VICTORIA UNIVERSITY OF WELLINGTON

Te Whare Wananga o te Upoko o te Ika a Maui

School of Engineering and Computer Science

Te Kura Mātai Pūkaha, Pūrorohiko

Optimal sizing of microgrids: A comparison of herd-behaviour-oriented meta-heuristics

By

Roomana Khalid

Supervisors: Prof Alan Brent, Dr Soheil Mohseni

Thesis presented in partial fulfilment of the requirements for the degree of Masters of Engineering by Thesis in Te Wāhanga Ahunui Pūkaha–Wellington Faculty of Engineering

February 2022

Abstract

The strategic long-term planning and design optimisation of renewable and sustainable energy systems, and particularly microgrids (MGs), is essential for the most effective use of limited resources, especially as the deployment of localised, distributed energy generation systems increases. The main objective of such integrated resource planning exercises is to minimise total discounted system costs, whilst adhering to a set of interlinked technical constraints, including reliability. This results in a non-deterministic polynomial time-hard (NP-hard) problem, for which no polynomial time solution exists. This has therefore brought to light the importance of utilising meta-heuristic optimisation algorithms.

Meta-heuristics are higher-level general strategies inspired by natural phenomena, which can be adapted to yield a near-globally-optimum solution to NP-hard problems by iteratively improving the position of candidate solutions under a pre-defined measure of quality or time. Given the approximate nature of meta-heuristics, they have been found to have different efficiencies in different applications due to the fundamental differences in the form of the underlying objective functions – and the nonlinearities and non-convexities involved. Accordingly, testing the efficiency of new meta-heuristics in different areas is an active research area.

In this context, a review of the MG sizing literature has identified that the performance of a number of state-of-the-art, herd-behaviour-oriented meta-heuristics has not yet been addressed, namely the wild horse optimiser (WHO), the artificial hummingbird algorithm (AHA), the artificial gorilla troops optimiser (AGTO), the marine predator algorithm (MPA), the equilibrium optimiser (EO), and the moth-flame optimisation algorithm (MFOA). In response, this study carried out a systematic performance comparison of the above-mentioned algorithms by benchmarking them against the well-established meta-heuristic in the literature, namely the particle swarm optimisation (PSO). To this end, two stand-alone battery-supported MGs were modelled, which provide an efficient solution for the electrification of personal passenger and utility fleets, in addition to serving residential and commercial loads. The first MG integrates solar photovoltaic (PV) and wind resources, while the second MG is solely driven by solar PV panels – both backed by battery storage. Moreover, to effectively coordinate the charge scheduling of integrated electric vehicles (EVs) – for improved cost solutions – specific rule-based dispatch strategies were developed. The conceptual MGs were then populated for three communities residing on Aotea–Great Barrier Island, in Aotearoa–New Zealand, who currently suffer from the unreliability of privately purchased, smaller-scale renewable energy systems.

The comparative summary-statistics-based results obtained from the application of the proposed method, parametrised for the two MG configurations of interest, to the three community cases, reveal the important role of newly advanced meta-heuristics in optimising a statistically robust, minimum cost solution to the associated MG asset allocation problem. Comprehensive capital budgeting, cash flow, and energy flow analyses, as well as various univariate sensitivity analyses, have, furthermore, verified the validity and effectiveness of the proposed optimised systems in providing an integrated, reliable, affordable, clean, secure platform for serving residential, commercial, and EV-charging loads in remote and island communities.

Acknowledgements

I would like to thank all the people who have supported me in the successful completion of this thesis.

Especially thanks to my supervisors Prof. Alan Brent and Dr. Soheil Mohseni for their continuous support, guidance, encouragement and patience and have shown faith in me.

I also would like to thanks head of school, post graduate coordinator, student advisor, and all my colleagues at the university who have contributed in the creation of productive environment at the campus.

I would love to mention my family who helped me out through the tough situations and was patient with me. Especially I would dedicate to my parents and my husband, Haris who have encouraged and backed me through this period and also done an incredible job instilling the love of education within me.

Table of Contents

List of Figures

List of Tables

Chapter 1: Introduction

This chapter provides the background information to the study and establishes the research rationale. The research objectives are then defined along with the research design and strategy.

1.1. Background

Providing electricity to the estimated 1 billion people remaining without access globally has been found to be particularly challenging given the costs associated with the expansions of conventional power networks to remote areas with geographically challenging terrain (Shieh *et al*., 2019). This brings to light the importance of distributed energy generation technologies that are sited close to the point of consumption, such as wind turbines (WTs), solar photovoltaic (PV) panels, micro-hydropower plants (MHPPs), and so forth. Distributed energy generation provides an effective platform for the electrification of remote areas, as well as decarbonising power supply (Papageorgiou *et al.*, 2020). The flexible architecture of microgrids allows for the optimal integration of distributed renewable energy sources (RESs) into the system – towards increasing the penetration of renewables in both urban regions and remote, rural localities.

In recent years, the microgrid concept has emerged to integrate several clean energy micro-sources into a dispatchable (controllable) system with a prescribed reliability level (Shieh *et al*., 2019). The U.S. Department of Energy defines a microgrid as "*a group of interconnected loads and distributed energy resources within clearly defined electrical boundaries that acts as a single controllable entity with respect to the grid*" (Ton and Smith, 2012).

Microgrids are typically associated with high capital, replacement, as well as operation and maintenance costs (Manfren *et al*., 2011). Also, non-dispatchable RESs, such as solar PV and wind are plagued by power output variability – as they depend on weather conditions. Despite high costs and variability in power output of RESs, there are several technical, economic and environmental benefits to implementing microgrids (AlSkaif *et al.*, 2017).

The optimal sizing of the components of microgrids is necessary to ensure a cost-minimal power supply whilst adhering to a set of operational and planning constraints. Accordingly, many studies in the literature have focused on developing MG capacity planning optimisation methods. For example, Yang *et al*. (2007) and (Diaf *et al.*, 2008) have presented exact mathematical optimisation-based approaches to designing a microgrid considering the loss of power supply probability (LPSP) reliability indicator. The major issues associated with analytical approaches to microgrid sizing are the strong assumptions and simplifications involved, which lead to significant simulation-to-reality gaps, especially in terms of the optimal cost of the system (Hlal *et al.*, 2019).

Alternatively, meta-heuristic algorithm techniques are increasingly utilised to approximate solutions to energy planning optimisation problems due to their applicability to the original (unreduced) problems. For instance, Bilal *et al.* (2013) have calculated the optimal size of WTs, PV panels, and battery packs to ensure the reliability of the system based on cost minimisation using a genetic algorithm-based solution approach. Radosavljević *et al*. (2016) have proposed optimising the energy and operational management of grid-connected microgrids. The optimisation of the system is achieved by utilising the particle swarm

optimisation (PSO) technique. Diab *et al.* (2019) have proposed a model that minimises the cost of electricity subject to meeting certain reliability levels for systems integrating solar PV panels, WTs, diesel generators, and battery storage systems (BSSs). The underlying hybrid microgrid is optimised using the moth-flame optimisation, whale optimisation, water cycle, and hybrid particle swarm-gravitation search algorithms with the performances compared. However, less attention has been devoted to optimising the size of microgrids using newly developed herd-behaviour-oriented meta-heuristic algorithms such as the artificial hummingbird algorithm (AHA), marine predator algorithm (MPA), and artificial gorilla troops optimiser (AGTO). Accordingly, the extent to which these algorithms might outperform the well-established algorithms is not yet known.

It is also noteworthy that New Zealand aims to achieve net-zero carbon emissions by 2050. Currently, around 40% of primary energy supply and more than 75% of electricity demand is met by RESs in New Zealand. Also, New Zealand holds the third place in the Organisation for Economic Cooperation and Development (OECD) in terms of the share of renewable electricity generation (MBIE, 2020a). This makes case studies in New Zealand prime candidates for evaluating the effectiveness of new methods.

1.2. Research rationale

It has been identified in the literature that meta-heuristic algorithms are able to increase the accuracy of optimal sizing of microgrid components compared to exact mathematical optimisers. For energy storage-supported microgrids integrating variable renewable technologies, particularly solar and wind resources, it is especially important to obtain the cost-minimal size of the components due to their high capital costs.

As the above review of the mainstream literature indicates, several scholars have presented meta-heuristic-based microgrid sizing approaches considering the cost objective. However, less attention has been given to the planning, and design optimisation, of microgrids with 100% renewable energy sources and with high reliability constraints using state-of-the-art herd-behaviour-oriented meta-heuristics.

Accordingly, research is needed on the optimisation of the whole-life cost of MGs using state-of-the-art herd-behaviour-oriented meta-heuristics. To this end, the optimisation problem needs to be derived based on minimising the total net present cost of the system subject to the standard operational and planning constraints.

1.3. Research objectives

This research aims primarily to assist the decision-making processes considering the whole life-cycle cost associated with microgrids' planning and optimal sizing. Specifically, the research objectives of the study are:

> O1: Identify the main factors that influence the economics and configurations of microgrid systems.
>
> O2: Establish a general meta-heuristic-based modelling framework to yield the optimisation of microgrids.
>
> O3: Conduct a case-study analysis within a New Zealand context to verify and validate the proposed meta-heuristic-based microgrid designing model.

O4: Examine and compare the efficiency of well-established and state-of-the-art meta-heuristic algorithms, when applied to the problem at hand.

1.4. Research design

This research follows a deductive reasoning approach by collecting evidence based on a case-study analysis to address the research problem. The deductive approach starts and ends with the 'theory', as illustrated in Figure 1, and follows the exploratory and descriptive phases (Van Wyk and Taole, 2015). In this context, a set of questions were formulated to explore the different scenarios for microgrid design optimisation, such as:

- "What are the most influential contributing factors to the design optimisation of microgrids?"
- "To what extent is a herd-behaviour-oriented meta-heuristic-based design of microgrids able to improve the costing of such systems?"
- "What are the implications of total cost minimisation during the planning phases of micro-grids?"

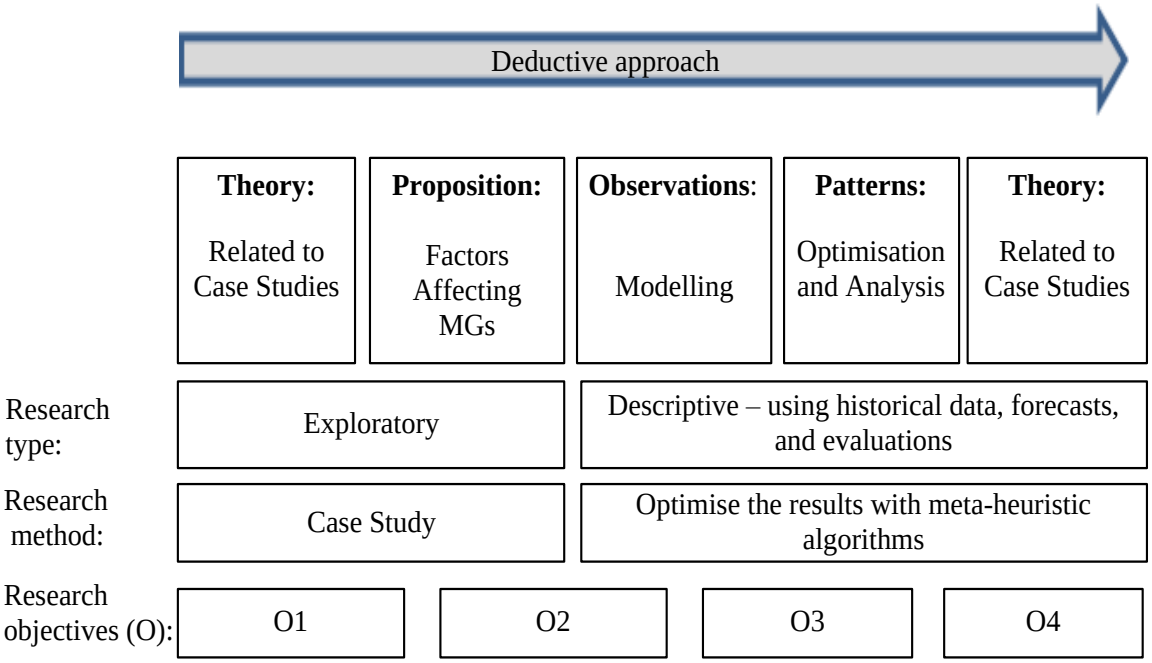

Figure 1.Illustration of the deductive approach of the research

Van Wyk and Taole (2015) classify research design types according to primary data and existing data. Primary data links to case studies, surveys, programme evaluations, and so forth, whereas existing data deals with historical studies, numeric data, and statistical data. This study uses a combination of primary and existing data.

1.5. Research strategy

The following steps were undertaken for the study:

Step 1: Review the literature on design optimisation of micro-grids using well-established and state-of-the-art meta-heuristics.

Step 2: Explore the possible applications of design optimisation of microgrids within a New Zealand context.

Step 3: Develop a modelling framework that optimises the cost objective, particularly life-cycle cost minimisation. More specifically, the objective function consists of the associated costs and continuous decision variables representing the size of components in the candidate pool.

Step 4: Test the performance of various meta-heuristics when embedded within the proposed model and applied to the underlying design optimisation problem.

Step 5: Verify the proposed model through comprehensive scenario-testing and in-depth sensitivity analyses.

Step 6: Systematically measure the impact of the proposed model in improving the cost-effectiveness of micro-grid systems.

Chapter 2: Literature review

2.1. Introduction

This chapter reviews the mainstream literature on the optimal capacity planning of micro-grids (MGs). To this end, first, the literature review methodology explains the steps taken to identify and select the eligible studies for review. The review of the relevant literature then lays the foundation for the identification of the main factors that influence the economics and configurations of MGs. This, in turn, provides a platform for illustrating the pathways and the associated barriers to the energy transition towards renewable energy resources from conventional energy generation. A thematic characterisation of the literature, furthermore, highlights the notable actions taken by developed and developing countries to surmount the identified barriers, including the use of advanced computational planning models and novel MG configurations. This paves the way for positioning the novelty of this study, summarised in the previous chapter, within the identified gaps in knowledge.

2.2. Literature review methodology

Inspired by Cronin *et al.* (2008), a hybrid literature review methodology was adopted, which includes the 'classic' and 'systematic' literature review components. Fig. 2 summarises the literature review process (Cronin et al., 2008).

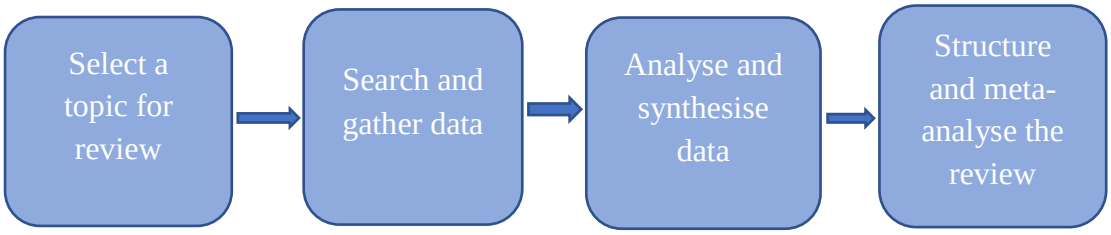

Figure 2. The literature review process adapted from (Cronin et al., 2008).

The selected topic for the literature review was the optimal sizing and capacity planning of MGs, and the wider transition to renewable energy economy by means of MGs. To search for relevant studies in the literature, a systematic review was carried out to identify the papers published *from 2002 to 2021* using selected keywords in the Google Scholar database and the advanced database provided by the library of Te Herenga Waka—Victoria University of Wellington. The publication types were limited to journal and conference articles, as well as book chapters. The selected keywords to search the literature are summarised in Table 1, which are categorised into more specific components of the MG sizing problem, as well as the relevant dimensions. The identified studies were also checked for eligibility by reviewing their titles, keywords, and tables of contents. The selected studies for review were then analysed and synthesised by carrying out a critical review of the main body of the publications. Finally, in the fourth step, the reviewed publications were structured and meta-analysed in terms of their findings to identify the knowledge gaps. The meta-analysis also entailed linking the wider thematic findings of the literature review to the research questions of this thesis.

Table 1. Keywords used to search the MG sizing literature.

Component	Keywords
Role in energy transition	Energy transition, decarbonisation
Topology	Micro-grid system, AC micro-grids, DC micro-grids
Economics	Micro-grid economics, capital cost
Renewable energy potentials	Solar energy, wind energy, renewable energy potentials
Case study	100% renewable energy
Long-term planning	Planning of micro-grid, design of micro-grid, sizing of micro-grid, optimal capacity of micro-grid
Configuration	Grid-connected, isolated, islanded, off-grid, stand-alone

Table 2 provides a summary of the identified studies from the systematic literature review. A thematic characterisation of the included studies for review, in accordance with the wider scope of the thesis, is presented in the following sections.

Table 2. Summary of the previous work on the planning and designing of MGs.

Micro-grid configuration	Type of loads	Battery storage	Optimisation approach	Optimisation algorithm(s)	Objective function(s)	Case study site	Reference(s)
PV, WT, CHP	Industrial and residential	No	Reduce gradient method	-	Investment and maintenance costs	East coast of USA	(Augustine *et al.*, 2012a)
PV, WT, FC, CHP	Commercial	No	Meta-heuristic	PSO	Operating cost	Unspecified	(Nikmehr and Najafi Ravadanegh, 2015)
PV, WT, FC, DG	Unspecified	No	Meta-heuristic	NSGA-II	Operating cost	Unspecified	(Karuppasamypandiyan *et al.*, 2019)
DG	Unspecified	No	Meta-heuristic	NSGA-II, Fuzzy logic	Power loss, stability	Algeria distribution network	(Mosbah *et al*., 2017)
PV, WT, DG	Residential	Yes	Meta-heuristic	NSGA-II	Operational cost and power loss	Unspecified	(Vergara *et al*., 2015)
PV, WT, MTs, main grid	Residential and agriculture	No	Meta-heuristic	PSO	Operating cost	Unspecified	(Kerboua *et al*., 2020)
PV, biomass	Residential and agriculture	Yes	Meta-heuristic	PSO, IWO	TNPC, LPSP	Unspecified	(Samy and Barakat, 2019)
PV, WT, DG	Unspecified	Yes	Meta-heuristic	CSOA, BFOA	Capital, O&M	Unspecified	(Alsmadi *et al.*, 2019)
FC, DG, main grid	Unspecified	Yes	Traditional method	Static dispatch	Operating cost	Unspecified	(Liu *et al.*, 2010)
PV, WT, FC, MT, main grid	Unspecified	Yes	Meta-heuristic	PSO	TNPC	Unspecified	(Razmi and Doagou-Mojarrad, 2019)
PV, WT, FC	Unspecified	Yes	Meta-heuristic	BSA, MFOA	Operating cost	Unspecified	(Suresh and Ganesh, 2019)
WT	Unspecified	Yes	Meta-heuristic	SHO	Operating cost	Tamil Nadu	(Rajesh *et al*., 2021)
PV, WT, MT, main grid	Residential	No	Incentive-based	-	Operational cost and power loss	Unspecified	(Monfared *et al.*, 2019)

			strategy				
PV, MT, main grid	EV, PHEV	No	Exact method	MILP	Operating cost	Unspecified	(Rasouli *et al.*, 2019)
WT, Boiler, CHP	EV, industrial	Yes	Exact method	MILP	Operating cost	Unspecified	(Lekvan *et al.*, 2021)
PV	EV, residential	Yes	Simulink	Phaser mode	Operating cost	Unspecified	(Cetinbas *et al*., 2019)
PV, WT, main grid	EV, residential	Yes	Traditional method	SA	Operating cost	Unspecified	(Liu *et al.*, 2020)
CHP, boiler, PV, LDG	EV, residential	No	Exact method	MILP	Operating cost	Unspecified	(Hosseinnia and Tousi, 2019)
PV, WT, CHP, boiler	EV, residential	Yes	Meta-heuristic	WOA	Operating cost	Newcastle, England	(Afrooz *et al.*, 2019)
PV, WT, FC, DG, MT	EV, load (unspecified)	No	Meta-heuristic	WOA	Power loss	Unspecified	(Sahu *et al*., 2020)
PV, hydrogen, FC	EV, residential	No	Meta-heuristic	NSGA-II	Operational cost and power loss	Yuxi, China	(Huang *et al.*, 2019)
PV, WT	Unspecified	Yes	Simulink	-	TNPC, LPSP	Corsica Island	(Diaf *et al.*, 2008)
PV, WT	Unspecified	Yes	Meta-heuristic	NSGA-II	TNPC	Unspecified	(Sarkar and Bhattacharyya, 2012)
PV, WT	Unspecified	Yes	Meta-heuristic	HGA	Operating cost	Shandong, China	(Lu *et al.*, 2017)
PV, WT	Unspecified	Yes	Meta-heuristic	NSGA-II	Operating cost	Portuguese distribution network	(Haddadian and Noroozian, 2017)
PV, WT	Unspecified	Yes	Meta-heuristic	NSGA-II, MOPSO	TNPC, LPSP	Malaysia	(Hlal *et al.*, 2019)
PV, WT, DG	Residential	Yes	Meta-heuristic	MOSaDE	COE, LPSP	Yanbu, Saudi Arabia	(Ramli, Bouchekara and Alghamdi, 2018)
PV, main grid	Residential, industrial	No	Meta-heuristic	EA	Power loss	Unspecified	(Chaspierre *et al*., 2017a)

PV	unspecified	No	Meta-heuristic	WHO	Compare efficiency of PVs	Unspecified	(Ramadan *et al.*, 2021)
Unspecified	EV	No	Meta-heuristic	AHA	Cost, efficiency	Unspecified	(Yin, Zhang and Jiang, 2021)
PV, WT, DG	Unspecified	Yes	Meta-heuristic	AGTO	Power loss	Unspecified	(Ali *et al.*, 2021)
Main grid	Unspecified	No	Meta-heuristic	MPA	Fuel cost, power losses	Unspecified	(Alharthi *et al.*, 2021)
Main grid	Unspecified	No	Meta-heuristic	MPA	Power loss	Unspecified	(Wadood *et al.*, 2021)
WT, DG, PV	Unspecified	Yes	Meta-heuristic	MPA	RES sensitivity analyses	Unspecified	(Yakout *et al.*, 2021)
PV	Unspecified	No	Meta-heuristic	MPA	PV statistical analysis	Unspecified	(Bayoumi *et al*., 2021)
PV, WT, DG	Unspecified	Yes	Meta-heuristic	WOA, WCA, MFOA, PSOGSA	COE, LPSP	Unspecified	(Zaki Diab *et al.*, 2020)
PV, WT, main grid	Unspecified	No	Meta-heuristic	EO, WOA, SCA	Operating cost	Unspecified	(Ahmed *et al.*, 2021)
PV, WT	Residential, commercial, EV-charging loads	Yes	Meta-heuristic	MFOA, PSO, WHO, AHA, AGTO, MPA, EO	TNPC	Great Barrier Island, New Zealand	This study

Key: AHA = Artificial Hummingbird Algorithm, AGTO = Artificial Gorilla Troops Optimiser, BFOA = Bacterial Foraging Optimisation Algorithm, BSA = Bat Search Algorithm, CSOA = Cuckoo Search Optimisation Algorithm, COE = Cost of Electricity, CHP = Combine Heat and Power, DG = Diesel Generator, EV = Electric Vehicle, EA = Evolutionary Algorithm, FC = Fuel Cell, HGA = Hierarchical Genetic Algorithm, IWO = Invasive Weed Optimisation, LDG = Local Dispatchable Generators, LPSP = Loss of Power Supply Probability, MTs = Micro-turbines, MOPSO = Multi-Objective Particle Swarm Optimisation, MOSaDE = Multi-Objective Self-Adaptive Differential Evolution algorithm, MFOA = Moth Flame Optimisation Algorithm, MPA = Marine Predator Algorithm, MILP = Mix Integer Linear Programming, NSGA-II = Non-dominating Sorting Genetic Algorithm, O&M = Operation and Maintenance Cost, PV = Photovoltaic, PHEV = Plug-in Hybrid Electric Vehicle, PSO = Particle Swarm Optimisation, PSOGSA = Particle Swarm-gravitational Search Algorithm, SA = Simulated Annealing Algorithm, SCA = Sine Cosine Algorithm, SHO = Selfish Herd Optimiser Algorithm, TNPC = Total Net Present Cost, WT = Wind Turbine, WOA = Whale Optimisation Algorithm, WHO = Wild Horse Optimiser, WCA = Water Cycle Algorithm.

2.3. Topology, configuration, and structure of MGs

The deployment of smart MGs has been found to be a key enabler of the energy transition away from fossil fuels as part of the wider decarbonisation efforts (Shah Danish et al., 2019). More specifically, smart MGs provide an effective platform for the optimal system integration of renewable energy sources (RESs) – towards increasing their penetration in conventional power systems and driving the reliable, affordable, clean electrification interventions tailored to remote communities. A review of the relevant literature reveals that site-specific plans are essential to cost minimisation, in view of the different potentials of renewables in different locations, as well as differences inherent in load profiles. Also, variable renewables, such as solar photovoltaic (PV) panels and wind resources require backup storage systems to ensure reliable and cost-effective energy supply, and are best managed using smart MGs (Sims, Rogner and Gregory, 2003).

In this context, wind and solar PV technologies have been found to be the most widely employed resources. Also, given the daily and seasonal power generation complementarities that exist between solar PV and wind, they are commonly implemented together (Kaldellis, 2002). Furthermore, on a global scale, renewable electrification using hydro resources has also been found to be the most technologically developed scheme, although heavily constrained by social and environmental barriers (Kaldellis, 2002). More specifically, social preferences towards hydro resources are difficult to predict and inherently uncertain, especially with regard to their development in remote areas. Moreover, the well-established biomass resources in the literature include forestry residues and landfill gas, which have a significant potential for development in rural areas, although suffering from sustainable management and logistics barriers. Other power generation and storage technologies considered in the identified studies include, but are not limited to, combined heat and power (CHP) units, electrolysers, fuel cells (FCs), hydrogen storage systems, and micro-turbines (MTs). In terms of connection to the wider utility grid, both grid-connected and -isolated systems are well-studied in the relevant reviewed literature.

In terms of topological architecture, both alternating current (AC) and direct current (DC) MGs are well-explored in the relevant reviewed literature. A major difference in terms of application is that AC-linked MGs are mostly utilised in active distribution systems, whereas DC-linked MGs are more commonly developed in greenfield sites where a large share of loads are DC – mobile phones, computers, LED lights, and so forth. In grid-connected applications, AC and DC MGs form the backbone of smart grids where loads can be cooperatively/intelligently served using the smart grid-wide resources during normal and emergency conditions (Alam, Chakrabarti and Ghosh, 2019).

Moreover, the literature review reveals that smart MGs driven by RESs are commonly backed by integrated energy storage systems (ESSs) to deliver a reliable power supply. Accordingly, in terms of energy balance, the total energy supplied by renewables and power imports (in the case of grid-connected systems) is not exactly equal to the total energy consumption due to the power and energy conversion losses involved. Additionally, AC MGs integrated into active distribution networks are associated with high resistance losses in distribution lines due to low operating voltages. Therefore, specifically developed voltage control schemes factored into the relevant reliability measures of the optimisation problems are prevalent in the relevant reviewed studies, which have shown to be effective in improving the economics of the designed systems. Additionally, it has been reported that the energy

conversion losses of DC-coupled MGs are lower than those of AC systems, mainly as a result of the increased efficiency of the underlying converters (Elsayed *et al*., 2015).

The evidence from the review of the relevant literature also suggests that off-grid electrification initiatives using stand-alone MGs have facilitated the provisioning of reliable, cost-effective, sustainable energy to remote and less economically developed communities over the last two decades, particularly in cases that are plagued by difficult geographical terrain – where grid connection and electricity transmission become difficult. Yet, despite these achievements, the literature review reveals that additional methodological advancements for the optimal coordination of dispatchable devices, as opposed to the conventional cycle-charging dispatch strategies, are needed to better align variable generation with demand (Hlal *et al.*, 2019).

2.3.1. Main advantages of MGs

Given their popularity in the relevant reviewed literature for the resilient integration of new loads and distributed energy resources (DERs), this section provides a summary of the advantages of MGs, namely:

- The ability to operate during sudden disruptions in the grid or blackout (improved resilience and reliability);
- Reduced losses and improved efficiency of the system operation;
- Bolstered cyber-security;
- Promoting clean energy;
- Efficient utilisation in remote areas; and
- Improving community well-being.

It is also noteworthy that the MG behaves as a complex zone when integrated into a wider utility network due to the integrated DC components. Moreover, Fig. 3 depicts the general schematic diagram of the most common MG configuration in the reviewed literature, namely the battery-backed, renewables-driven architecture (Mumtaz and Bayram, 2017).

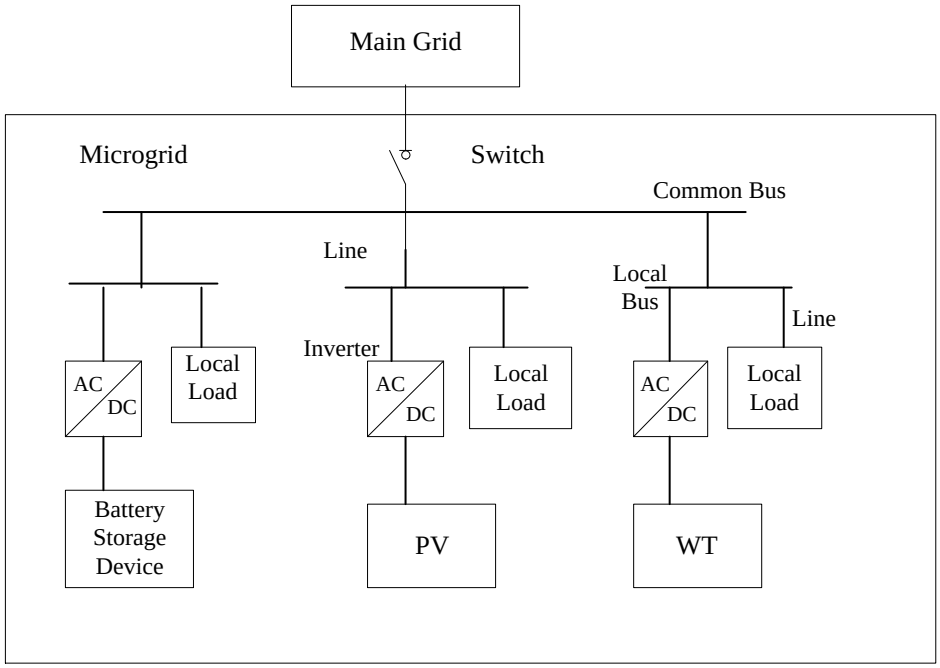

Figure 3. General model of a battery-backed, renewables-driven MG.

2.4. Factors affecting the economics of MGs

To objective of MG sizing is to determine the optimal combination of resources with minimum cost subject to a set of technical constraints. However, based on the evidence in the reviewed literature, the implementation of the optimal solution is associated with technical, economic, social, and regulatory barriers that make the realisation of MGs with a high penetration of RESs challenging. Some of these barriers could be linked to immature technology, while others arise due to the specific conditions of the country or region of interest (Diaf et al., 2008). While Table A1 in Appendix A summarises and sub-categorises the above barriers, the following sections provide a detailed discussion of such barriers, with a particular focus on technical barriers due to their particular relevance to the scope of this study.

2.4.1. Technical barriers

The major technical barriers to RE project developments are limited infrastructure maturity, energy storage complexities, lack of onsite operation and maintenance resources, and non-ideal performance of equipment in real-world conditions (Seetharaman *et al.*, 2019).

2.4.1.1. Non-dispatchable renewable resources

One of the significant challenges of the integration of RESs is the associated inherent variability in power generation (Edris, 2012). For example, the power outputs of solar PV and wind turbine (WT) technologies depend on specific day-to-day and seasonal meteorological conditions, which have direct implications for the size of the integrated storage systems, which are vital for improved dispatchability reasons. The uncertainties in forecasts of non-dispatchable power outputs might also result in oversized generation components, which in

turn, increase the total discounted cost of MGs. For oversized solar PV plants, this additionally results in increased voltage control complexities (Mahmoud *et al.*, 2014). The degree of complexity increases as the dimension of the system components increases due to the correlations that exist between the associated uncertain factors, notably given the complementarities of different RESs (Badal *et al.*, 2019).

The review of the relevant literature also identifies that solar PV and wind resources are the most favoured generation technologies for the provision and proliferation of clean energy using MGs – see Fig. 4 for an indication of wind generation capacity as a proportion of total electricity generation in selected countries' energy mix (MBIE, 2020b). In view of the above-discussed uncertainty in power outputs of solar PV and WT technologies, more advanced control systems are needed to cost-effectively and reliably meet the loads.

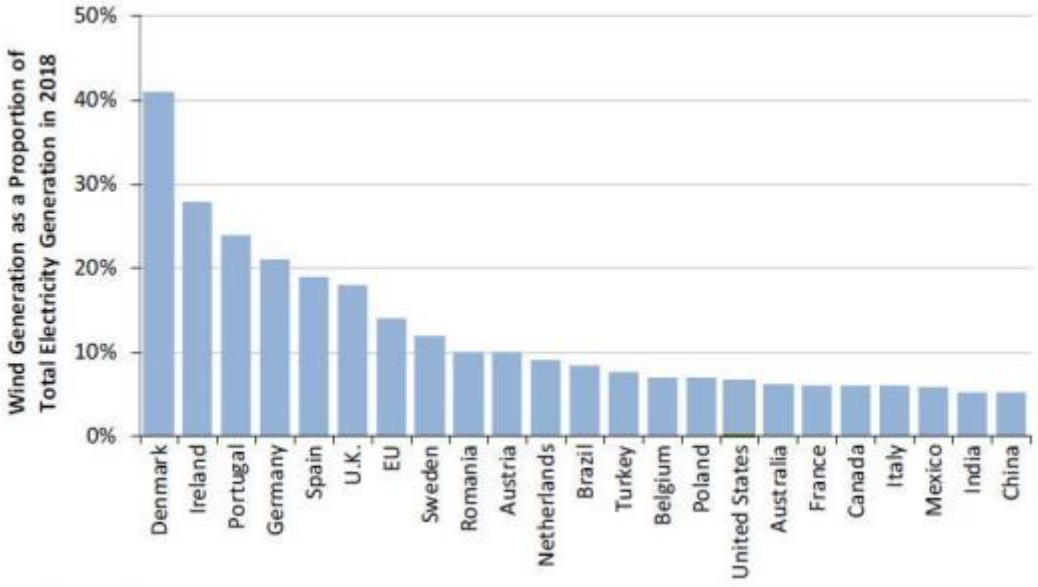

Figure 4. Penetration of wind turbines in selected countries' energy mix (MBIE, 2020b).

The relevant reviewed literature has also discussed the technical challenges associated with dispatchable RESs (notably, biopower generation plants), albeit significantly less than non-dispatchable resources. Specifically, the review identifies the following notable challenges associated with biopower generation: greenhouse gas production, provisioning of sufficient feedstock supply, and higher generation costs compared to fossil fuel-based power plants and non-dispatchable renewables (Sims, Rogner and Gregory, 2003). Also, for large-scale biopower schemes, the levelised cost of energy increases as the capacity and consequently the distance of the generation facility from load consumption points increases for air quality reasons. Furthermore, excess moisture in pellets could reduce the electricity generation efficiency in large-scale biopower plants as a result of thermal efficiency reduction due to excess heat absorption. On the other hand, if biomass resources lose extra moisture, it could also lead to additional production costs as a result of reduced efficiencies (Iqbal *et al.*, 2014). Therefore, biomass resources require adequate moisture for efficient power generation, which is a challenging task. This, consequently, induces uncertainty in power outputs of biopower plants, which is difficult to quantify probabilistically. Such unquantified uncertainty factors can also lead to unforeseen voltage variations, especially on a MG scale (Kumar *et al.*, 2016).

2.4.1.2. Energy storage complexities

The review has also identified salient inadequacies with regard to the standards and guidelines of energy storage integration that are critical for the reliable operation of highly renewable MGs. Such inadequacies have also hindered the large-scale commercialisation of fundamentally new storage technologies, which has direct negative implications for the large-scale integration of variable renewables (Radosavljevic *et al.*, 2016). This is especially so with respect to the important role of energy storage systems on the efficient management of energy flow from generation to consumption (in a balanced manner) necessary to maintain the power quality (Hussain *et al.*, 2017). The review has also confirmed that battery storage is the most favoured storage technology, not only in remote, off-grid applications to support variable renewables, but also in grid-connected systems that participate in deregulated electricity markets and run advanced energy arbitrage mechanisms (Zhao *et al.*, 2018). It is also worth emphasising that battery storage technologies replace diesel generators in the previous generation of MGs, commonly known as hybrid renewable energy systems (Zaki Diab *et al.*, 2019).

The literature review also finds that battery storage is widely characterised by energy and power capacities, which are held fixed per unit of storage considered, as is the MG topology (Hlal *et al.*, 2019). Other salient characteristics of battery storage considered during the capacity planning and design phases include efficiency, operating temperature, depth of charge and discharge, lifespan, and energy density (Zaki Diab *et al.*, 2019). Furthermore, deep cycle batteries are commonly promoted in the literature, the efficiency of which varies from 70% to 90% (Divya and Østergaard, 2009). Some of the commonly used batteries in the literature are discussed in more detail in the following sections.

2.4.1.2.1. Lithium-ion (Li-ion)

The advantages of Li-ion battery in MG development applications include high energy density, efficient trade-offs between specific energy and specific power ratings, safe operating temperatures, and relatively long expected life (Agua *et al.*, 2020), (Zhang *et al.*, 2018). However, the main limitation of Li-ion batteries is the significant impact of depth-of-discharge on their lifespan, which warrants advanced, more expensive operational strategies (Zhao *et al*., 2018).

2.4.1.2.2. Lead-acid (LA)

The lead-acid battery is currently the most widely utilised battery technology in remote, off-grid MGs (Zhang *et al.*, 2018). As its main advantages, it offers deep cycle discharge capacity and low self-discharge rates at a comparatively low price due to its well-established, mature technology base, while its charge and discharge efficiencies could vary from 50% to 95%. However, it has low specific energy, relatively low charge and discharge power capacities, poor performance in low temperatures, and limited cycle life – with repeated deep cycling significantly reducing the battery life (Zhao *et al.*, 2018).

2.4.1.2.3. Vanadium redox-flow

The main advantages of vanadium redox-flow batteries include high energy efficiency, long cycle life, short response time, and independently adjustable power rating and energy capacity. However, they are currently associated with higher capital and operation and

maintenance costs, mainly as a result of using capital-intensive ion-exchange membranes, which typically contribute to around 40% of the total battery cost. They additionally suffer from low volumetric energy storage capacity as a result of the low solubility of the active species in the electrolyte. The literature review has identified the important role of vanadium redox-flow batteries in power quality improvement due to their high charge/discharge power capacities (Leung *et al.*, 2012).

2.4.1.2.4. Sodium-sulphur (NaS)

The sodium-sulphur battery technology is a mature system with established experience and the middle cost per capacity compared to other battery technologies. It also has almost no self-discharge and extremely quick response time (high energy density, energy capacity, and power density), making it suitable for responding to changes in demand in a MG in steady state conditions. It also benefits from a high recycling rate due to the use of less toxic materials. However, its main disadvantage is that it requires a heat source to maintain the temperature of the liquid electrode; the operating temperature of NaS batteries is 574 K-624 K. This makes it impractical for residential and small-scale commercial use cases. More importantly, the heat source needed for the continuing operation of the battery drains part of the battery's efficiency, which reduces its overall efficiency and incurs additional costs due to the necessity of adding heat exchange systems (Kawakami *et al.*, 2010).

2.4.1.2.5. Nickel-metal hydride (NiMH)

The nickel-metal hydride (NiMH) battery has the advantages of low memory effect, good environmental performance, profitability of recycling, long service life, and relative inexpensiveness (Zhao *et al.*, 2018). However, it is plagued by high self-discharge rates (25%-35% per month), limited cycle life (performance deteriorates after less than 300 cycles if repeatedly deep discharged), low charging/discharging power capacities, and high maintenance costs (Zhu *et al.*, 2013).

As the above review of some of the batteries used in MGs indicates, different battery storage technologies are associated with different specifications; notably, energy density, specific power, specific energy, charge/discharge power capacity, self-discharge, and maximum allowable depth-of-discharge. This necessitates a comprehensive, multi-case-study-oriented comparative study of various battery technologies to aid the associated decision-making on the optimal MG capacity planning and unit sizing during the long-term strategic planning phases. It is noteworthy that the differences in the specifications of different battery technologies affects the energy balance analyses in the typical year-long operational scheduling stage, with consequent changes in the optimal equipment size and associated total discounted life-cycle cost of MGs (Gamarra and Guerrero, 2015). Furthermore, such comprehensive battery selection studies can provide an effective platform for more profitable renewable energy project developments with associated lower energy curtailments and lost loads.

2.4.1.3. Lack of operation and maintenance culture

Given that renewable energy technology is comparatively new and less optimally developed, there exists a lack of knowledge and expertise in operation and maintenance (O&M). This results in lower than expected efficiencies with non-optimal operations and non-regular maintenance. That is, the maximum efficiency could be achieved only if the technologies are

optimally operated with a well-defined maintenance schedule. It is also necessary to check the availability of well-suited equipment, components, and spare parts in local markets during the prior techno-economic feasibility assessments, as the import of the equipment might incur a high initial cost, increasing the overall estimated cost of the project (Seetharaman *et al.*, 2019).

2.4.2. Economic barriers

The literature review also reveals that the main factors underpinning the economic and financial barriers are high upfront cost requirements, lack of relevant financial institutes, lack of investors, and less government subsidies in developing, oil-exporting countries (Steffen, 2020). These factors have hindered the global proliferation of RE. The following sections more specifically discuss the identified economic barriers.

2.4.2.1. Competition with fossil fuels

According to the International Energy Outlook report of the U.S. Energy Information Administration (EIA, 2016), fossil fuels (mainly coal, natural gas, and oil) are expected to supply 78% of the global energy used (aggregated over all sectors) in 2040. For indicative purposes, Fig. 5 shows the global primary energy consumption by fossil fuel sources until 2019 and energy is measured in terawatt-hours (TWh) (Global Fossil Fuel consumption, 2019). Most notably, coal is still a major source of power generation due to its abundance in many countries, making it relatively inexpensive and accessible compared to renewable energy technologies. Also, natural gas-fired power plants and natural gas combined-cycle power plants make up a significant portion of developing, fossil-fuel-exporting countries' power generation mix (Dulal *et al.*, 2013).

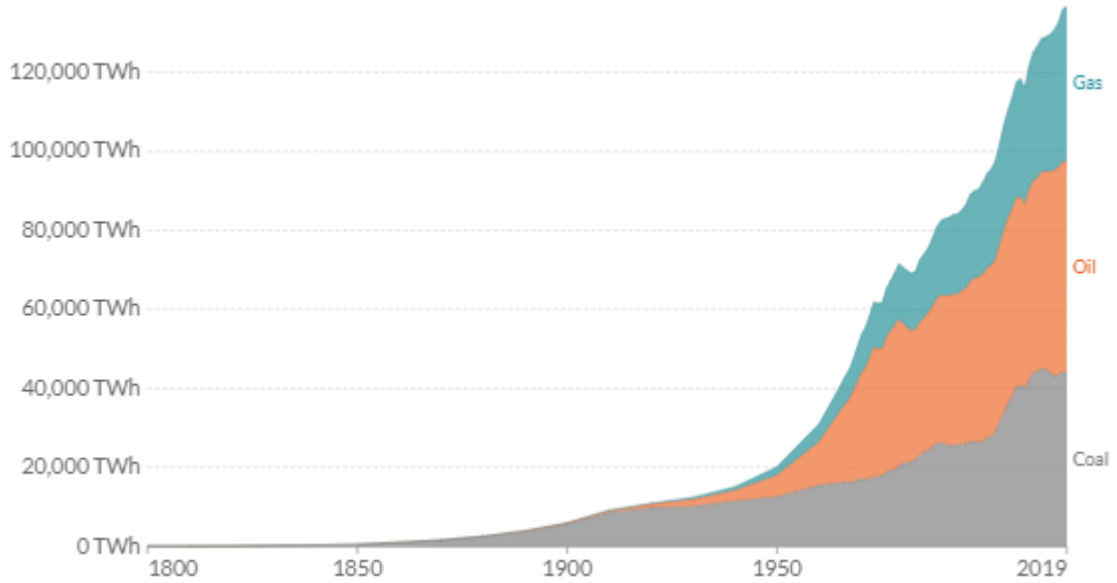

Figure 5. Global primary energy consumption by fossil fuel sources until 2019.

2.4.2.2. Subsidies of energy generation

In developing, fossil fuel-exporting countries, fossil fuel-fired power plants are still receiving significantly higher government subsidies compared to renewable energy generation

schemes, making a high penetration of RESs in the generation mix an uneconomical option for the power industry. For example, natural gas, which has a significant 70% share in Iran's power generation mix, received $35 billion in subsidies in 2020 (Financial Tribute, 2021).

2.4.2.3. Renewable energy investment with limited financing institutions

In the lack of tailored financial instruments and organisations, renewable energy developments can be financed using corporate finance or project finance structures. The corporate finance structure is based on a balance sheet (for instance, a utility), whereas the project finance structure is based on an off-balance sheet in a legal entity. It has also been found that private developers are responsible for a large share of market openings across various scales of renewable energy development. Furthermore, it has been recognised that, while high-risk renewable energy projects might need to be funded from public funding sources, it is still private actors that draw on public finance instruments to push renewable energy to new frontiers (Steffen *et al.*, 2018).

Moreover, securing financing at competitive rates with those of fossil fuel energy projects is a substantial barrier for renewable energy developers in the developing world. In this light, a hybrid debt-equity finance structure is promoted in the literature. More specifically, debt is defined as the portion of the investment procured by external lenders and supported by the project's financial flows or the credit of the corporate. On the other hand, equity represents the value that would be returned when all the project assets are liquidated based on future cash inflows generated by the project. In this context, determining the optimal percentage of debt and equity in the project's financial structure requires holistic risk-aware capital budgeting analyses (Krupa, Poudineh and Harvey, 2019).

2.4.2.4. Cost of capital

Renewable energy projects are associated with high initial investment costs, which are exacerbated by inefficiencies in technologies, resulting in relatively long net payback periods – the amount of time it takes to recoup the cost of investment – that leave investors behind (Hainz and Kleimeier, 2012). Both energy-as-a-service and community-financed business models suffer from high initial capital costs – an issue that is more pronounced where more stringent lending standards are in place, making it more difficult to borrow money without having substantial credit (Ansari *et al.*, 2013).

2.4.3. Social barriers

Despite broad public support for renewable energy, in some regions, the transition to renewables away from conventional sources (or more specifically, the siting of infrastructure) has faced local resistance and opposition due to a lack of quality information. That is, the review indicates that although a lot of work has been conducted on public attitudes towards sustainable energy equipment, true understanding of the dynamics of social acceptance has remained elusive due to the scarce consideration of all the determinants of social acceptance at the same time (Devine-Wright, 2007).

2.4.3.1. Symbolic aspects of facility siting

A review of the literature indicates that there is a need to more systematically study the symbolic aspects of renewable energy infrastructure siting disputes due to the very few

empirical studies exploring such dimensions. A discursive approach has also been utilised in a number of recent studies to better understand the public resistance to the siting of WTs, solar PV panels, and micro-hydro generation systems, which have shown how rhetorical and communicative dimensions at the social-psychological level can positively impact the decisions of individuals and local communities involved in renewable energy siting disputes (Steffen *et al.*, 2018), (Devine-Wright, 2007).

2.4.3.2. Not-in-my-backyard phenomenon

The not-in-my-backyard phenomenon describes the situations in which individuals oppose the nearby development of a technology or service, despite general, abstract support of the idea. The notable reasons behind the not-in-my-backyard behaviour are found to be landscape impact, environmental degradation, noise concerns, government giveaways of public lands to private solar and wind farm developers, and lowering local property values (Grafström *et al.*, 2020), (Nasirov *et al.*, 2015), (Smith and Klick, 2007).

2.4.3.3. Land use

Inherent land-per-unit-of-power-produced characteristics of WTs and solar PV panels make conflict over land use and project siting, resulting in the objection of farmer communities to the development of renewable energy projects near their lands (Steffen, 2020). Accordingly, a growing body of research has been devoted to reducing the land use impact of non-dispatchable renewables. To this end, combining renewable power with other land uses, notably agriculture, as well as installing solar panels on rooftops, have been reported to be the most effective interventions to minimise land use conflicts. Also, the direct involvement of communities in renewable energy planning and land use zoning has been recognised as an effective policy to alleviate such concerns (Jeslin Drusila Nesamalar, Venkatesh and Charles Raja, 2017), (Gross, 2020).

2.4.3.4. Lack of skilled labour

The literature review also identifies the lack of skilled professionals in designing, building, operating, and maintaining renewable energy and storage technologies a significant barrier for a smooth transition to a low-carbon economy (Ansari *et al.*, 2013). That is, not only is bridging the skills gap key for energy access, but it also plays a significant role in achieving 100% renewable energy (Karakaya and Sriwannawit, 2015). More strikingly, driving the post-COVID19 renewable energy transformation requires additional investment and innovation in higher education, as well as long-term investments in staffing.

2.4.4. Legal and regulatory barriers

A number of legal and regulatory barriers to sustainable energy systems have also been identified, namely: lack of legal frameworks and standards for independent power generators, limited transmission line access, liability insurance requirements, and lack of equipment standards (Beck and Levine, 2004), (Stokes, 2013).

2.4.4.1. Lack of legal frameworks and standards for independent power generators

In many developing countries, electricity companies are still monopolistic from generation to transmission to distribution. In such conditions, where there is a lack of standardised legal

frameworks, independent electricity generators are not able to enter the market and invest in sustainable energy systems with energy-as-a-service business models. Also, such circumstances lead to ad-hoc-based, non-systematic power purchase agreements, which make the planning and management of renewable energy development particularly challenging (Sun and Nie, 2015), (Beck and Levine, 2004).

2.4.4.2. Limited transmission line access

Where conventional power utilities control a monopoly on transmission lines, they may not allow emerging renewable energy generation companies to fairly access the transmission lines. Equitable access to transmission lines is of utmost importance for newly established renewable energy generation companies, notably wind farms and large-scale biopower plants, as they may be sited far from consumption nodes. Accordingly, a set of well-defined and consistent rules are necessary to effectively avoid right-of-way disputes (Zhang *et al.*, 2014), (Beck and Levine, 2004).

2.4.4.3. Liability insurance requirements

Small-scale renewable energy systems, particularly solar PV-driven household and community systems, which feed back into the grid during the periods of excess generation under net metring tariffs, may require liability insurance. This is because when those small generators continue to supply back into the wider utility grid, when upfront lines are disconnected for repair purposes, can cause injury to repair crews, although modern protective devices can prevent the so-called "islanding" issue (Stokes, 2013), (Beck and Levine, 2004).

2.4.4.4. Lack of equipment standards

Standardisation within the renewable energy supply chain is essential to guarantee that the equipment and spare parts are manufactured in compliance with technical regulations. Effective development of the relevant standards requires extensive verification processes based on benchmarking against a set of criteria. It also entails conformity assessment processes through independent, third-party certifications or other verification processes (Emodi, Yusuf and Boo, 2014), (IRENA, 2013).

2.5. Drivers of renewable energy

The review of the relevant literature has also identified that the drivers of renewable energy development can be broadly classified into the following four groups, or a combination thereof: (i) climate change mitigation, (ii) energy security, (iii) energy access, and (iv) socio-economic growth. These drivers are discussed in more detail in the following sections, which are also summarised in Table A2 in Appendix A.

2.5.1. Climate change mitigation

Addressing climate change by limiting global temperature rise to well below 2 degrees Celsius – or to strive for 1.5 degrees Celsius – is a major driver of renewable energy proliferation efforts (Shah Danish *et al.*, 2019). Given the fact that energy use accounts for around two-thirds of total greenhouse gas emissions with the power generation sector recognised as a major contributor, decarbonisation of the energy sector, including the power

sector, using renewables is at the forefront of efforts. While the share of renewable in the global power generation mix is around 29%, it is projected to increase to approximately 60% by 2030 (Papageorgiou *et al.*, 2020).

2.5.2. Energy security

Particularly relevant to the provisioning of clean and affordable energy to remote and less economically developed communities is energy security, given the fact that most remote communities currently rely on diesel as the primary energy source. In addition to the negative climate impact, the use of diesel in remote areas has important negative energy security implications. In this setting, the use of local renewable energy systems that use well-diversified technologies has been shown in the literature to be able to increase energy security in remote, off-grid applications, whilst additionally reducing the associated energy costs (Verbruggen *et al.*, 2010).

2.5.3. Energy access

While global access to electricity has been steadily increasing over the past few decades, 940 million people (13% of the world) still do not have access to electricity. In the pre-MG era, this was mainly attributed to the cost-inefficiency of extending a power line to the electricity grid. However, the emergence of advanced, smart MGs, accompanied by unprecedented improvements in the cost-effectiveness and efficiency of renewable and storage technologies, has provided an effective platform to accelerate the progress in electrifying remote and low-income communities (Shieh, Ersal and Peng, 2019). Also, the integration of advanced water purification, filtration, and treatment systems, as well as water desalination systems, into the stand-alone MGs tailored to communities that do not have access to safe driving water has provided them with effective clean water solutions in several instances (Okedu, Salmani and Waleed, 2019).

2.5.4. Socio-economic growth

The human development index and per capita income have been shown to be directly correlated with per capita energy use (Steffen, 2020). That is, measuring the amount of electricity usage of a community is an important social and economic indicator, with direct implications for health, education, and the wider welfare of people (Dalton *et al.*, 2015), (Pahle, Pachauri and Steinbacher, 2016), (Karytsas and Theodoropoulou, 2014). In this context, off-grid, integrated, smart energy systems that produce electricity locally using RESs are found to be an effective tool for sustainable rural development with their potential to deliver multi-faceted socio-economic benefits, including net job creation and greater social inclusiveness (IRENA, 2017).

2.6. MG capacity planning optimisation

Determining the optimal combination of the size of the components integrated into MGs, such as solar PV panels, WTs, micro-hydro power plants, battery storage systems (BSSs), and hydrogen-based energy storage systems to name a few, requires evaluating the operational performance of the candidate combinatorics in an intelligent (optimisation-based) manner for reasons of computational tractability (Jin *et al*., 2021). It is also noteworthy that MG design and operation are inter-connected problems, as the operational strategy affects the equipment capacity required, while the capacity of the system can limit the optimal operation

exercise. Uncertainties in forecast data additionally influence the operation of the system and their impact propagates upward to the optimal sizing problem (Gamarra and Guerrero, 2015). In addition to the aleatory sources of uncertainty, the MG capacity planning optimisation problem and the associated decision-making processes are subject to various epistemic uncertainties, which arise from the lack of knowledge about future scenarios that cannot be modelled probabilistically (Billinton and Huang, 2008).

In this context, both analytical solutions and meta-heuristic-based algorithms have been employed in the literature to yield the optimum MG designs subject to a set of technical and economic constraints in the operational and planning levels. The following sections classify the wider MG sizing approaches and critically review the most vigorous approaches to MG design and investment planning optimisation in the relevant reviewed literature.

2.6.1. Classification of MG sizing approaches

As mentioned above, all the MG sizing approaches involve evaluating various designs by determining the operational performance of the system at discrete time-steps over some time period, which makes them computationally complex. The classic approach to MG sizing is using exact mathematical programming techniques, such as linear programming, mixed-integer linear programming (MILP), mixed-integer nonlinear programming (MINLP), and dynamic programming. While these techniques are relatively fast, they suffer from a lack of accuracy due to the necessity of making several decompositions and mean-field approximations for application to the non-deterministic polynomial time-hard (NP-hard) MG sizing problem with integrated nonlinear and non-convex objective functions, as well as planning- and dispatch-level constraints (Baños *et al.*, 2011). A growing body of literature has also formulated multi-objective models for the strategic, long-term MG capacity planning optimisation in the presence of multiple criteria. This strand of the literature has considered the optimisation of reliability, greenhouse gas emissions, curtailed energy, self-sufficiency, and resilience objectives simultaneously to the total discounted cost of the system, rather than considering them as constraints to the classic single-objective, least-cost-oriented MG sizing practice. The overarching goal of multi-objective energy planning optimisation is to make effective decisions in the presence of trade-offs between a number of competing objectives. The mainstream exact mathematical optimisation-based approach in the literature for multi-criteria MG planning optimisation is found to be the ε-constraint method. The ε-constraint method is essentially an algorithm transformation method, the main advantage of which is that it enables controlling the density of the representation of each objective by assigning a set of equidistant grid points to other objectives and treating them as constraints. However, breaking down a multi-objective problem into several single-objective problems and solving them for various input settings is a computationally costly method for large-scale problems. That is, the main disadvantage of the ε-constraint method is that it fails to generate a set of non-dominated solutions in a single run (Mavrotas, 2009), (Puchinger and Raidl, 2006).

To address the computational intensiveness of closed-form solution algorithms in inherently NP-hard MG sizing applications, a recent, growing body of literature has focused on the utilisation of meta-heuristic-based solution approaches to the MG capacity planning optimisation problem. The main advantage of meta-heuristics is that they can be readily applied to the relevant full models, whereas they are principally limited by the so-called “no free lunch” theorem, which postulates that no single meta-heuristic is universally the best-performing algorithm for all algorithms. This necessitates comprehensive, multi-test-case-oriented efficiency testing of meta-heuristics, especially given the rapid advancements in this

highly active field (Gamarra and Guerrero, 2015), (Mohseni, Brent, Burmester, *et al.*, 2021). In view of the approximate nature of meta-heuristics, they involve iterative, nature-inspired master processes to guide and modify the operation of the underlying heuristics (low- or high-level procedures) to effectively yield high-quality solutions (Fouskakis and Draper, 2002). In single-objective, least-cost-based MG sizing applications, this entails the evaluation of the fitness of each search agent/particle/individual of the meta-heuristics at each iteration by evaluating the associated operational performance of the candidate solution set. The solution set consists of the size of components as decision variables and the associated total discounted cost of the system. The iterative process of searching for the cost-minimal solution then continues until reaching the stopping criterion, which is commonly a maximum number of iterations. Additionally, multi-objective variants of meta-heuristics have been found to be particularly effective in solving multi-criteria MG design optimisation problems compared to analytical methods. A review of the relevant literature also finds that the multi-objective evolutionary algorithms employed in MG sizing applications can be broadly classified into Pareto-based and non-Pareto-based classes. The Pareto-based algorithms have been found to be more popular in the literature given their potential to generate useful insights on the best-compromise solutions.

Moreover, in terms of the subordinate heuristics employed, meta-heuristics can be generally categorised into the following two classes:

Trajectory meta-heuristics: Trajectory meta-heuristics typically use a single agent at a time to trace out a path over the course of iterations. The commonly used meta-heuristics in this category include the simulated annealing (SA), the tabu search (TS), the greedy random adaptive search procedures (GRASP), the evolutionary strategy (ES), and the iterated local search (ILS) (Gamarra and Guerrero, 2015).

Population-based meta-heuristics: Population-based meta-heuristics use multiple search agents, which interact with each other and trace multiple paths as the iterations continue. The most commonly used meta-heuristics in this category include the genetic algorithm (GA) and the particle swarm optimisation (PSO) (Gamarra and Guerrero, 2015).

Furthermore, various hybridisations of meta-heuristics have been proposed and employed in the MG capacity planning literature. The main idea behind the hybridisation of different meta-heuristics is to exploit the advantage of one meta-heuristic for addressing the limitation of another, leading to a rich and fruitful ground for the cross-fertilisation of different ideas of meta-heuristic optimisation. In addition, the meta-heuristic hybridisation efforts can be mainly classified into sequential and parallel efforts, with the parallel algorithms benefitting from faster running times (Blum *et al.*, 2011).

Moreover, the non-Pareto-based, multi-objective meta-heuristics, alternatively referred to as single objective-based multi-objective meta-heuristics, commonly employ the weighted sum method to combine all multi-objective functions into one scalar, composite objective function. This class of algorithms has the advantage of determining a single unique solution for actual implementation. However, it fails to provide decision-making support for the identification of a preferred solution from the set of Pareto-optimal solutions, as opposed to the provision of a set of alternatives. The approach is commonly considered to be subjective given that it involves the direct allocation of the weights by decision-makers (Vergara *et al*., 2015). On the other hand, Pareto-based multi-objective optimisation algorithms provide the non-dominated set of the entire feasible decision space. To illustrate, where one solution

dominates the other, it means that it is strictly better than the other solution in at least one objective, but no worse than it in all objectives. Given a set of multi-criteria solutions, the non-dominated solution set is defined as a set of all the solutions which are not dominated by any member of the solution set. The set of non-dominated solutions in the feasible decision space is called the Pareto-optimal set. Also, the boundary represented by the set of all points mapped from the Pareto-optimal solutions is referred to as the Pareto-optimal front (Deb, 2001), (Baños *et al.*, 2011).

It is noteworthy that two major components of all meta-heuristics, which generate an initial random population of solutions and evolve them towards the global optimality, are intensification and diversification, alternatively referred to as exploitation and exploration, respectively. The exploitation phase is responsible for effective long-range jumps around the global search space, while the exploitation phase seeks to perform efficient local search near the global optima. An optimal trade-off between these two components is necessary to ensure global optimality (Blum and Roli, 2003).

In addition, the existing MG techno-economic analysis software tools in the industry and academia can be broadly classified into two categories. The first category adopts a full-factorial approach to the MG sizing problem; the noteworthy tools in this class are the original HOMER and RETScreen software packages, the main limitation of which is the so-called 'combinatorial explosion' when considering a large number of candidate technologies or increasing the fidelity of the decision space. The second class of MG techno-economic feasibility assessment tools use simplified exact mathematical optimisation algorithms. The most popular software packages in this category are HOMER Pro, Hybrid2, iHOGA, REopt, and DER-CAM. Expectedly, these software packages suffer from the same limitations of the aforementioned analytical solution approaches to MG planning (Mendes *et al.*, 2011).

2.6.2. Major trends in meta-heuristic-based MG sizing approaches

The literature review indicates a number of major trends in meta-heuristic-based MG sizing. Notably, the particle swarm opposition (PSO) (Kennedy and Eberhart, 2005) and the genetic algorithm (GA) (Jong, 1988), as well as their multi-objective variants, have been found to be the dominant meta-heuristics used in the literature. For instance, Nikmehr and Ravadanegh (2015) have proposed a PSO-based solution algorithm for the optimal sizing of grid-connected MGs, which is aware of the optimal power exchange decisions between the MG and the main utility grid. The PSO has also been employed by Samy and Barakat (2019) for the optimal sizing of a MG considering solar PV and biomass generation resources and its performance is benchmarked against the invasive weed optimisation (IWO) considering the total net present cost (TNPC) as the main objective subject to limitations on the maximum allowable total excess energy fraction and the loss of power supply probability (LPSP).

A PSO-based MG sizing solution algorithm has also been proposed for both grid-connected and islanded solar PV/wind MGs in (Razmi and Doagou-Mojarrad, 2019), which has been shown to generate statistically robust and valid results to the MG capacity planning problem. In another instance, Karuppasamypandiyan *et al.* (2019) have used the non-dominated sorting genetic algorithm-II (NSGA-II) to simultaneously optimise the cost and greenhouse gas emissions of a MG integrating WTs, solar PV panels, and fuel cells in conjunction with a diesel generator. Mosbah *et al.* (2017) have also proposed a solution approach for the simultaneous optimisation of the cost and voltage stability of grid-connected MGs using the NSGA-II algorithm. In addition, in a comprehensive, multi-case-oriented study, Hlal *et al.*

(2019) have shown that the NSGA-II algorithm yields more statistically robust solutions in MG planning applications incorporating several conflicting objectives compared to the multi-objective PSO, though at the cost of increased computational complexity.

Also, more recently, the moth-flame optimisation algorithm (MFOA) (Mirjalili, 2015), which is inspired by the navigation mechanism of moths at nights (referred to as transverse orientation), has shown to be an efficient algorithm in MG sizing applications in several studies. For example, (Mohseni *et al.*, 2021) have shown that the MFOA-optimised MG sizing solution outperforms those of the GA, the PSO, the hybrid GA-PSO, the harmony search algorithm, the simulated annealing algorithm, the artificial bee colony algorithm, the ant colony optimiser, and the ant lion optimiser.

The literature review also indicates that hybrid meta-heuristics have gained significant attention in recent years (Altbawi *et al*., 2021). For example, Suresh and Ganesh (2019) have shown the higher efficiency of a hybrid MFOA-bat search algorithm (BSA) for capacity planning of MGs integrating solar PV, WTs, fuel cells, and battery storage resources, compared to the MFOA and the BSA alone. Another novelty of their research is the consideration of both active power and reactive power during the design phase of MGs, which is shown to be important for improved quality of the power supply.

A growing body of the literature has also explored the optimal integration of electric vehicles (EVs) into MGs, which has important implications for the dispatch of the system (Monfared *et al.*, 2019). For example, Rasouli *et al.* (2019) have presented a MILP approach for the optimal system integration of EVs into systems that are mainly driven by solar PV and micro-turbine resources. They have additionally quantified the uncertainties in forecasts of EV-charging loads, electricity market prices, residential loads, as well as the power outputs from solar PV and micro-turbine technologies. A similar MILP-based modelling approach for the optimal integration of EVs has been employed by Lekvan *et al.* (2021) for application to systems integrating wind resources, boilers, combined heat and power units, storage technologies, as well as responsive loads. They have also characterised the uncertainties in wind speed and load demand. Furthermore, a fundamentally different modelling framework based on the simulated annealing (SA) algorithm, has been formulated by Yi *et al.* (2020) for the integration of EV-charging loads, in conjunction with solar PV and wind resources, whilst additionally factoring the optimal power exchange schedules with the wider utility grid into the analyses.

2.6.3. Potential of state-of-the-art meta-heuristics

As the above overview of the MG planning literature has shown, meta-heuristic algorithms are playing an increasingly important role in the optimal planning and designing of renewable and sustainable energy systems. Fig. 6 shows a summary of the percentage contribution of different sources of inspiration for the meta-heuristics in the literature (Dragoi and Dafinescu, 2021).

The review has also identified model-order reduction as an effective tool for handling the inherent computational expensiveness of meta-heuristics. For instance, Cagnano *et al.* (2018) have used a reduced model of voltage control profile, while optimising the size of the components of the network. Similarly, Chaspierre *et al.* (2017) have presented a reduced-order model to simplify the distribution network under planning. Ramli *et al.* (2018) have also considered a lower-than-standard resolution for wind speed, solar irradiance, ambient

temperature, and load data, while optimising a MG integrating solar PV, WT, and diesel generator technologies. Similarly, Augustine *et al.* (2012) have used representative days to reduce the computational expensiveness of optimising the total planning cost of a MG.

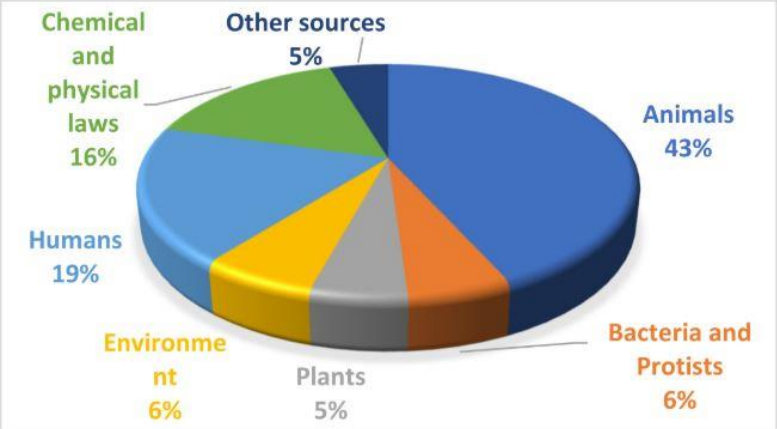

Figure 6. Distribution of inspiration sources of meta-heuristics in the literature (Dragoi and Dafinescu, 2021).

There also exists a growing body of evidence in the literature lending support to the argument that newly advanced (state-of-the-art) meta-heuristics have the potential to improve the optimality (quality) of energy optimisation solutions, including MG sizing solutions, compared to the well-established algorithms. For instance, Ramadan *et al.* (2021) have shown that the wild horse optimiser (WHO), which is a biology-based algorithm inspired by the social life behaviour of wild horses – dominating, grazing, leading, chasing, and mating – performs better than the evolutionary algorithm (EO) and the gradient-based optimiser (GBO) in modelling the nonlinearity of solar PV panels. In another instance, Abdollahzadeh *et al.* (2021) have shown the outperformance of the artificial gorilla troops optimiser (AGTO) to the well-established meta-heuristics in modelling the frequency response in energy systems integrating solar PV panels, WTs, diesel generators, and battery storage devices. They have also verified the statistical robustness and validity of their findings by repeating the simulations for a variety of battery storage technologies. Furthermore, Alharthi *et al.* (2021) have shown that a multi-objective variant of the marine predator algorithm (MPA) has a superior efficiency to the well-established multi-objective meta-heuristics in optimal dispatching applications of energy systems where several conflicting objectives – energy losses, total cost, carbon dioxide emissions, and fuel costs – are considered concurrently. Wadood *et al.* (2021) have additionally shown the effectiveness of the MPA compared to conventional meta-heuristics in minimising the total operational time of relays, which has salient implications for the reduction of interference and failure of MG systems. In another instance, Ahmed *et al.* (2021) have demonstrated the superior effectiveness of the equilibrium optimiser, first introduced by Faramarzi *et al.* (2020), in multi-objective MG energy management problems where cost minimisation, as well as the maximisation of voltage profile and system stability, are simultaneously factored into the associated analyses.

2.7. Conclusions

This chapter has reviewed the wider literature on the optimal capacity planning of grid-connected and stand-alone MGs. To this end, a literature review methodology has been devised to identify and select the eligible studies for review. The review of the relevant

literature has then laid the foundation for the identification of the main factors that affect the economics and configurations of different configurations of MGs. This, consequently, has allowed for illustrating the pathways of and the associated barriers to the energy transition towards renewable energy resources from conventional energy generation. A thematic characterisation of the literature, furthermore, has highlighted the salient innovative ideas proposed in the literature to surmount the identified barriers, including the use of advanced computational planning models and novel MG configurations. Accordingly, this chapter has paved the way for positioning the novel contributions of this study, presented in the following chapter, within the identified gaps in knowledge.

Chapter 3: Meta-heuristic-based modelling framework

3.1. Introduction

This chapter addresses Research Objective 2, which seeks to develop a general meta-heuristic-based modelling framework to yield the optimal configuration and sizing of micro-grids (MGs). To this end, it first presents the mathematical modelling of the components of three conceptual test-case MG systems. It then proceeds to illustrate the rule-based dispatch strategy developed to decide the operational schedules of the systems. Subsequently, the developed test-case systems with pre-defined dispatch strategies are employed to parametrise the proposed modelling framework. They additionally serve to verify the effectiveness of the proposed MG sizing model, which uses the forecasts of solar irradiance, wind speed, and power load demand data as inputs.

Collectively, the components of the proposed MGs are solar photovoltaic (PV) panels, wind turbines (WTs), battery storage systems (BSSs), and various power converters. More specifically, MG 1 is driven by wind and solar PV resources, whereas MGs 2 and 3 are assumed to be solely driven by solar PV power. The employed power conversion apparatuses can be classified as DC/AC inverters, AC/DC converters, and DC/DC converters. The project lifetime is considered to be 25 years, in accordance with the lifetime of the most durable component, namely solar PV panels. The following sections present the mathematical modelling of the test-case MG systems and their energy management strategies, as well as the overall meta-heuristic-based MG sizing framework parametrised for the test cases, which entails MG life-cycle cost minimisation subject to a set of operational- and planning-level constraints, notably reliability.

3.2. Micro-grid 1

The schematic diagram of the first stand-alone MG system is depicted in Fig. 7. It uses solar PV and WT technologies for power generation, which are supported by a BSS. A dump load is also considered to be able to maintain the balance of power supply and demand when total non-dispatchable generation outstrips total loads. Furthermore, the optimal size of all power conditioning devices that lie between the generation/storage components and the DC bus is assumed to be equal to the optimal size of the devices they couple to the common DC bus. Moreover, as it can be seen from the figure, the total load on the system can be broken down into residential, commercial, and electric vehicle (EV)-charging loads. Accordingly, the optimal capacities of the residential and commercial loads' inverter, as well as the EV-charging loads' inverter, are controlled by the relevant peak demands. The following sections mathematically model the components of MG 1 and define the operational strategy of the network.

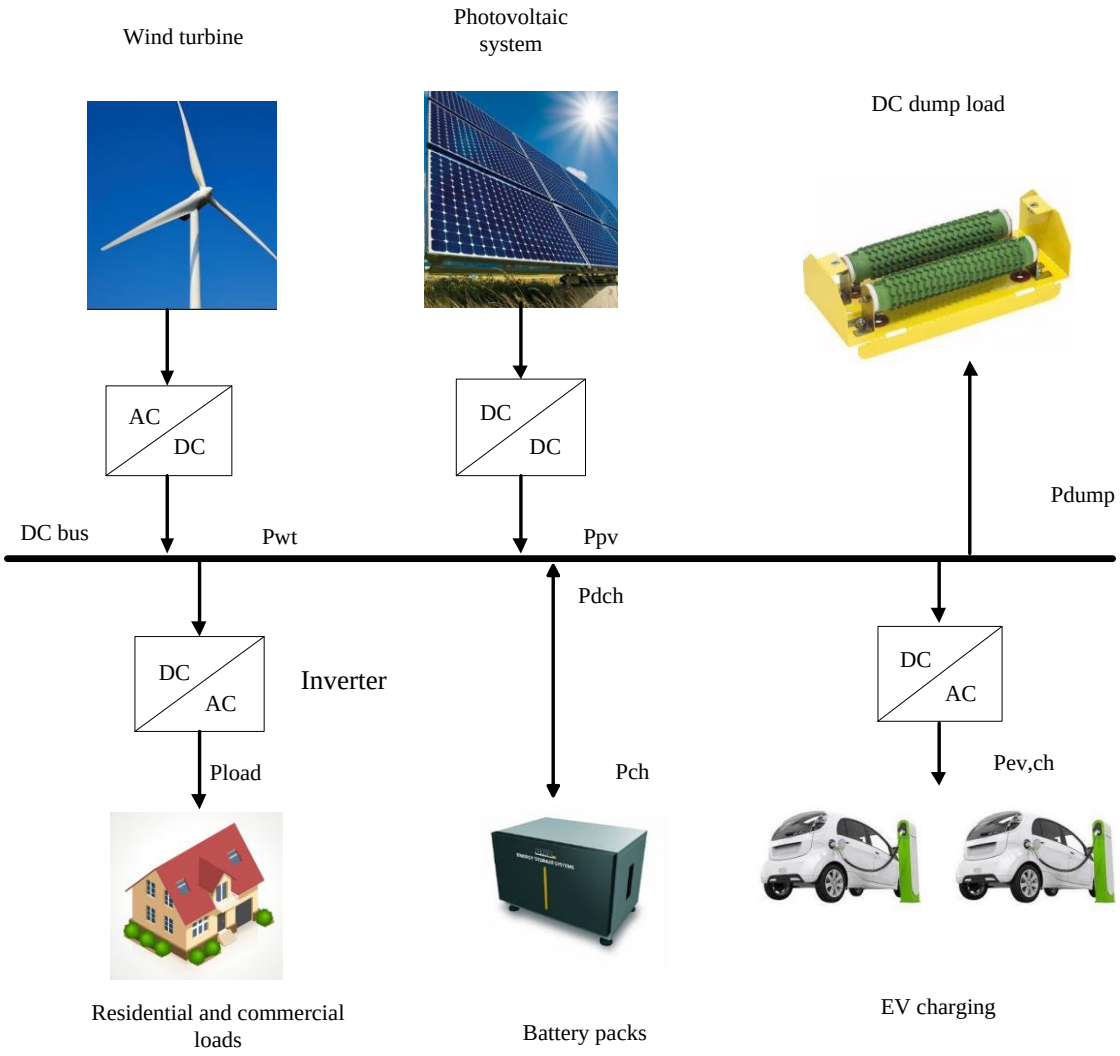

Figure 7. Schematic diagram and energy flow of MG 1.

3.2.1. Wind turbines

The 3-blade Senwei SWT-50 kW wind turbine is selected, which has a rated power of 50 kW AC with a hub altitude of 34 m. The characteristic curve of the WT is shown in Fig. 8. The wind speed data, measured at the height of h_{ref}, is normalised to the hub height h using the following equation (Ramli *et al.*, 2018):

$$V_h = V_{ref} \times (h/h_{ref})^r, \quad (1)$$

where V_{ref} is the reference wind speed recorded at the height of h_{ref}, r is an exponent in the range [0.1, 0.25], which reflects the characteristics of the terrain. Given the non-flat, tree-covered land characteristics of the site, r is considered to be 0.2 in this study.

Stewart and Essenwanger, (1978) have derived the power output from WTs as a more flexible version of the general Weibull distribution of WT power output, which can be expressed as:

$$P_{WT}(t) = N_{WT} \times \begin{cases} 0; & if\ v < v_{cin}\ or\ v > v_{Cout} \\ P_{rated} \times \left(\frac{v(t)^3 - v_{Cin}^3}{v_{rated}^3 - v_{Cin}^3}\right); & if\ v_{cin} \leq v < v_{rated} \\ P_{rated}; & if\ v_{rated} \leq v \leq v_{Cout} \end{cases} \quad (2)$$

where P_{WT}, P_{rated}, $v(t)$, v_{Cin}, and v_{Cout} respectively denote the power output from the WT (kW), the turbine's rated power (kW), normalised wind speed (m/s) at time-step t, as well as the associated cut-in and cut-out wind speeds (kW). Also, N_{WT} is the optimum number of WTs, which is determined at each iteration of the optimal sizing process as a decision variable.

The selected turbine has a lifetime of 20 years. Also, the rated, cut-in, and cut-out wind speeds of the turbine are 9.5 m/s, 3.5 m/s, and 20 m/s, respectively. Furthermore, the capital investment and replacement costs of the WT are $65,000/unit, while its O&M cost is $2,600/unit/year.

It should be noted that all costs are cited in the 2021 New Zealand dollars throughout this study.

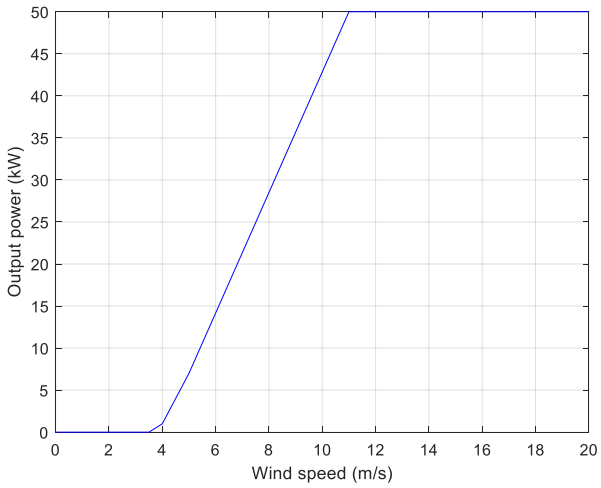

Figure 8. Characteristic curve of the SWT-50kW wind turbine.

(Senwei Model SWT-50kW - Variable Pitch Wind Turbine, 2021).

3.2.2. Photovoltaic panels

In this study, the Half Cut PERC Mono Photovoltaic solar panel is considered. The panel has a rated capacity of 330 W with an expected lifetime of 25 years. Eq. (3) can be used to calculate the aggregate power output from the solar generation system at time-step t:

$$P_{PV}(t) = N_{PV} \times DF \times G_t(t)/1000, \quad (3)$$

where N_{PV} is the optimum number of solar panels, which is updated at each iteration of the sizing process, and $G_t(t)$ is the global solar irradiance (W/m^2) at time-step t. It should also be noted that the power output from the solar panels decreases over time due to degradation – induced by wiring losses, frame corrosion, high temperatures, dust layer, and so forth.

Therefore, a calendar-induced degradation factor (DF) of 85% is taken into account for the solar PV generation system (Mohseni *et al.*, 2019). Also, a tilt angle of 36˚ was considered for the PV panels.

Furthermore, the associated capital investment and replacement costs of the panels are $335/unit, while their O&M costs are considered to be $6/unit/year. Moreover, the lifetime of solar panels is 25 years; hence, no replacement occurs over the project lifespan.

3.2.3. Battery storage system

The 14-kWh Tesla Powerwall battery pack is considered in this study, which has a lifetime of 10 years. Also, the associated capital investment and replacement costs are $390/unit, while the O&M cost is $2/unit/year.

Furthermore, the following equality constraint is used to ensure that the battery bank's state of charge (SOC) at each time-step t is aware of the underlying charging and discharging processes (Chen *et al.*, 2012):

$$E_b(t) = E_b(t-1) + (P_{ch}(t) \times \eta_{ch}) \times \Delta t - (P_{dch}(t)/\eta_{dch}) \times \Delta t, \quad (4)$$

where P_{ch} is the battery bank's charging power, P_{dch} is the battery bank's discharging power, while η_{ch} and η_{dch} are the charging and discharging efficiencies of the battery packs, respectively, both of which are assumed to be 95% in this study.

Moreover, the energy content of the overall BSS is subject to the following constraint, in line with physical, real-world conditions (Chen *et al.*, 2012):

$$E_b^{min} \leq E_b(t) \leq E_b^{max}, \quad (5)$$

where E_b^{min} and E_b^{max} are the minimum and maximum allowable energy contents of the BSS. More specifically, E_b^{max} is controlled by the optimal capacity of the battery bank, while E_b^{min} is controlled by the maximum depth of discharge (DOD) of the battery packs, which is mathematically expressed in Eq. (6) (Kwon *et al.*, 2006). Also, the maximum DOD is set to 90%.

$$E_b^{min} = \frac{100-DOD}{100} \times E_b^{max}.$$

3.2.4. EV-charging station

An electric vehicle (EV) charging station was also considered to serve the EV-charging loads. For the site under consideration, 10 medium-sized plug-in personal passenger EVs and 5 medium-sized plug-in utility EVs were planned for integration into the conceptual MG. To this end, 7.6-kW SOLAREDGE SE7600H-US EV-chargers with an accompanying single-phase DC/AC inverter was considered, which has an overall efficiency of 99%. The lifetime of the overall EV-charging unit is 20 years. The associated capital and replacement costs of the EV-charging unit including the DC/AC inverter costs are $4,000/unit, while the O&M cost of the station is $160/unit/year.

It is noteworthy that the optimal size of the EV-charging station is not treated as a separate decision variable, but rather it is determined based upon the peak EV-charging load following

the specifically developed dispatch strategy. Accordingly, the cost of the station is exogenously added to the optimal whole-life cost of the system.

3.2.5. Power conversion apparatuses

The following converters are considered in this study:

1. The Red Prime AC/DC converter is used for the integration of 50-kW WTs. The converter's efficiency and lifetime are 98% and 15 years, respectively;

2. The SAMLEX IDC-360A-24 DC/DC converter is used to couple the 360-W solar PV panels to the common DC bus. The converter has an efficiency of 85%, and a lifetime of 15 years; and

3. The Eaton DG1 IP21 DC/AC inverter is utilised to supply the AC residential and commercial loads from the DC bus. The rated capacity, efficiency, and lifetime of the selected inverter are 50 kW, 96%, and 20 years, respectively. Similar to other converters in the system, it does not form part of the decision variable vector, and is calculated outside the model based upon the expected total residential and commercial loads. (Mohseni *et al.*, 2021).

Table 3 presents a summary of techno-economic specifications of the selected components in the candidate pool for MG 1. It is noteworthy that all costs are cited in 2021 New Zealand Dollars.

Table 3. Techno-economic specifications of the candidate components of MG 1.

Component	Manufacturer part number	Capital cost	Replacement cost	Operation and maintenance cost	Lifetime (years)
Wind turbine	Senwei SWT	$65,000/unit	$65,000/unit	$2,600/unit/year	20
Solar PV panel	Half Cut PERC	$335/unit	$335/unit	$6/unit/year	25
Battery	POWERWALL	$390/unit	$390/unit	$2/unit/year	10
AC/DC inverter	Red Prime	$4,770/unit	$4,770/unit	$382/unit/year	15
DC/DC inverter	SAMLEX IDC	$50/unit	$50/unit	$0.04/unit/year	15
Inverter	Eaton DG IP21	$8,000/unit	$8,000/unit	$320/unit/year	20
EV-charger	SOLAREDGE	$4,000/unit	$4,000/unit	$160/unit/year	20

3.3. Energy management of MG 1

A rule-based energy management strategy is specifically developed to ensure that generation always satisfies demand. To this end, the battery storage linking variables are used. Three main dispatch strategies tailored to different scenarios are considered for the operation of MG 1, which are detailed in the following sections.

3.3.1. Generation meets total demand

In this scenario, the total power output from renewable generation technologies is equal to the sum of residential, commercial, and EV-charging loads, which can be mathematically modelled as:

$$P_{PV}(t) + P_{WT}(t) = P_{load}(t)/\eta_{inv} + P_{EV}(t)/\eta_{EV}, \quad (7)$$

$$E_b(t + \Delta t) = E_b(t), \quad (8)$$

$$P_{EV,del}(t) = P_{EV}(t), \quad (9)$$

where P_{load} is the total residential and commercial load on the system at time-step t, P_{EV} and $P_{EV,del}$ are the expected EV-charging load and the actual power delivered to EVs at time-step t, respectively, while η_{inv} and η_{EV} respectively denote the efficiencies of the residential/commercial loads' inverter and EV chargers.

3.3.2. Excess generation

In this scenario, it is assumed that the aggregate power output from renewable energy generation technologies is greater than the total load demand (including the EV-charging loads). Accordingly, the excess energy generation is stored in the BSS. The operational strategy of the system can be mathematically modelled as:

$$P_{ch}(t) = P_{PV}(t) + P_{WT}(t) - (P_{load}(t)/\eta_{inv}) - (P_{EV}(t)/\eta_{EV}\ ), \quad (10)$$

$$E_b(t + \Delta t) = E_b(t - 1) + P_{ch}(t) \times \eta_{ch} \times \Delta t, \quad (11)$$

$$P_{EV,del}(t) = P_{EV}(t). \quad (12)$$

3.3.3. Excess residential and commercial loads

In this scenario, the total residential/commercial load demand is greater than the total power output from renewable energy generation technologies. Therefore, the battery bank is discharged to meet the residential and commercial loads as far as possible. However, for reasons of energy efficiency, the EV-charging load is not served by discharging the stationary battery bank, which leads to the loss of total EV-charging loads, in addition to potentially part of the residential and commercial loads. This scenario can be mathematically modelled as:

$$P_{dch}(t) = (P_{load}(t)/\eta_{inv}) - P_{PV}(t) - P_{WT}(t), \quad (13)$$

$$E_b(t + \Delta t) = E_b(t - 1)\ - (P_{dch}(t)/\eta_{dch}) \times \Delta t, \quad (14)$$

$$P_{EV,del}(t) = 0, \tag{15}$$

$$Q_{EV}(t) = P_{EV}(t). \tag{16}$$

Where residential and commercial load shedding is necessary to maintain the power balance of the system, the associated lost load can be obtained from the following equation:

$$Q_{load}(t) = P_{load}(t) - \left(P_{PV}(t) + P_{WT}(t) + \left(\frac{E_b(t) - E_b^{min}}{\Delta t}\right) \times \eta_{dch}\right) \times \eta_{inv}. \tag{17}$$

More specifically, the onsite storage is used to its maximum capacity to meet the residential and commercial loads. Yet, despite doing so, there exists unserved demand, apart from unsupplied EV-charging loads.

3.4. Micro-grids 2 and 3

The second and third BSS-supported MGs are expected to generate electricity solely by solar PV panels, in accordance with Fig. 9. Also, the mathematical models of the associated components – solar PV panels, the battery bank, the EV-charging station, and system-wide converters – are the same as those presented for MG 1. Note that MGs 2 and 3 are indeed the same, and the reason for the separate numbering is to minimise the potential ambiguity given the presentation of three case studies in the next chapter.

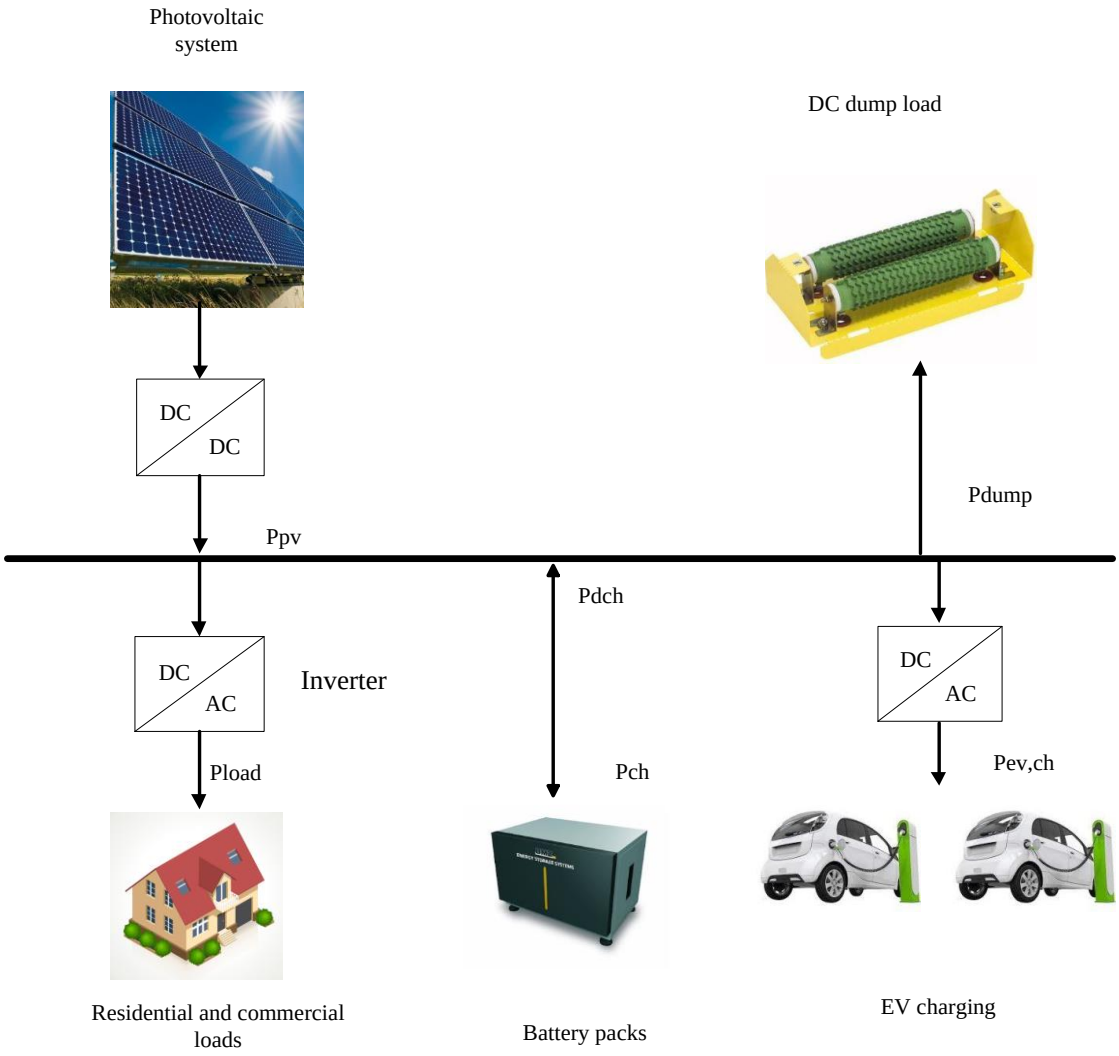

Figure 9. Schematic diagram and energy flow of MGs 2 and 3.

3.5. Energy management of MGs 2 and 3

Similar to MG 1, a rule-based, cycle-charging energy management strategy was formulated for MGs 2 and 3, which seeks to balance generation and demand with the aid of the BSS, given the variability inherent in the power output of the solar PV plant. Accordingly, the following three main energy dispatch scenarios were considered for the operation of MGs 2 and 3.

3.5.1. Generation meets total demand

In this scenario, the total power output from the solar PV generation system is equal to the sum of residential, commercial, and EV-charging loads; hence:

$$P_{PV}(t) = (P_{load}(t)/\eta_{inv} + P_{EV}(t)/\eta_{EV}), \quad (18)$$

$$E_b(t + \Delta t) = E_b(t), \quad (19)$$

$$P_{EV,del}(t) = P_{EV}(t), \quad (20)$$

where P_{load} represents the total residential and commercial loads at time-step t, P_{EV} and $P_{EV,del}$ are the expected EV-charging load and actual power delivered to EVs at time-step t, respectively, while η_{inv} and η_{EV} are the efficiencies of the residential/commercial loads' inverter and EV chargers, respectively.

3.5.2. Excess generation

In this scenario, it is assumed that the total power output from the solar PV generation system is greater than the total load demand (including the EV-charging loads). Accordingly, the excess energy generation is stored in the BSS. The operational strategy in this scenario can be mathematically modelled as:

$$P_{ch}(t) = P_{PV}(t) - (P_{load}(t)/\eta_{inv}) - (P_{EV}(t)/\eta_{EV}\ ), \quad (21)$$

$$E_b(t + \Delta t) = E_b(t) + P_{ch}(t) \times \eta_{ch} \times \Delta t, \quad (22)$$

$$P_{EV,del}(t) = P_{EV}(t). \quad (23)$$

3.5.3. Excess residential and commercial loads

In this scenario, it is assumed that the total solar PV generation falls short of the total residential and commercial power load demand. Accordingly, the BSS is discharged to serve the residential and commercial loads. Similar to MG 1, the stationary battery storage is not used to charge the EVs to minimise energy conversion losses. Also, a separate equality constraint is employed to model the entirely unserved demand of EVs during the periods where the total residential and commercial loads exceed the solar PV generation. The following equations mathematically model this operating scenario:

$$P_{dch}(t) = (P_{load}(t)/\eta_{inv}) - P_{PV}(t), \quad (24)$$

$$E_b(t + \Delta t) = E_b(t)\ - (P_{dch}(t)/\eta_{dch}) \times \Delta t, \quad (25)$$

$$P_{EV,del}(t) = 0, \quad (26)$$

$$Q_{EV}(t) = P_{EV}(t). \quad (27)$$

Furthermore, the total lost residential and commercial loads, following the potential depletion of the battery storage can be obtained from the following equation:

$$Q_{load}(t) = P_{load}(t) - \left(P_{PV}(t) + \left(\frac{E_b(t) - E_b^{min}}{\Delta t}\right) \times \eta_{dch}\right) \times \eta_{inv}. \quad (28)$$

3.6. MG life-cycle cost estimation methodology

The objective of the proposed MG life-cycle cost estimation method is to minimise the whole-life cost of off-grid MGs based on net present valuations subject to a set of operation- and planning-level constraints. More specifically, the objective function consists mainly of the size of the equipment multiplied by the associated per-unit cost factors, as (Chen *et al.*, 2012):

$$NPC_c = N_c \times (C_{cc} + \text{RC} \times \text{SPPW} + (\frac{C_{o\&m}}{CRF(i,T)}) - \text{SV}), \quad (29)$$

where NPC_c is the net present cost of component c, while N_c, C_{cc}, $C_{o\&m}$, and RC represent the optimal capacity, capital cost, operation and maintenance cost, and replacement cost of the MG component c, respectively. Also, SPPW, CRF and SV respectively denote the single payment present worth, capital recovery factor, and salvage value of the corresponding component.

The salvage value can be determined as follows:

$$\text{SV} = \text{RC} \times \frac{L - (T - L \times \left[\frac{T}{L}\right])}{L}, \quad (30)$$

where L and T respectively denote the expected life-cycle of the associated component (years) and the expected life-cycle of the MG system (years), which is considered to be 25 years.

Furthermore, the SPPW represents the present value of a one-time cash outflow corresponding to a series of equal future payments, which can be modelled as:

$$\text{SPPW} = \sum_{n=1}^{Y} \frac{1}{(1+i)^{L \times n}}, \quad (31)$$

where $Y = \left[\frac{T}{L}\right]$, and i is the real interest rate, which is assumed to be 6% in this study.

Moreover, the capital recovery factor is the ratio of a constant annuity to the corresponding present value for a considered length of time, which can be calculated as follows:

$$\text{CRF}(i,\text{T}) = \frac{i(1+i)^T}{(1+i)^T - 1}. \quad (32)$$

Accordingly, the total net present costs of MGs 1 to 3 can be modelled as:

$$\text{TNPC}_{\text{MG 1}} = \text{NPC}_{\text{PV}} + \text{NPC}_{\text{WT}} + \text{NPC}_{\text{BSS}} + \text{NPCC}_{\text{CONV}} + \text{NPC}_{\text{EV-Charger}} + \textit{pen1} + \textit{pen2}, \quad (33)$$

$$TNPC_{MG\ 2,\ 3} = NPC_{PV} + NPC_{BSS} + NPC_{CONV} + NPC_{EV\text{-}Charger} + pen1 + pen2, \quad (34)$$

where NPC_{PV}, NPC_{WT}, NPC_{BSS}, NPC_{CONV}, and $NPC_{EV\text{-}Charger}$ respectively denote the net present costs of the PV panels, WTs, the BSS, the converters, and EV-chargers. Also, *pen1* and *pen2* are the penalty terms (as sufficiently large values) associated with not meeting the desired reliability levels in serving the residential/commercial and EV-charging loads, respectively. That is, they are employed to mark the positions in the search space where any of the imposed constraints are violated as infeasible equipment size combinations.

The equivalent loss factor (ELF) is used to measure the reliability of the system, which unlike other relevant reliability indicators, is aware of both the frequency and magnitude of lost loads. In the context of this study, the ELF associated with unmet residential/commercial and EV-charging loads can be expressed as:

$$ELF_{load} = \frac{1}{n}\sum_{t=1}^{n}\frac{Q_{load}(t)}{P_{load}(t)}, \quad (35)$$

$$ELF_{EV} = \frac{1}{n}\sum_{t=1}^{n}\frac{Q_{EV}(t)}{P_{EV}(t)}, \quad (36)$$

where n is the number of time-steps in the planning horizon. In this study, the ELF_{load} associated with the residential/commercial loads was assumed to be 0, while the ELF_{EV} associated with EV-charging loads was considered to be 0.005.

The minimisation of the objective function is additionally subject to a number of other constraints, as (Xu *et al.*, 2018), (Chen *et al.*, 2012):

$$P_{ch}^{min} \leq P_{ch}(t) \leq P_{ch}^{max}, \quad (37)$$

$$P_{dch}^{min} \leq P_{dch}(t) \leq P_{dch}^{max}, \quad (38)$$

$$E_b^{min} \leq E_b(t) \leq E_b^{max}, \quad (39)$$

$$E_b(1) = E_b^{max}, \quad (40)$$

$$E_b(8{,}760) \geq E_b(0). \quad (41)$$

Specifically, Eqs. (37)–(39) ensure that, at each hour of the MG operation, the charging and discharging power capacities of the storage, as well as its energy content, lie within the associated pre-defined ranges. Also, Eq. (40) assumes that the battery bank is initially full-charged to adequately handle the peaks that occur early in the time-series load data without oversizing. Furthermore, for balanced analyses, Eq. (41) ensures that the energy in-store at the last hour of the representative one-year operating horizon is not lower than the pre-specified initial battery state of charge. Recall that the operational analyses are carried out over a one-year horizon with hourly granularity.

It is also noteworthy that the decision variables (size of the solar PV panels, WTs, and the BSS) are enforced to lie within the range [0, 1000].

3.7. Overview of the proposed modelling framework

Fig. 10 displays the flowchart of the proposed modelling framework for the capacity planning optimisation of off-grid MGs, which is parameterised for the conceptualised MGs. As the figure shows, first, all input data are loaded. The meta-heuristic algorithm employed to optimise a solution to the problem at hand is then initialised before iteratively updating the position of the individuals.

At each iteration, energy balance analyses are carried out to guide the search process based on the unmet residential/commercial and EV-charging loads, as well as other violated constraints. The process of updating the optimal size of the equipment, and in turn, the estimated total net present cost of the MG is continued until reaching the stopping criterion (maximum number of iterations).

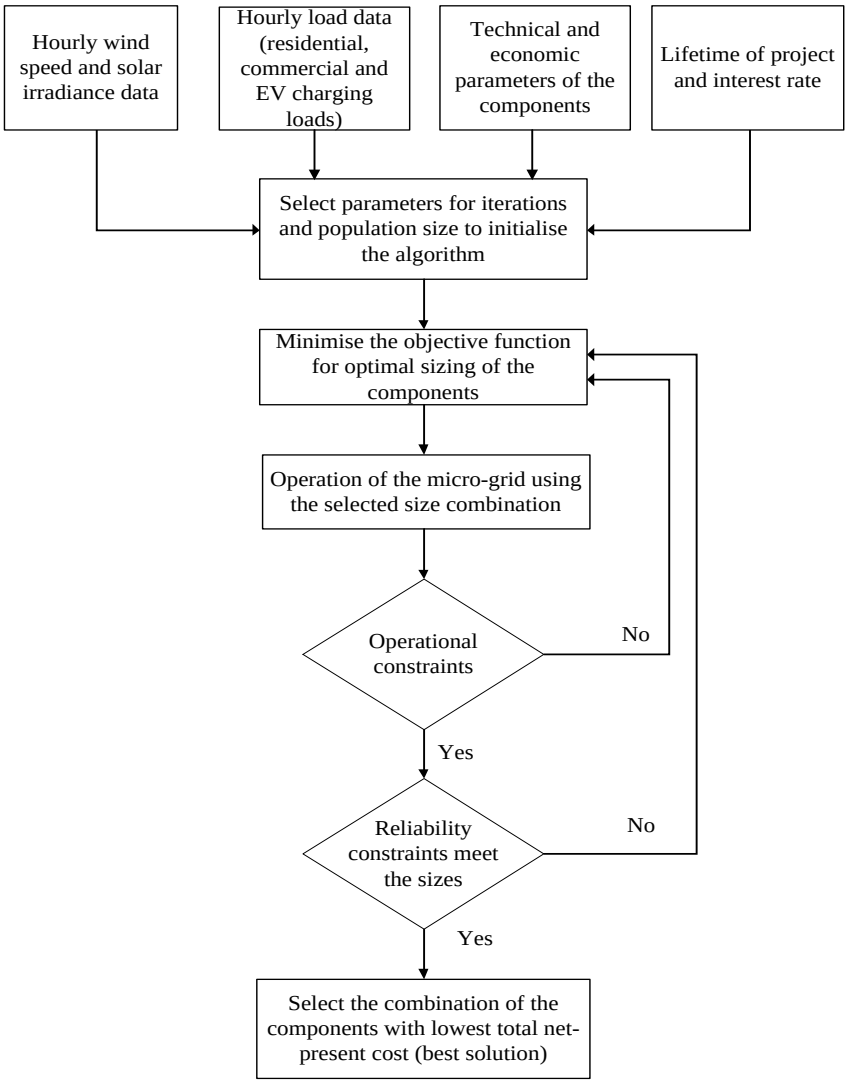

Figure 10. Flowchart of the meta-heuristic-based MG sizing modelling framework.

3.8. Conclusions

This chapter has developed the overall meta-heuristic-based off-grid MG capacity planning optimisation method, which employs net present cost valuations, the equivalent loss factor

reliability index, and a specifically developed rule-based, cycle-charging dispatch strategy in the presence of EV-charging loads. The operational planning model is novel in that (i) it minimises the probability of oversizing the components by discharging the battery storage to its maximum capacity during the periods where total residential/commercial loads fall short of total renewable power generation, and (ii) it entails distinct rules for serving residential/commercial and EV-charging loads. The proposed model has been parametrised for two stand-alone, battery-supported system topologies feeding residential/commercial and EV-charging loads. The first system is driven by a combination of solar PV panels and WTs, whereas the second system is driven by solar PV panels alone. A further salient feature of the proposed model is considering separate reliability indices for meeting residential/commercial and EV-charging loads, based on which distinct penalty factors have been formulated. Finally, the flowchart of the proposed model has been presented, which shows an in-depth overview of the general modelling framework, within which various meta-heuristic algorithms can be embedded to optimise a solution to the derived off-grid MG capacity planning problem. The techno-economic specifications of the selected components have, furthermore, been presented, which are used as input data for the application of the model to the case studies. The next chapter presents and discusses the time-series input data, including the forecast meteorological and energy consumption profiles, for the sites of interest.

Chapter 4: Case study – Aotea–Great Barrier Island

4.1. Introduction

This chapter presents the input data supplied to the proposed meta-heuristic-based MG designing model for the cases of interest within an Aotearoa–New Zealand context. First, the overall graphical and climatic conditions of the case study sites are briefly described. The chapter then proceeds to more specifically detail the meteorological and energy consumption data forecasts. To this end, the derived hourly forecasts of solar irradiance and wind speed time-series data – based on the corresponding historical data retrieved from the relevant databases – as well as the energy consumption forecasts – based on the aggregation of appliance-level loads (including residential/commercial power loads) and EV-level loads (EV-charging loads) – are presented. The profiling of meteorological and load demand data is carried out separately for the three case communities residing on Aotea–Great Barrier Island, Aotearoa–New Zealand.

4.2. Geographical and climatic background

Aotea–Great Barrier Island is situated in the outer Hauraki Gulf, 100 km north-east of central Auckland, with an area of 285 square kilometres and the following coordinates: latitude –36.26˚S and longitude 175.49˚E. It is the sixth-largest island of Aotearoa–New Zealand. According to the 2018 census, the island has a usually resident population of 936 people (Census, 2018). However, the total population of the island increases significantly over holiday periods due to tourism.

4.2.1. Climatic conditions of Aotea–Great Barrier Island

Aotea–Great Barrier Island is richly endowed with solar resources in summer, with a daily average of 11.3 hours of sunlight during the summertime according to the SolarView database of NIWA (2019). More specifically, December is the sunniest month – with 6.4 hours of sunlight per day (on average) – whereas May is associated with the least sunlight hours – with an average of 3.3 hours of sunlight per day.

In terms of wind resources, October is the windiest month, with an average maximum wind speed of approximately 34 km/h, whereas April is the weakest month in terms of wind resources, with an average minimum wind speed of around 14 km/h. The solar and wind resources exhibit significant complementary characteristics. Prior techno-economic feasibility assessments have estimated that harnessing solar and wind resources for electricity generation is able to serve the energy needs of the island's inhabitants in a reliable, affordable, self-sufficient, and sustainable manner (Park, 2021).

As mentioned above, the solar irradiance data were retrieved from the NIWA's SolarView database, while the wind speed data were collected from the Cliflo database of NIWA (2020). To this end, 15 years' worth (2007 to 2021) of hourly-basis, year-round historical solar irradiance and wind speed records (8,760 data points) were collected from the relevant databases for the three micro-communities residing on the island, namely: Medlands (MG 1), Tryphena (MG 2), and Mulberry Grove (MG 3).

4.3. Meteorological data

The meteorological data requirements of the three MGs are as follows: solar irradiance (MGs 1–3), and wind speed (MG 1). It should be recalled that MG 1 integrates both solar photovoltaic (PV) and wind turbine (WT) technologies, whereas MG 2 and MG 3 are driven solely by solar PV resources. That is, prior techno-economic feasibility and business case analyses have indicated that the WT technology is an unviable choice for MGs 2 and 3 given the associated hilly, tree-covered terrain. Therefore, unlike MG 1, the WT technology has not been considered in the candidate pool for MGs 2 and 3. Fig. 11 shows the geographical locations of the three communities considered for off-grid MG installations. In terms of geographical location, MGs 2 and 3 are about 6.3 km and 8.1 km far from MG 1, respectively.

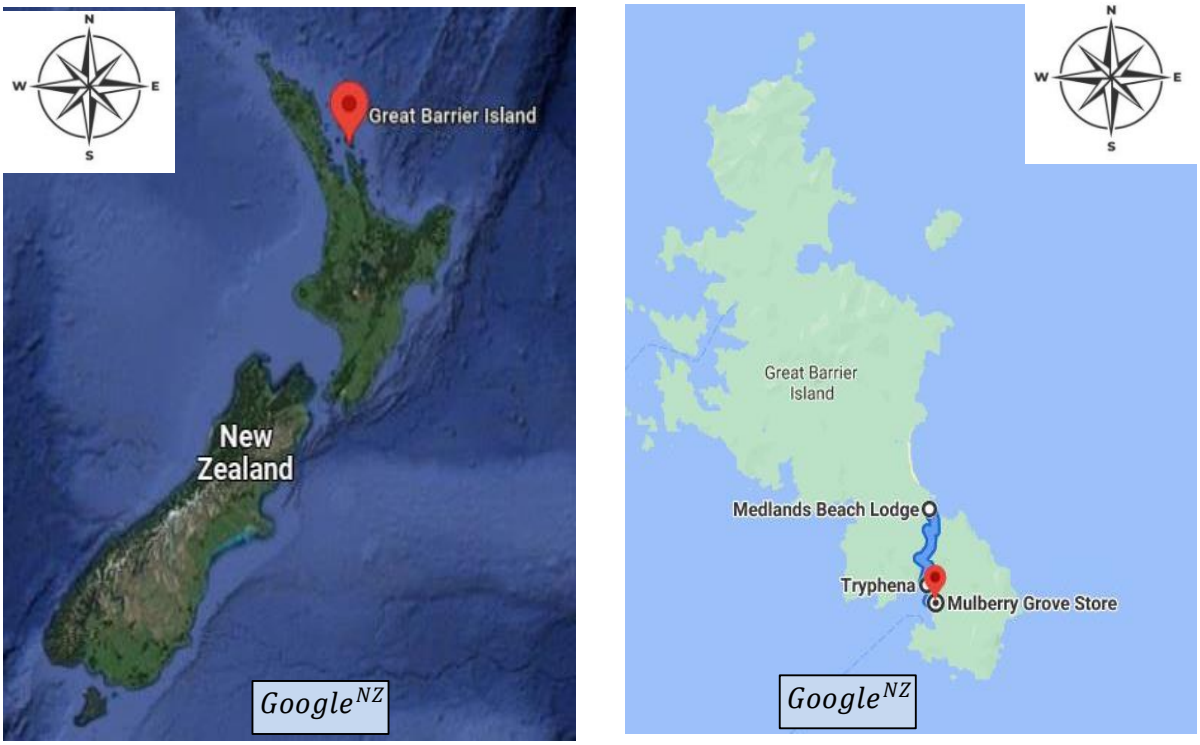

Figure 11. Locations of the conceptualised MGs for installation on Aotea–Great Barrier Island (image courtesy of Google Earth™ mapping service).

4.3.1. MG 1: Medlands

Medlands is close to the south-eastern end of Aotea–Great Barrier Island. Fig. 12 shows the corresponding monthly mean daily profiles for solar irradiance and wind speed. Note that the associated one-year time-series data were converted to monthly averaged 24-h data streams not only for reasons of better visualisation, but also for use in the reduced version of the original model in the next chapter. It is also noteworthy that the solar irradiance data were retrieved for solar PV panels with a tilt angle of 36˚.

(a)

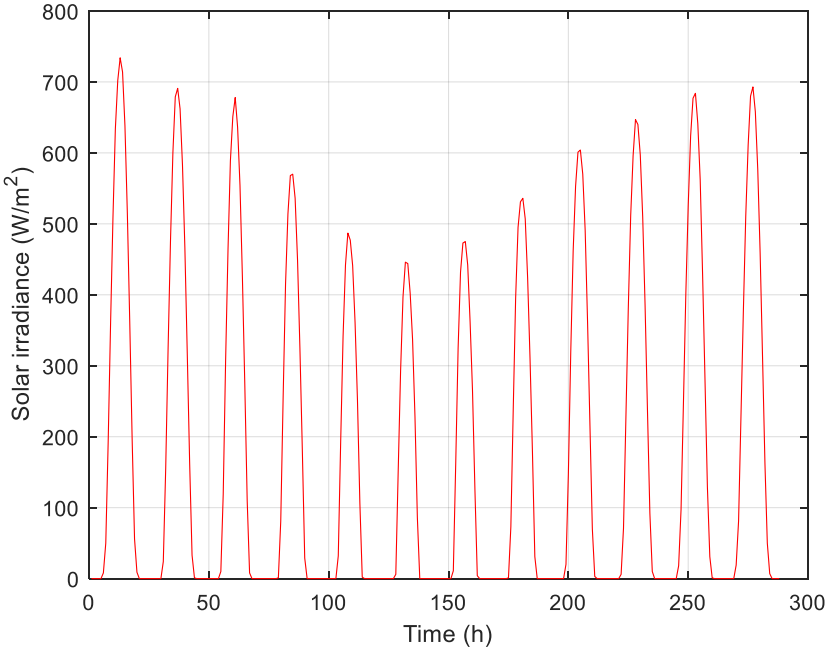

(b)

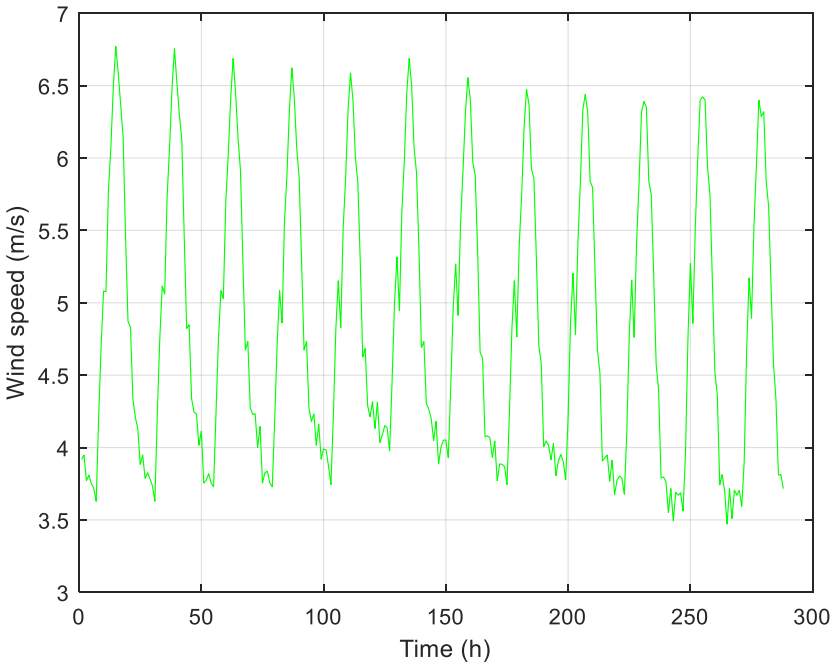

Figure 12. Monthly mean daily solar irradiance and wind speed profiles for MG 1: (a) solar irradiance (W/m^2), and (b) wind speed (m/s).

4.3.2. MG 2: Tryphena

Tryphena is situated at the south-western end of the island, which is about 6.3 km far from Medlands, and surrounded by hills and mountains. As noted earlier, MG 2 conceptualised for the Tryphena site is purely driven by solar PV resources. Fig. 13 depicts the monthly mean daily profile for solar irradiance at the Tryphena site. Again, it should be noted that the solar irradiance data were retrieved for solar PV panels with a tilt angle of 36˚.

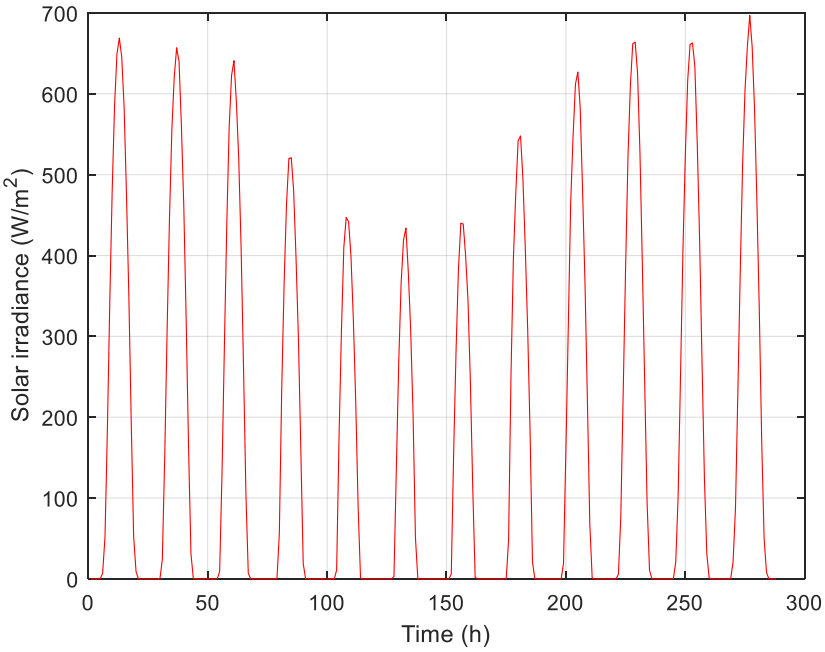

Figure 13. Monthly mean daily solar irradiance profile for MG 2 (W/m^2).

4.3.3. MG 3: Mulberry Grove

Mulberry Grove is a small community, which is about 8.1 km far from Medlands and 2 km far from Tryphena. As stated earlier, the MG conceptualised for the Mulberry Grove site is driven solely by solar PV resources (solar PV panels with a tilt angle of 36˚) as it is the only viable renewable power generation technology based on the associated pre-feasibility analyses. Fig. 14 depicts the monthly mean profile for solar irradiance at the Tryphena site.

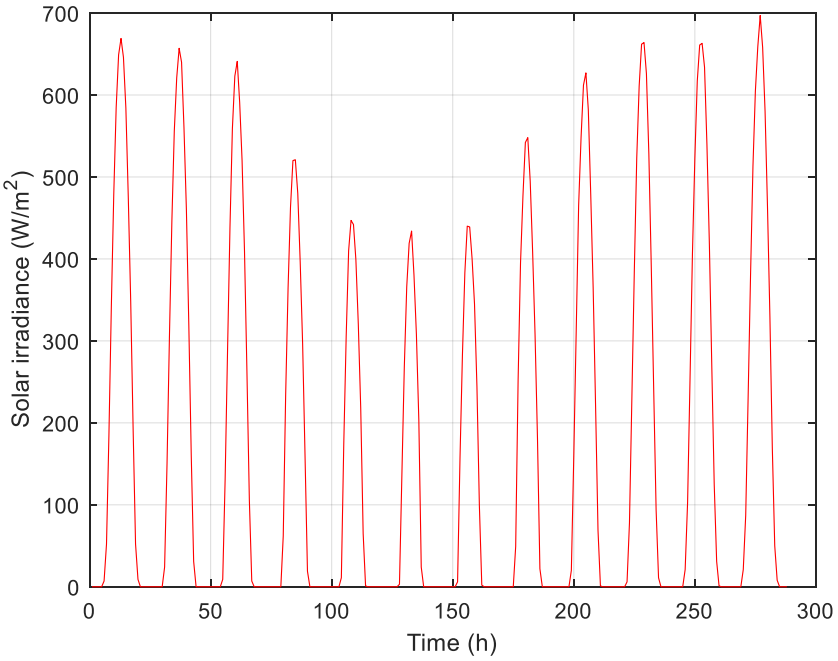

Figure 14. Monthly mean daily solar irradiance profile for MG 3 (W/m^2).

4.4. Energy consumption data

This section presents the derived load profiles of the three communities, which are loaded as inputs to the proposed MG sizing framework, along with the meteorological and techno-economic data. The following sections describe the total energy consumption data associated with each case, which are broken down into the constituent power load components, namely appliance loads and EV-charging loads.

4.4.1. Residential and commercial power loads

Table 4 presents the number of residential and commercial end-users of the cases of interest. As the table details, a total of 43 buildings were considered for the case of MG 1, while the total number of buildings connected to MG 2 and MG 3 were 36 and 18, respectively. The reason for a relatively higher number of buildings in MG 1 compared to MGs 2 and 3 is that it is recognised as the island's most popular location among visitors coming for holidays or leisure (Park, 2021).

Table 4. Number of buildings in the three MGs.

Micro-grid	MG 1	MG 2	MG 3
Load components	40 residential and 3 commercial loads	30 residential and 6 commercial loads	15 residential and 3 commercial loads
Total number of buildings	43	36	18

To derive the total appliance loads on the MGs, a novel energy consumption aggregation strategy was developed, which specifically considers the power consumption of frequently switched on-off appliances, occasionally running appliances, and continuously running appliances. The list of appliances considered for the cases studied and their corresponding hourly-resolved, customer-class-adjusted nominal power usages are detailed in Table B1 in Appendix B, while their detailed specifications are presented in Tables B2 and B3 (Gruber and Prodanovic, 2012). It is also noteworthy that low-temperature heating and cooking loads are assumed to remain non-electrified. Furthermore, while power load time-series of 8,760 data values are considered in the full, non-reduced variant of the proposed model, the corresponding monthly mean daily load forecast profiles for MGs 1–3 are respectively displayed in Figs. 15–17 for the sake of improved visualisation. As it can be observed from the figures, the total appliance load demand on MG 1 is (expectedly) greater than those of MGs 2 and 3. The reader is referred to Figs. B1–B3 in Appendix B for an illustration of the typical energy consumption profile of households (MGs 1–3), commercial buildings (MGs 1–3), and a pub (MG 2), respectively.

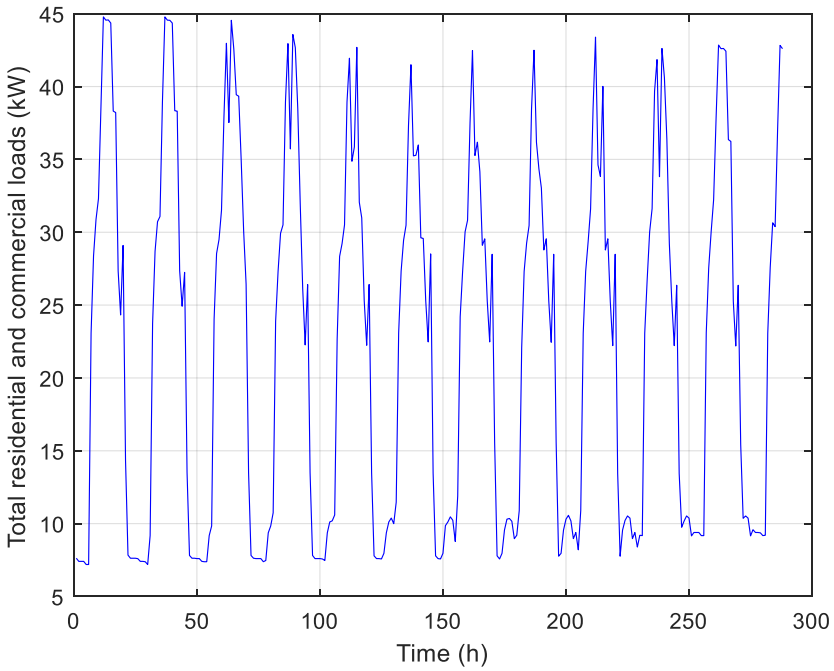

Figure 15. Forecasted monthly mean daily profile for the total appliance energy consumption of the Medlands site (kW).

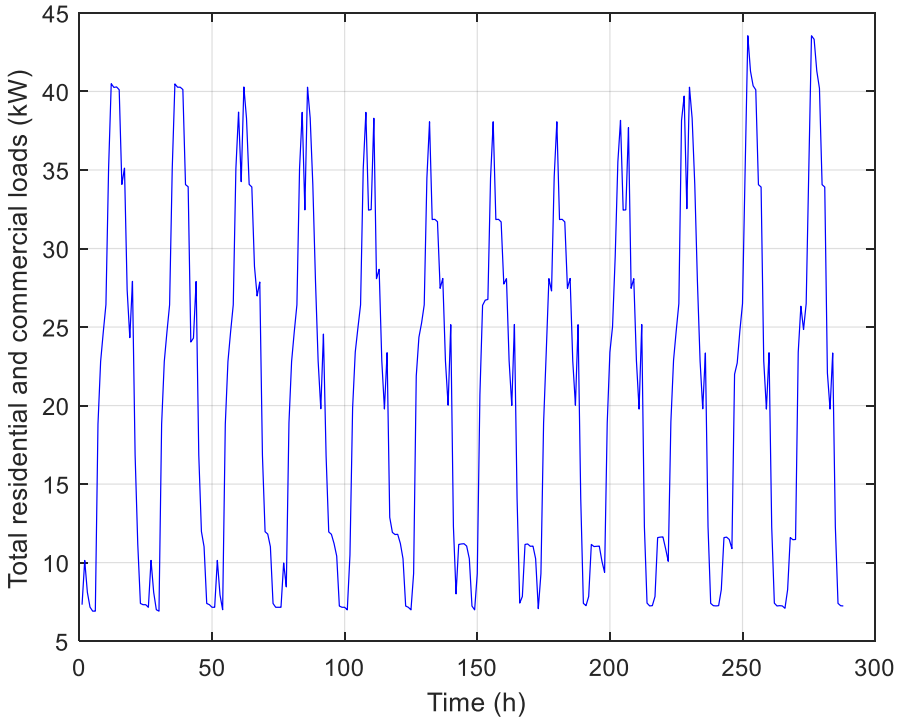

Figure 16. Forecasted monthly mean daily profile for the total appliance energy consumption of the Tryphena site (kW).

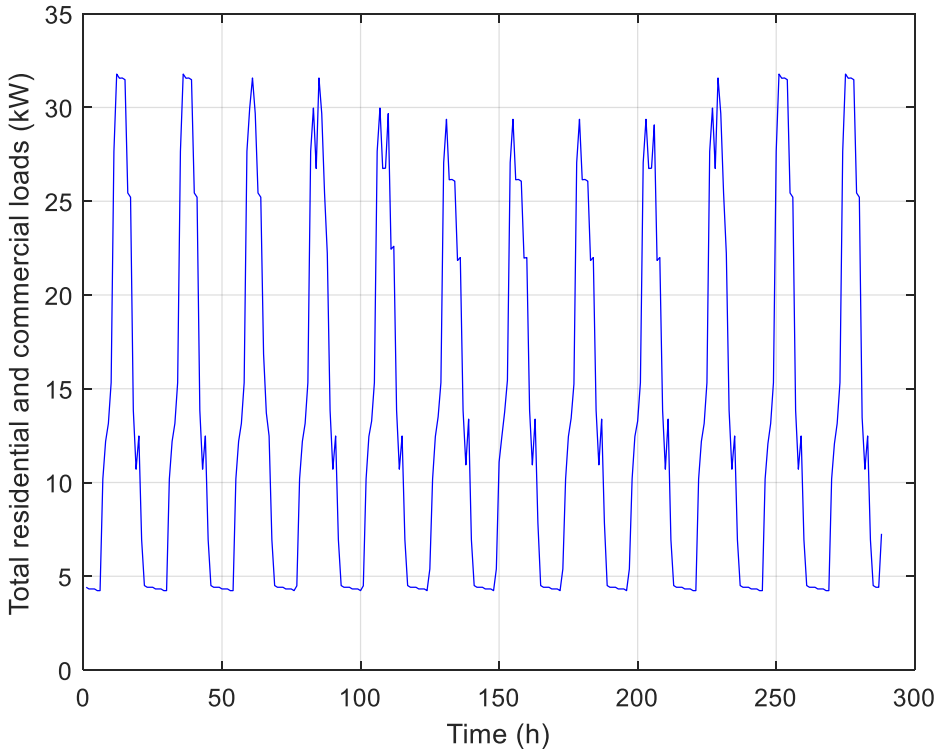

Figure 17. Forecasted monthly mean daily profile for the total appliance energy consumption of the Mulberry Grove site (kW).

4.4.2. EV-charging loads

In general, the fleet of electric vehicles (EVs) can be categorised into five main classes, namely: (i) private EVs, (ii) utility EVs, (iii) commercial EVs, (iv) electric goods trucks, and (v) electric buses (Su *et al*., 2019). In this study, private EVs and utility EVs are considered for integration into the conceptual systems, in accordance with the transportation needs of the sites of interest.

In this context, private EVs were selected to be of the model Nissan Leaf, which has a charging power capacity of 6.6 kW and a battery capacity of 40 kWh, which provides 270 kilometres of range. Furthermore, the utility EVs were chosen to be of the model LDV EV-80, which has a charging power capacity of 6.6 kW and a battery capacity of 56 kWh, which provides 190 kilometres of range (Su *et al.*, 2019).

A rule-based energy management strategy was additionally developed to decide the timing of EV charging – as part of the specifically developed rule-based, cycle-charging expert decision support system for the dispatch of the entire system. To coordinate the charging of EVs in MG 1, it was assumed that the charging of the 10 private EVs and 5 utility EVs occurs during the period between 9 p.m. and 5 a.m. using level-1 chargers. The reason behind the aforementioned scheduling strategy of EV-charging loads is to flatten the overall net load demand (total loads minus total renewable power generation) and improve the load factor, and consequently reduce the excess renewable power curtailments, as well as the size of the capital-intensive stationary battery bank – and, therefore, the total discounted system cost. Recall that the excess renewable power generation that cannot be stored in the battery bank – due to capacity and/or charging power limits – is spilt in a dump load. On the other hand, if the battery bank is not able to fully meet the loads, load shedding is necessary, which leads to an increase in the loss of load probability, necessitating greater storage capacities.

It was also assumed that the private EVs were charged every alternate day, whereas the utility EVs are charged on a daily basis. Fig. 18(a) displays the forecasted total energy demand of EVs on MG 1 for a typical representative day – during the off-peak hours. For simplified analyses, it was assumed that the energy consumption of EVs remains the same for the 365 days of the baseline representative year of the MG operation. That is, the effect of weekdays versus weekend days on the charging behaviour is neglected. It is also noteworthy that the same EV charger model can be used for both private and utility EVs, in view of their similar charging power capacities. It should also be recalled that the EV-charging load is assumed to be left unmet during the periods where the onsite stationary battery bank is in the discharge mode for reasons of energy efficiency.

The number of private and utility EVs were also respectively set to 10 and 5 in MGs 2 and 3. However, given the different dynamics that take place in MGs 2 and 3 compared to MG 1 (due to the absence of WTs), the charging of EVs is scheduled to occur during the period between 12 p.m. and 4 p.m. More specifically, as mentioned earlier, the loads on MGs 2 and 3 are met solely by solar PV generations. This is the main reason why the EV-charging is scheduled to take place during the afternoon hours. It is also noteworthy that the total EV-charging load is evenly distributed amongst the EVs in the pool considering the associated pre-defined charging hours.

(a)

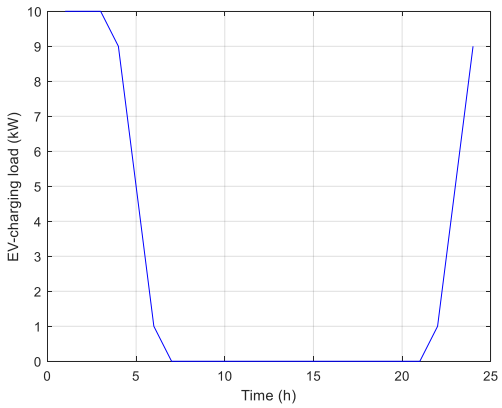

(b)

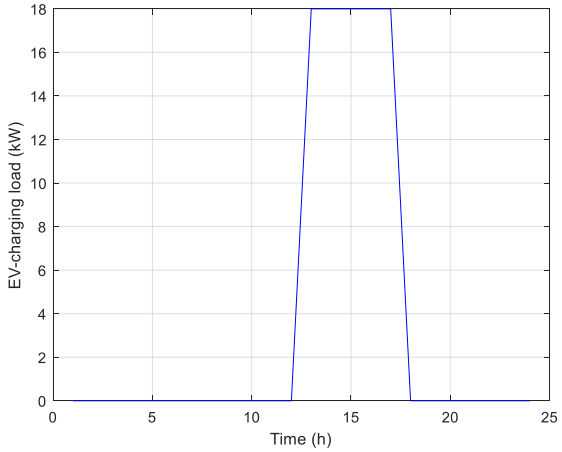

Figure 18. Illustration of the aggregate charging pattern of EV-charging loads (kW): (a) MG 1, and (b) MGs 2 and 3.

4.5. Conclusions

This chapter has presented and discussed the meteorological and load demand data forecasts associated with MGs 1–3, which are respectively tailored to the Medlands, Tryphena, and Mulberry Grove sites on Aotea–Great Barrier Island, Aotearoa–New Zealand. The forecasted time-series data – solar irradiance, wind speed, residential/commercial loads, and EV-charging loads – have also been comparatively analysed. Furthermore, the differences in the scheduling strategies of EV-charging loads using level-1 chargers in MG 1 and MGs 2 and 3 – in accordance with the associated topological differences – are explained. The derived time-series data are utilised as inputs to the proposed meta-heuristic-based off-grid MG sizing model parametrised for the notional MGs 1–3, which are populated for the three cases of interest, with the associated numeric simulation results presented and discussed in the next chapter.

Chapter 5: Simulation results and discussion

5.1. Introduction

This chapter addresses Research Objective 4, which seeks to compare the efficiency of the well-established and competitively selected, state-of-the-art, herd-behaviour-oriented meta-heuristic algorithms in long-term off-grid micro-grid (MG) planning applications. The results obtained from the application of the meta-heuristics under consideration to the MG sizing cases of interest are then comparatively evaluated. The comparative analyses of the efficiencies of the meta-heuristics incorporate various summary statistics to systematically measure the accuracy and precision of the algorithms. The section then proceeds to provide comprehensive univariate sensitivity analyses that provide important insights into the robustness of the system costs and configurations to changes in load demand and power outputs of renewable energy technologies. Finally, case-specific cash flow, energy flow, and capital budgeting analyses substantiate the technical feasibility and economic viability of the project proposals before verifying the validity of the model through a direct comparison of the results of the Medlands test-case system with those of the industry-leading software package for MG sizing, namely HOMER Pro.

5.2. Selected meta-heuristics and simulation setup

The conceptual MG 1 incorporates solar photovoltaic (PV) panels, wind turbines (WTs), and a battery storage system (BSS), while MG 2 and MG 3 are solely driven by a solar PV generation system supported by a battery bank. The three MGs were assumed to be stand-alone systems tailored to providing clean electricity to remote areas. A number of state-of-the-art meta-heuristic algorithms, namely the moth-flame optimisation algorithm (MFOA), the wild horse optimiser (WHO), the artificial hummingbird algorithm (AHA), the artificial gorilla troops optimiser (AGTO), the marine predators algorithm (MPA), and the equilibrium optimiser (EO) were selected for comparative performance analyses and benchmarking against the well-established meta-heuristic in the field, namely the particle swarm optimisation (PSO). The algorithms were also used to test the technical feasibility and economic viability of the conceptual MGs, as well as to verify the effectiveness of the proposed method in yielding cost-optimal solutions. To this end, the relevant meteorological and load demand data were supplied to the proposed method – within which the above-mentioned algorithms are separately embedded for comparative analyses – with the following resolutions: (i) monthly-averaged daily profiles of 12 months × 24 hours or 288 data points (considering model reduction), and (b) hourly-resolved, year-round profiles of 8,760 data points (without model reduction).

The model was simulated on the Intel® Core™ i5-4310M, 2.70 GHz CPU processor with a RAM of 8 GB. The coding was performed in the MATLAB R2020b software.

5.2.1. Performance comparison of the selected algorithms

Inspired by a relevant framework recently developed in (Mohseni and Brent, 2020), a statistics-oriented meta-heuristic performance ranking technique was specifically designed to rank the efficiency of the meta-heuristics of interest in MG equipment capacity planning applications. The proposed ranking technique incorporates the following five descriptive statistics: the standard deviation, mean, and median of the total net present costs (TNPCs)

obtained throughout 30 independent simulation runs, as well as the associated best-case and worst-case results out of the 30 trials of optimising a solution to the three MG sizing problems. The standard deviation measures the amount of variation or dispersion of the population of TNPC outputs, while the mean of the set of TNPC observations represents the arithmetic average of the values – and indicates the central tendency of the values. Also, the median is the value separating the higher half of the population of TNPC outputs from the lower half. The mean of the results, as well as the best-case and worst-case solutions, indicate the accuracy of the algorithms under comparison, whereas the median and standard deviation values indicate the precision of the algorithms over 30 independent trials. Furthermore, for the sake of fair comparisons, the population size (number of search agents), the maximum number of iterations, as well as the upper and lower bounds of the decision variables were respectively set to 100, 200, 10000, and 0 in all simulations.

Table 5 presents the total discounted system costs obtained from the application of the algorithms, the comparative efficiency of which is under investigation, to the optimal equipment capacity planning problem of the three MG instances over 30 simulation runs, whilst accounting for the model reduction technique. The rank order of the algorithms is determined by taking the average of the descriptive statistics for each MG sizing case first (Avg. 1) – which determines the case-specific scores of meta-heuristics when applied to the optimal MG sizing problems of interest – and then taking the average of the resulting scores over the three cases (Avg. 2). The following points should be noted for a better interpretation of the comparative results presented in Table 5:

1. Low standard deviation values indicate that data are clustered around the mean (i.e., the data values are concentrated close to the mean), whereas high standard deviation indicates that data are more spread out (i.e., the data values show more variation from the mean).

2. A standard deviation equal to zero indicates that there is no spread in data.

3. When the mean value is greater than the median value, the distribution curve is skewed to the right (positively skewed). On the other hand, when the median value is greater than the mean value, the distribution curve is skewed to the left (negatively skewed).

4. The best-case and worst-case values respectively indicate the minimum and maximum TNPCs obtained over 30 independent simulation runs.

5. The AGTO and the MPA have almost the same performance, and therefore decimal values were specifically considered for the comparison of their efficiencies.

The comparative results presented in Table 5 are revealing in the following ways:

1. The MFOA and the EO have the best and worst performances, respectively. More specifically, the summary-statistics-based meta-heuristic comparison framework confirms that the MFOA outperforms the other six algorithms investigated, namely the PSO, the WHO, the AHA, the AGTO, the MPA, and the EO. The utilisation of the MFOA for the optimal sizing of the cases of interest reduces the expected TNPC by \$2,647 (~1%), \$2,864 (~1%), and \$6,037 (~2%) for MG 1, MG 2, and MG 3, respectively, compared to the EO, which is the least well-performing meta-heuristic.

2. The standard deviation of the TNPC outputs of the MFOA and the EO when applied to the third MG are both equal to 0. This indicates the robustness of the MFOA in yielding the globally optimal solution, whilst substantiating the comparative inefficiency of the EO in MG planning applications.
3. Based on the Avg. 2 metric, the following rank order can be established for the meta-heuristics under comparison: the MFOA > the AGTO > the MPA > the AHA > the PSO > the WHO > the EO.

Table 5. Summary-statistics-based efficiency comparison of the selected meta-heuristics applied to the three MG planning cases.

Alg.	Sys.	St. Dev.	Best	Worst	Mean	Median	Avg. 1	Score	Avg. 2	Rank
PSO	MG 1	1523	438,177	444,152	439,070	438,611	440,003	6		
	MG 2	126	426,553	427,241	426,576	426,553	426,731	4	5	5
	MG 3	974	272,791	278,123	272,968	272,791	274,168	5		
MFOA	MG 1	296	435,539	436,589	435,651	435,539	435,830	1		
	MG 2	218	423,689	423,720	423,223	423,218	423,462	1	1	1
	MG 3	0	266,754	267,000	266,754	266,754	266,816	1		
WHO	MG 1	37689	438,171	515,553	468,126	438,171	465,005	5		
	MG 2	1	426,553	426,554	426,553	426,553	426,553	7	6	6
	MG 3	1	272,791	272,792	272,791	272,791	272,791	6		
AHA	MG 1	106	435,838	436,287	435,972	435,944	436,010	3		
	MG 2	737	431,073	434,475	431,265	431,075	431,972	6	4	4
	MG 3	1	266,999	267,004	267,001	267,000	267,001	3		
AGTO	MG 1	256	435,791	436,546	435,945	435,804	436,021	2		
	MG 2	1	431,073	431,074	431,073	431,073	431,073	5	3	2
	MG 3	1	266,999	267,000	266,999	266,999	266,999	2		
MPA	MG 1	1	438,171	438,173	438,171	438,171	438,171	4		
	MG 2	1	426,553	426,554	426,553	426,553	426,553	2	3.33	3
	MG 3	1	272,791	272,793	272,791	272,791	272,791	4		
EO	MG 1	2400	438,186	445,214	439,341	438,219	440,240	7		
	MG 2	1	426,553	426,554	426,553	426,553	426,553	3	6	7
	MG 3	0	272,791	272,793	272,791	272,791	272,791	7		

Furthermore, Table 6 presents the optimal mix of the technologies in the candidate pool for the three cases, which represent the best-case performance of the meta-heuristics considering input data reduction. It can be observed from the table that, compared to the AHA and the AGTO, the MFOA allocates more WTs in the case of MG 1 to reduce the need for a large battery storage capacity. Also, although the number of WTs selected by the MFOA for MG 1 is equal to those optimised by the PSO, the WHO, the MPA, and the EO, it returns comparatively lower capacities for the solar PV plant and the BSS. This can be explained by the MFOA's unique feature of dynamically rebalancing exploration – the early stages of the optimisation process that represents the long-range movement of search agents – for improved exploitation – the local search around promising regions of the search space identified in the exploration phase. Such rebalancing procedure is found to be particularly

useful for optimising a solution in the general multi-dimensional, nonlinear, non-convex shape of the decision space of MG sizing problems.

It is noteworthy that the size of the inverter does not constitute part of the solution set, as it is calculated exogenously (outside the model) based upon the peak load demand. It should also be noted that the optimal size of each component is rounded up to the nearest integer given the continuous nature of the selected meta-heuristics. The associated TNPCs were, accordingly, rounded up to the nearest integer.

Table 6. Optimal mix of the candidate technologies and the corresponding TNPCs for the three cases optimised by the selected algorithms in their best performance considering data reduction.

Alg.	Sys.	PVs (no.)	BSS (no.)	WTs (no.)	TNPC ($)
PSO	MG 1	127	390	3	438,177
	MG 2	792	261	N/A*	426,553
	MG 3	541	134	N/A*	272,791
MFOA	MG 1	102	381	3	435,539
	MG 2	784	261	N/A*	423,689
	MG 3	523	135	N/A*	266,754
WHO	MG 1	127	391	3	438,171
	MG 2	792	261	N/A*	426,553
	MG 3	541	134	N/A*	272,791
AHA	MG 1	209	424	2	435,838
	MG 2	796	267	N/A*	431,073
	MG 3	536	127	N/A*	266,999
AGTO	MG 1	208	424	2	435,791
	MG 2	796	267	N/A*	431,073
	MG 3	536	127	N/A*	266,999
MPA	MG 1	127	391	3	438,171
	MG 2	792	261	N/A*	426,553
	MG 3	541	134	N/A*	272,791
EO	MG 1	127	390	3	438,186
	MG 2	792	261	N/A*	426,553
	MG 3	541	134	N/A*	272,791

*N/A = Not applicable because the WT is not considered as a candidate technology in MG 2 and MG 3.

Fig. 19 depicts the convergence curves of the selected meta-heuristics in their best runs when applied to MG 1 considering input data reduction. It can be observed from the figure that the MFOA, the AGTO, and the MPA have almost the same convergence behaviour, whereas the AHA, the PSO, and the WHO take more iterations to converge. The figure also reveals that the weaker performance of the EO can be explained by its premature trapping in poor local optima. These observations collectively confirm the comparable simulation speed of the MFOA to the fastest meta-heuristics in the candidate pool – for efficiency comparisons.

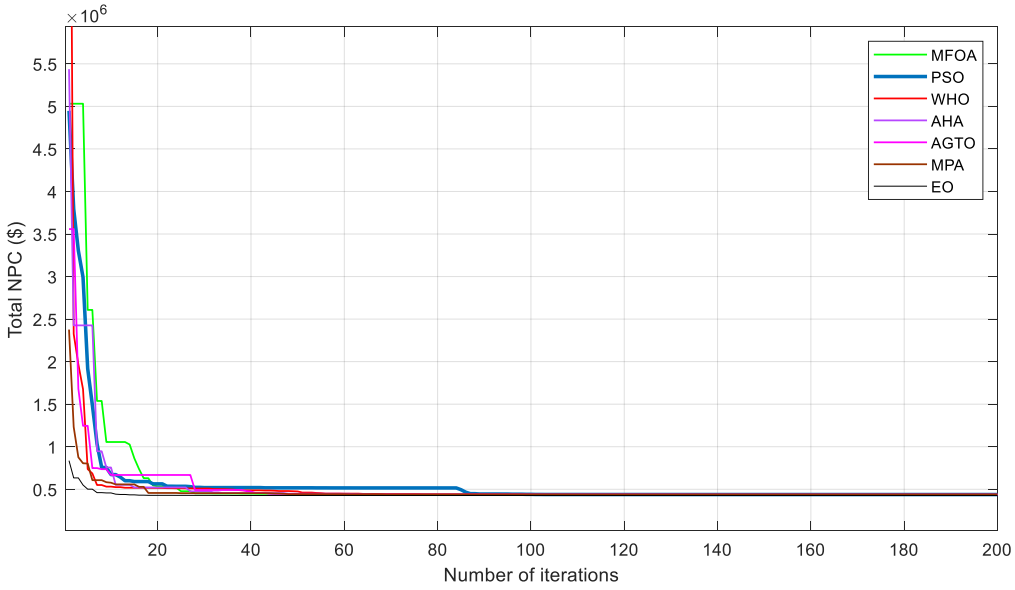

Figure 19. Best-case convergence curves of the selected meta-heuristics when applied to MG 1 considering input data reduction ($).

5.3. Verification of the MFOA with and without model reduction

To verify the effectiveness of the model-order reduction technique employed, this section compares the results obtained from the application of a reduced variant of the model that considers representative days (with 288 data points) to those of a non-reduced model (with 8,760 data points). To this end, the MFOA is used as the optimiser due to its validated superiority over the other algorithms in the previous section. Also, a single run was deemed sufficient given the considerably low (and in one case, zero) standard deviation of the MFOA revealed from the statistical performance analyses above. The associated comparative results (with and without input data reduction) are presented in Table 7.

Table 7. Optimal sizing solutions of the three MGs obtained from a single run of the MFOA with and without model reduction.

Case	Sys.	PVs (no.)	BSS (no.)	WTs (no.)	TNPC ($)
With model reduction	MG 1	102	381	3	435,539
	MG 2	784	261	N/A*	423,689
	MG 3	523	135	N/A*	266,754
Without model reduction (full model)	MG 1	480	84	3	435,330
	MG 2	779	259	N/A*	420,900
	MG 3	530	118	N/A*	260,446

*N/A = Not applicable because the WT is not considered as a candidate technology in MG 2 and MG 3.

The computational time for the proposed model is approximately 5 minutes and 300 minutes for the cases with 288 and 8,760 data points, respectively. Accordingly, using a reduced variant of the model significantly reduces the computational expensiveness of simulations without a statistically significant impact on the resulting TNPCs, as shown in Table 7. More

specifically, the TNPCs yielded considering input data reduction are associated with inaccuracies of approximately 0.05%, 0.6%, and 2% respectively for MGs 1–3 compared to the corresponding full model versions. The above-mentioned deviations of the TNPCs optimised by the reduced model from the corresponding values obtained from the full model reveal the inverse correlation of the inaccuracy of model reduction with the overall size of the MG indicated by the average annual load. That is, the lower the size of the MG, the greater the inaccuracy of the model with input data reduction compared to the corresponding full model.

It is also noteworthy that the component size mix obtained for the case of MG 1 using the superior MFOA algorithm in the non-reduced input data scenario is less technically viable from a resiliency perspective – given the presence of a significantly smaller battery capacity – compared to the scenario with model reduction. This indicates that although using one-year-long time-series data during the MG planning phases is important for numeric simulations to better reflect globally optimum solutions, there might exist locally optimum solutions that provide a better trade-off between cost and resilience. However, this requires operating the system with component capacities obtained from the counterpart reduced models (with 288 data points) over full time periods (with 8,760 data points) to ensure that they adequately relax the relevant reliability and other operational- and planning-level constraints.

5.4. Scenario analyses for MG 1: Indicative impact analyses of the timing of EV charging

To evaluate the impact of the timing of EV charging on the costing and configuration of MGs, this section presents and discusses the results of scenario analyses carried out for MG 1, which integrates solar PV panels, WTs, a BSS, and EVs. To this end, the considered scenarios include: (i) scheduling the charging of EVs to the late evening and early morning hours (9 p.m. to 5 a.m.), (ii) shifting the EV-charging loads to the afternoon hours (12 p.m. to 4 p.m.), and (iii) exclusion of EV-charging loads. For better-informed decision-making support, each of the scenarios, additionally, address two cases, namely: (1) without solar PV generation, and (2) without WT generation. The simulations were carried out using the MFOA for a single run considering input data reductions to alleviate the computational burden.

5.4.1. Supplying the EV-charging loads in the late evening and early morning hours

Table 8 (a) presents the results of the optimum size of the components of MG 1, where the charging of EVs is scheduled to occur between the hours 9:00 p.m. to 5:00 a.m. It can be observed from the table that the exclusion of the solar PV plant from the candidate pool results in a slight decrease in the size of the BSS, but no significant change in the TNPC is expected compared to the baseline value. More specifically, a ~2% increase in the TNPC was observed, which equates to ~$9k. However, the case without a wind resource has had a more significant impact on the TNPC of the system. Specifically, a ~8% increase in the TNPC was observed (equating to ~$37k) due to the consequent modest increase in the size of solar PV panels and the BSS.

Table 8 (a). Relative importance of solar PV and WT plants on the economic viability of MG 1 with EV-charging loads supplied during the late evening and early morning hours.

Scenario	PVs (no.)	BSS (no.)	WTs (no.)	TNPC ($)
Baseline	102	381	3	435,539
Without PV	-	341	4	445,215
Without WT	614	474	-	472,087

5.4.2. EV-charging loads shifted to the afternoon hours

In this scenario, the EV-charging loads are shifted to the afternoon hours – specifically, from 12:00 p.m. to 4:00 p.m. – which has increased the TNPC by around 7% (equating to $32,156) compared to the original case where the EV-charging loads are served during the late evening and early morning hours (see Tables 8 (a) and (b)). The main underlying reason for this observation is the decreased load factor – defined as the average load divided by the peak load – which necessitates adding more solar PV capacity. Furthermore, the optimal capacity of the WT plant and the battery bank is increased in the solar PV-less case, as one would expect, with a consequent TNPC increase of ~2% (equating to $6k). On the other hand, the WT-less scenario indicates a TNPC increase of ~5% (equating to $21k), which corroborates the relatively more significant impact of the WT plant on the cost-effectiveness of MG 1 compared to the solar PV plant.

Table 8 (b). Relative importance of solar PV and WT plants on the economic viability of MG 1 with EV-charging loads shifted to the afternoon hours.

Scenarios	PVs (no.)	BSS (no.)	WTs (no.)	TNPC ($)
Baseline	397	205	3	467,695
Without PV	-	356	4	473,920
Without WT	667	470	-	489,093

5.4.3. No EV-charging loads

In this scenario, it is assumed that the transportation sector is not electrified. Expectedly, the TNPC is reduced compared to the other scenarios that consider the integration of EV-charging loads (see Tables 8 (a), (b), and (c)). Also, a comparison of the relevant solar PV-less and WT-less cases has provided another layer of evidence on the greater importance of WTs on the financial sustainability of the project compared to solar PV panels. More specifically, the PV-less case is associated with a total discounted system cost increase of ~3%, whereas the WT-less case is associated with a cost increase of ~8% compared to the associated baseline case.

Table 8 (c). Relative importance of solar PV and WT plants on the economic viability of MG 1 without EV-charging loads.

Scenarios	PVs (no.)	BSS (no.)	WTs (no.)	TNPC ($)
Baseline	211	398	2	426,284
Without PV	-	341	4	441,215
Without WT	614	474	-	468,087

5.5. Sensitivity analyses

Sensitivity analyses are useful to evaluate the effects of changes in input parameters on the total cost estimate and the corresponding MG configuration during the associated planning phases. Accordingly, a set of separate univariate sensitivity analyses are carried out to measure the robustness of the solutions to changes in the values of renewable power sources (on the generation side) and load demand (on the consumption side). The sensitivity variables on the generation side include solar irradiance and wind speed, which are inherently variable and weather-dependent, with the historical data retrieved from the SolarView tool and database of NIWA (2019), while the load demand data is specifically synthesised based on the forecast of the residents' appliance use. Also, the associated load demand sensitivity analyses provide insights into the impact of the potential variations of loads on the resulting MG cost and architecture – and can be effectively used to tailor the MG's sizing to the end-consumers' robustness and reliability preferences. Again, the simulations were carried out using the MFOA for a single run considering input data reductions.

As mentioned above, the impacts of the potential variations in solar irradiance, wind speed, and load demand were evaluated on the total net present cost (TNPC) and configuration of the conceptual MGs. To this end, the sensitivity analyses are conducted by increasing and decreasing the forecasted values of the sensitivity variables by 40% in 10% intervals.

The following scenarios were specifically considered in determining the effect of changes in relevant time-series patterns:

a) Fixed electricity load and solar irradiance, and varying wind speed.
b) Fixed electricity load and wind speed, and varying solar irradiance.
c) Fixed solar irradiance and wind speed, and varying electricity load.

The above-mentioned scenarios were also considered in two cases, namely with and without electric vehicle (EV) charging loads, for a more holistic analysis.

5.5.1. With EV-charging loads

a) Fixed electricity load and solar irradiance, and varying wind speed

The obtained results for MG 1 are presented in Fig. 20. As the figure shows, increasing the wind speed data from 10% to 40% of the original values steadily decreases the TNPC of the system. In addition, as shown in Table 9, this results in a rejection of the photovoltaic (PV) panels in all relevant scenarios, with a combination of the BSS and WTs providing the most economically viable choice for serving the load demand. The reason is that the wind resource is more abundant compared to solar irradiance. Also, from 20% increments in wind speed

onwards, the number of required WTs is reduced to 2 from the original 3 with an accompanying decrease in battery storage due to the increased capacity factor of the WT generation system. Furthermore, a 40% increment of wind speed is associated with a 36% reduction in the TNPC compared to the baseline value. This suggests the significant impact of the required degrees of robustness and reliability on the produced cost estimates.

On the other hand, for the scenarios with wind speed deviations in the range of −40% to −10%, no WT is selected due to an insufficient wind resource to make this technology economically viable. Consequently, the total cost of the system increases due a larger number of solar panels and battery packs required. Moreover, the insignificant changes in the size of the components and the cost of the MG for the scenarios of changing the wind speed from its original value to −40% of its original value (albeit no WT is selected in any of those cases) can be explained by the continuous formulation of the problem. In other words, the actual number of WTs is not exactly equal to 0, but it is rounded down to 0.

Table 9. Components' size estimates and the associated TNPCs by varying wind speed for MG 1 with EV-charging loads.

Variation (%)	PVs (no.)	BSS (no.)	WTs (no.)	TNPC ($)
−40	634	473	0	478,506
−30	645	477	0	484,817
−20	661	479	0	491,196
−10	696	479	0	504,305
Baseline	102	381	3	435,539
10	0	336	3	376,174
20	0	336	2	331,991
30	0	336	2	300,369
40	0	309	2	276,330

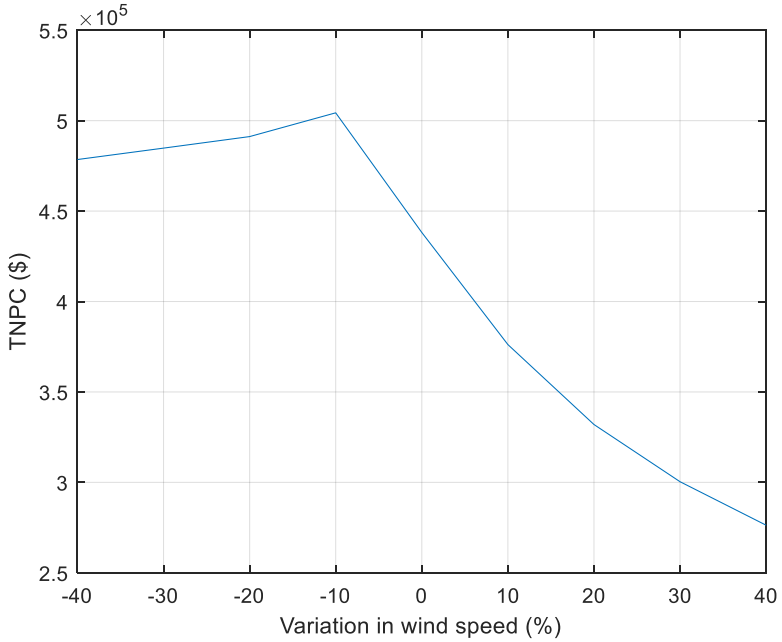

Figure 20. Effects of variation in wind speed on the costing of MG 1 with EV-charging loads.

b) Fixed electricity load and wind speed, and varying solar irradiance

For microgrid 1 (MG 1), increasing the value of solar irradiance from −40% of its original value to −20% of its original value results in zero PV panels with associated implications for the size of the BSS, WTs, and in turn, the TNPC, as illustrated in Table 10 (a). A further interesting observation is a significant rise in the size of the PV generation system from the case with −10% deviation in solar irradiance onwards. On the other hand, in the cases with a solar irradiance deviation of +10% to +40%, the TNPC steadily decreases, albeit insignificantly (specifically, 3% or $12k). However, the second and third MGs were found to be more sensitive to changes in solar irradiance increments. More specifically, a 18% (equating to $77k) and 19% (equating to $48k) cost reduction were observed for MG 2 and MG 3 at a +40% solar irradiance deviation compared to the baseline value, as presented in Tables 10 (b) and (c), and Fig. 21.

Table 10 (a). Components' size estimates and the associated TNPCs by varying solar irradiance for MG 1 with EV-charging loads.

Variation (%)	PVs (no.)	BSS (no.)	WTs (no.)	TNPC ($)
−40	0	341	4	445,215
−30	0	341	4	445,215
−20	0	341	4	445,215
−10	98	370	3	443,272
Baseline	102	381	3	435,539
10	103	386	3	435,171
20	107	391	3	430,681
30	250	404	0	426,989
40	389	404	0	423,161

Table 10 (b). Components' size estimates and the associated TNPCs by varying solar irradiance for MG 2 with EV-charging loads.

Variation (%)	PVs (no.)	BSS (no.)	TNPC ($)
−40	1243	297	605,397
−30	1066	297	542,312
−20	933	297	494,997
−10	861	275	457,955
Baseline	784	261	423,689
10	720	261	400,985
20	660	261	379,679
30	609	261	361,650
40	566	261	346,197

Table 10 (c). Components' size estimates and the associated TNPCs by varying solar irradiance for MG 3 with EV-charging loads.

Variation (%)	PVs (no.)	BSS (no.)	TNPC ($)
−40	720	231	385,458
−30	712	167	350,357
−20	625	166	318,838
−10	581	149	294,158
Baseline	523	135	266,754
10	492	134	255,324
20	451	134	240,769
30	416	134	228,452
40	387	134	217,896

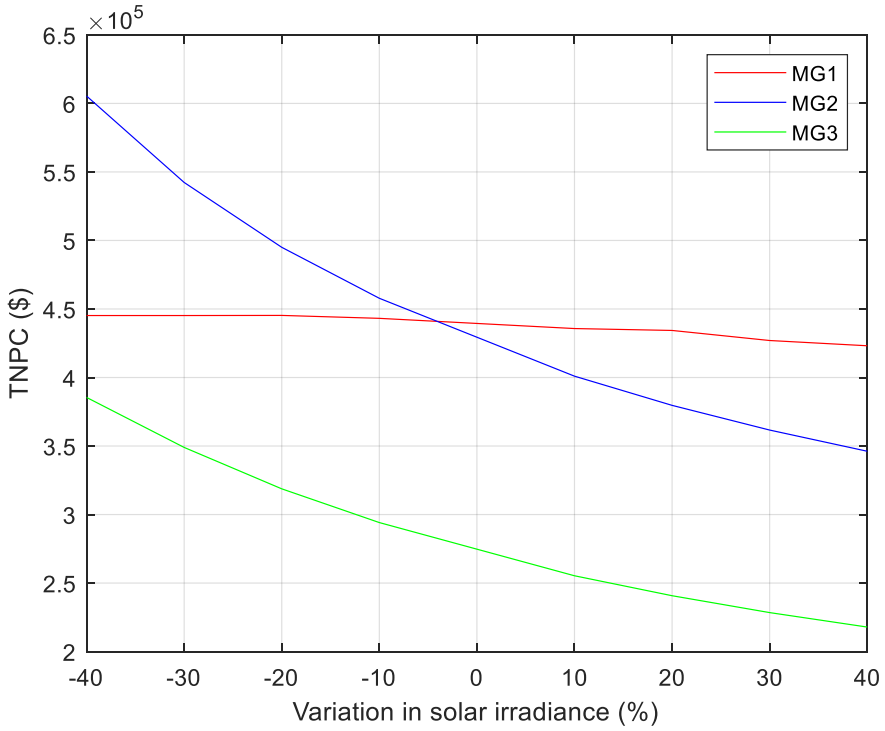

Figure 21. Effects of variation in solar irradiance on the costing of the three MGs with EV-charging loads.

c) Fixed solar irradiance and wind speed, and varying electricity load

A significant direct correlation was observed between the changes in load demand and the TNPC for all the three MGs under consideration, as it can be seen from Fig. 22. That is, the number of PV panels, WTs, and battery packs is more significantly influenced by the load on the MG compared to other inputs. This observation is consistent with prior findings in the literature (Mohseni *et al.*, 2019). At the extreme scenario (+40% deviation in load demand), the TNPC is increased by a significant 37% compared to the baseline scenario for MG 1 and MG 2. It can also be inferred from Table 11 and Fig. 22 that the sensitivity of the TNPC of the MG to changes in load demand, to some extent, depends on the original value of the total load it is expected to serve.

Table 11 (a). Components' size estimates and the associated TNPCs by varying load demand for MG 1 with EV charging-loads.

Variation (%)	PVs (no.)	BSS (no.)	WTs (no.)	TNPC ($)
−40	60	220	2	281,886
−30	65	269	2	321,275
−20	118	344	2	363,711
−10	105	294	3	405,257
Baseline	102	381	3	435,539
10	0	374	4	485,171
20	335	510	2	534,285
30	153	498	3	556,721
40	348	584	3	596,690

Table 11 (b). Components' size estimates and the associated TNPCs by varying load demand for MG 2 with EV-charging loads.

Variation (%)	PVs (no.)	BSS (no.)	TNPC ($)
−40	505	156	271,091
−30	577	182	309,939
−20	647	210	348,897
−10	720	235	387,701
Baseline	784	261	423,689
10	864	287	465,431
20	936	313	504,296
30	989	354	544,065
40	1045	393	583,710

Table 11 (c). Components' size estimates and the associated TNPCs by varying load demand for MG 3 with EV-charging loads.

Variation (%)	PVs (no.)	BSS (no.)	TNPC ($)
−40	279	81	152,666
−30	307	109	176,853
−20	330	160	211,078
−10	455	133	241,505
Baseline	523	135	266,754
10	588	148	296,232
20	619	173	320,290
30	681	175	349,116
40	727	189	366,582

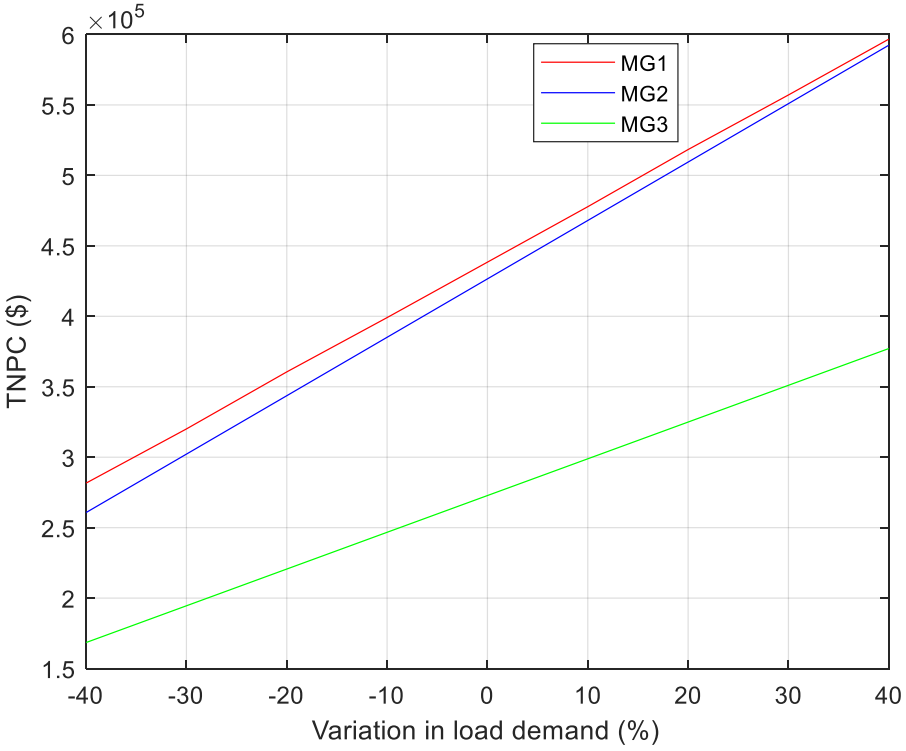

Figure 22. Effects of variation in load demand with EV-charging loads on the costing of the three MGs.

5.5.2. Without EV-charging loads

a) Fixed electricity load and solar irradiance, and varying wind speed

The obtained results in the EV-less case have revealed practically the same insights into the sensitivity of the MG capacity planning solutions to changes in key time-series inputs. This substantiates the validity of the obtained insights.

More specifically, increasing wind speed from −40% of its original value to −10% of its original value increases the TNPC, as presented in Table 12. In this case, given the absence of EV loads, only PV panels and stationary batteries are sufficient to serve the load demand. Then, for the wind speed variations in the range of −10% of the original value to +40% of the original value, the estimated TNPC decreases sharply, as shown in Fig. 23. More specifically, the TNPC is reduced by 37% as compared to the baseline case, which equates to a community saving of $155,669 in total energy costs.

Moreover, an increase in the TNPC is observed, despite the decrease in wind speed by 10% and the consequent absence of WTs in the associated solution set. This observation can be explained by the continuous formulation of the problem, as illustrated above.

Table 12. Components' size estimates and the associated TNPCs by varying wind speed for MG 1 without EV-charging loads.

Variation (%)	PVs (no.)	BSS (no.)	WTs (no.)	TNPC ($)
−40	634	473	0	474,506
−30	645	477	0	480,817
−20	661	479	0	487,196
−10	698	479	0	500,329
Baseline	211	398	2	426,284
10	0	336	3	372,174
20	0	336	2	327,036
30	0	336	2	304,317
40	0	336	2	270,615

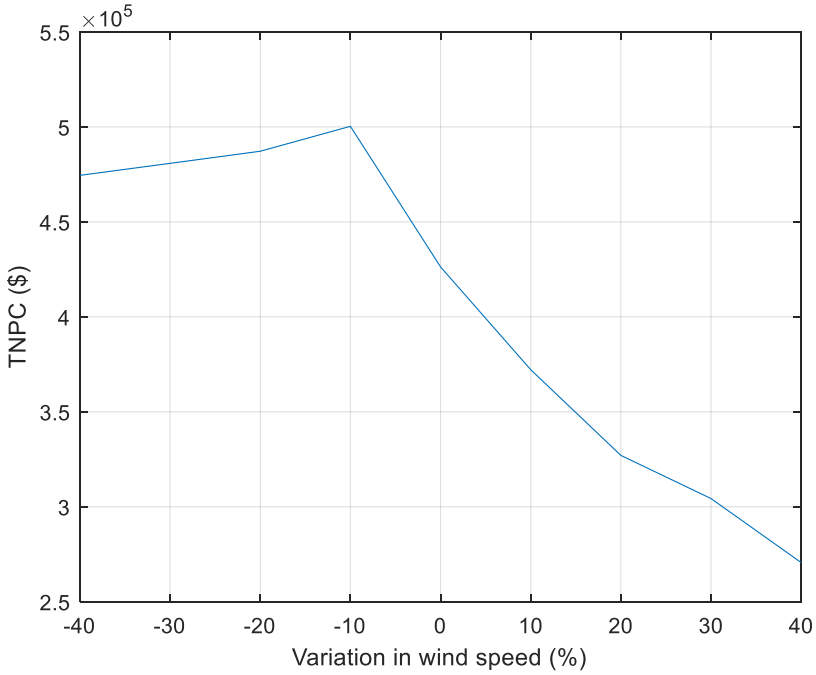

Figure 23. Effects of variation in wind speed on the costing of MG 1 without EV-charging loads.

b) Fixed electricity load and wind speed, and varying solar irradiance

As Table 13 (a) indicates, for MG 1, no change in the TNPC is observed for the deviation of solar irradiance from −40% of its baseline value to −20% of its baseline value, which can be primarily attributed to the relatively long step size (nameplate capacity) selected for WTs. Then, for the deviations in the range of −10% to +20% of the original irradiance values, the TNPC is steadily reduced due to the availability of better solar resources. However, an insignificant rise is observed in the TNPC at the deviations of +30% and +40%, which is mainly due to the presence of small values of WT capacity, though rounded down to 0 in the reported solution set. The sensitivity of the TNPC of MGs 2 and 3 to changes in solar irradiance are also presented in Tables 13 (b) and (c), respectively – and also visualised in

Fig. 24. As an indication, for a +40% solar irradiance deviation, the total discounted system cost reduction is found to be approximately 2%, 16%, and 20% respectively for MG 1, MG 2 and MG 3, respectively, which is comparable, on a percentage basis, to the case of 'with EVs'.

Table 13 (a). Components' size estimates and the associated TNPCs by varying solar irradiance for MG 1 without EV-charging loads.

Variation (%)	PVs (no.)	BSS (no.)	WTs (no.)	TNPC ($)
−40	0	341	4	451,215
−30	0	341	4	451,215
−20	0	341	4	451,215
−10	161	435	2	448,881
Baseline	211	398	2	426,284
10	220	401	2	425,706
20	503	470	0	425,005
30	506	488	0	431,794
40	520	490	0	431,280

Table 13 (b). Components' size estimates and the associated TNPCs by varying solar irradiance for MG 2 without EV-charging loads.

Variation (%)	PVs (no.)	BSS (no.)	TNPC ($)
−40	1092	311	554,823
−30	936	311	499,425
−20	819	311	457,883
−10	794	265	425,050
Baseline	718	262	396,720
10	652	262	373,556
20	598	262	354,255
30	552	262	337,924
40	513	262	333,926

Table 13 (c). Components' size estimates and the associated TNPCs by varying solar irradiance for MG 3 without EV-charging loads.

Variation (%)	PVs (no.)	BSS (no.)	TNPC ($)
−40	713	165	345,174
−30	611	165	329,029
−20	535	165	281,921
−10	517	136	260,797
Baseline	464	136	242,481
10	424	135	227,379
20	388	135	214,847
30	358	135	204,244
40	333	135	195,155

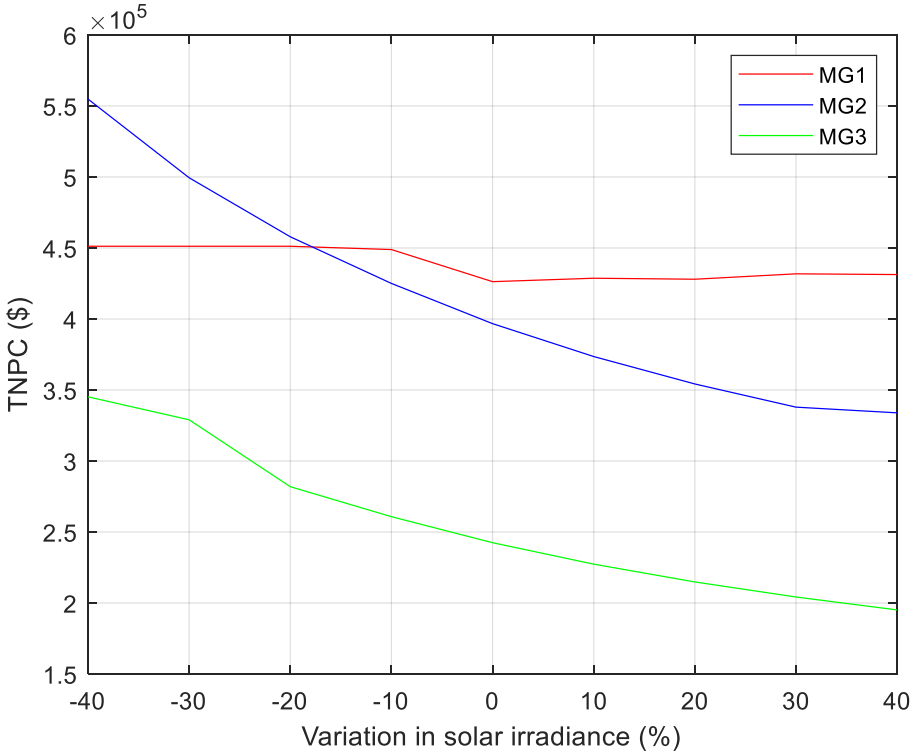

Figure 24. Effects of variation in solar irradiance on the costing of the three MGs without EV-charging loads.

c) Fixed solar irradiance and wind speed, and varying electricity load

Tables 14 (a), (b), and (c) present the results of the load demand sensitivity analyses for the three MG instances, respectively. As visualised in Fig. 25, the sensitivity of the TNPC of the MGs of interest to changes in load values follows approximately the same pattern as that in the corresponding case with EV-charging loads. This further verifies the validity of the obtained findings.

Table 14 (a). Components' size estimates and the associated TNPCs by varying loads for MG 1 without EV-charging loads.

Variation (%)	PVs (no.)	BSS (no.)	WTs (no.)	TNPC ($)
−40	76	241	2	276,721
−30	470	340	0	313,790
−20	531	386	0	359,710
−10	550	405	0	394,506
Baseline	211	398	2	426,284
10	231	452	2	480,037
20	815	599	0	523,395
30	323	543	2	565,850
40	138	525	4	593,239

Table 14 (b). Components' size estimates and the associated TNPCs by varying loads for MG 2 without EV-charging loads.

Variation (%)	PVs (no.)	BSS (no.)	TNPC ($)
−40	431	166	245,460
−30	502	184	280,125
−20	574	210	318,973
−10	646	236	357,845
Baseline	718	262	396,720
10	787	290	435,689
20	861	320	472,920
30	931	349	512,496
40	1004	370	552,073

Table 14 (c). Components' size estimates and the associated TNPCs by varying loads for MG 3 without EV-charging loads.

Variation (%)	PVs (no.)	BSS (no.)	TNPC ($)
−40	279	81	148,662
−30	326	95	172,092
−20	373	108	195,533
−10	419	122	218,975
Baseline	464	136	242,481
10	512	149	265,871
20	559	162	289,300
30	606	176	312,742
40	652	189	336,202

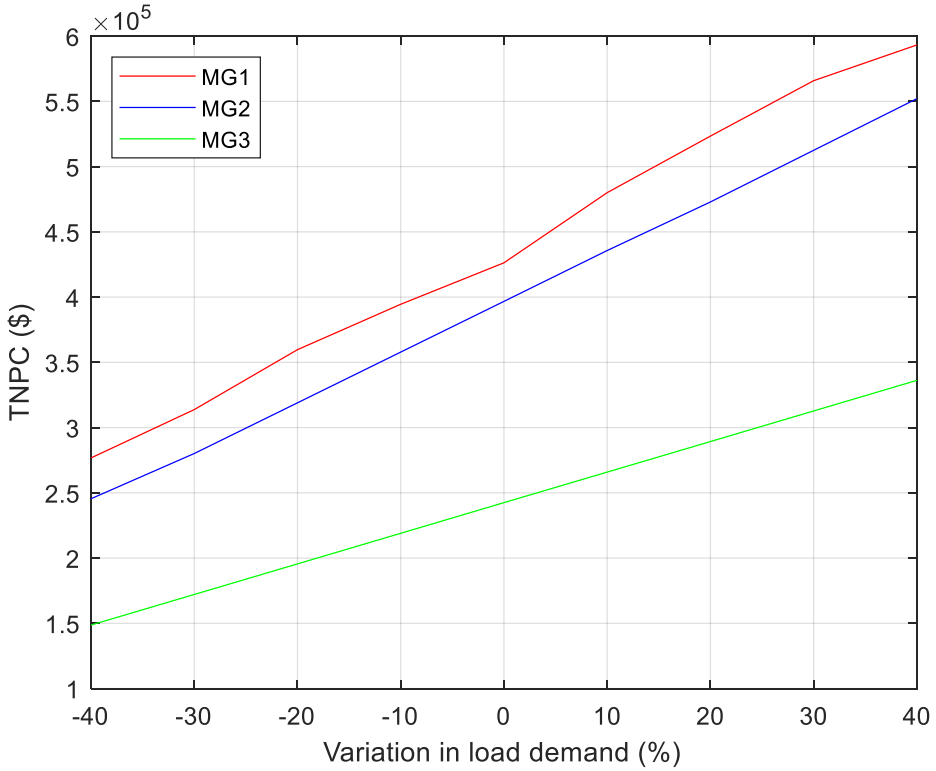

Figure 25. Effects of variation in load demand without EV-charging loads on the costing of the three MGs.

5.6. Cash flow analyses of the optimised MGs

The capital budgeting analyses were carried out in accordance with the best-case results of the MFOA for the three micro-grids considering 8,760-long time-series input data (without model reduction). As mentioned above, the best TNPCs of MGs 1–3 were respectively found to be $435,330, $420,900, and $260,446. Fig. 26 shows the contribution of the net present cost of the components, the optimal size of which constitute the decision variables, to the associated TNPCs, which additionally account for the costs of the inverter and EV chargers. It can be observed that the higher cost of MG 1 compared to the other two cases is mainly due to the added WT capacity needed to meet its comparatively larger load demand. It can also be inferred from the figure that MG 2 has the largest BSS and solar PV capacities. This can be, in large part, attributed to the absence of WTs in its generation mix (compared to MG 1) and the larger demand on its network (compared to MG 3).

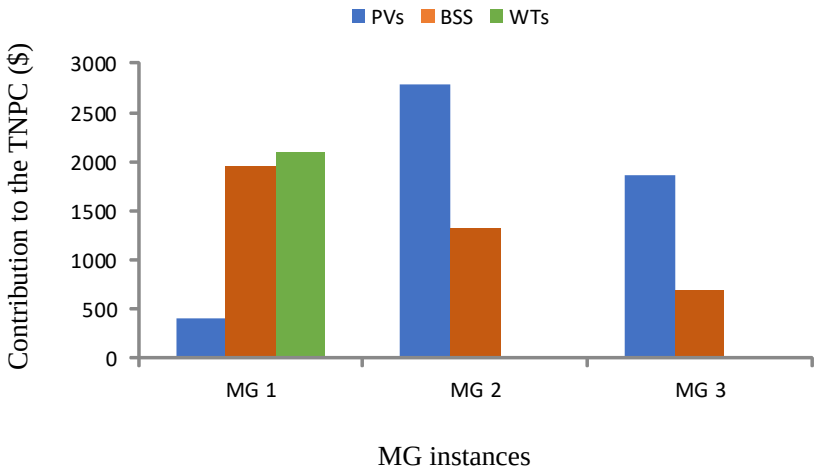

Figure 26. Breakdown of the TNPC into the net present costs of components for the three cases.

5.7. Energy flow analyses of the optimised MGs

The percentage contributions of different energy generation and consumption components to the total MG-wide energy generation and consumption are summarised in Fig. 27 for the solution set returned by the best run of the MFOA. For MG 1, approximately 85% of the total energy generation is attributable to solar PV panels, and 15% to WTs. On the consumption side, the sum of residential and commercial loads makes up around 67% of the total load, the EV-charging loads comprise around 10% of the total load, with a total loss of around 23% due to the non-ideal system conditions and unmet EV-charging loads – in view of the considered equivalent loss factor of 0.005 as the reliability index.

MGs 2 and 3 were solely driven by solar energy, meaning that solar energy is responsible for 100% of MG-wide energy produced. The energy consumption of the residential and commercial loads makes up around 52% of the total energy consumption in both cases. Also, in both cases, the EV-charging loads and total losses are responsible for around 11% and 37% of the total loads, respectively.

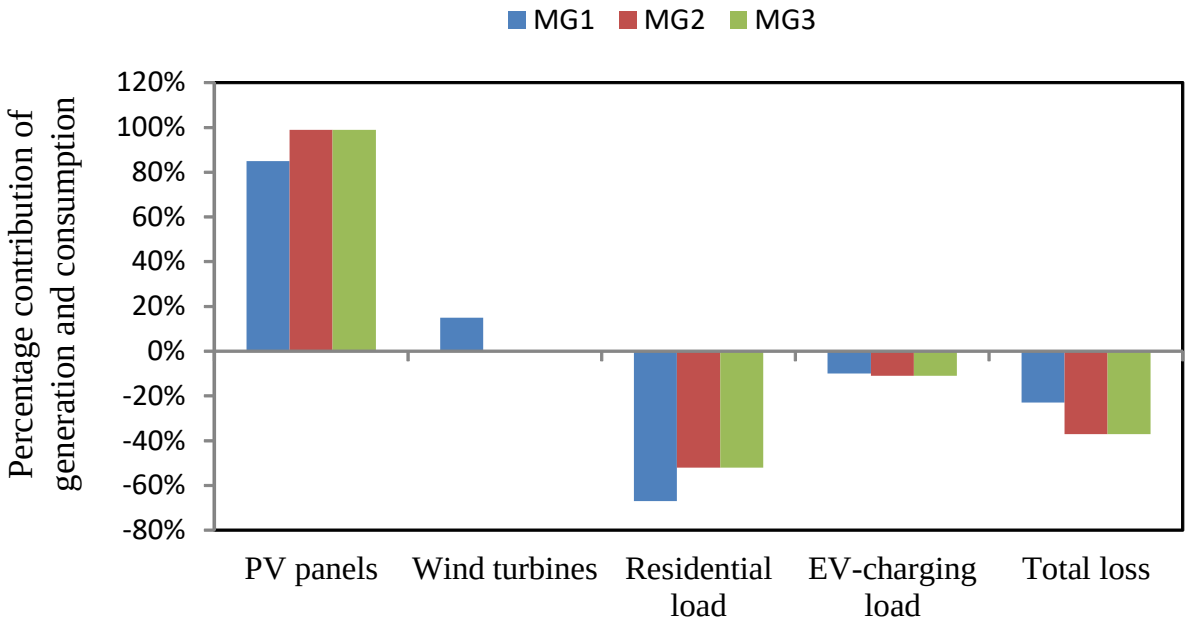

Figure 27. Balance of energy between the generation and consumption sides within the three simulated MGs.

5.8. Levelised costs of electricity of the optimised MGs

Current average retail price of domestic electricity in New Zealand is $0.29/kWh (MBIE, 2021). Table 15 presents the levelised costs of electricity of the three MG systems optimised by the proposed method in the best run of the MFOA. A comparison of the levelised costs of electricity associated with the optimised MGs with the current average retail price of electricity in New Zealand further supports the economic viability of the modelled MGs.

Table 15. Levelised costs of electricity associated with the optimised MGs.

System	LCOE ($/kWh)
MG 1	0.09
MG 2	0.10
MG 3	0.09

5.9. Capital budgeting analyses of the optimised MGs

To further support the financial sustainability of the simulated MGs using the best run of the MFOA, this section presents comprehensive financial appraisal analyses. To this end, the following three capital budgeting criteria are employed: the profitability index (PI), the discounted payback period (DPP), and the internal rate of return (IRR).

The PI refers to the ratio of the present value of the total investment over the project life-cycle to the associated capital investment expenditure. The higher the value of the PI, the

more attractive the project. The following equation can be used to calculate the PI (Gurau, 2012):

$$\text{PI} = 100 \times \frac{\sum_{t=0}^{T} I(1+i)^{-t} - TNPC}{Cap_T}, \quad (42)$$

where I is the annual income from the provisioning of energy services to end-consumers, Cap_T denotes the total capital investment in the baseline year, i is the real interest rate, and T is the expected service life of the conceptualised MG. Accordingly, it was assumed that the electricity rate is fixed at \$0.19/kWh (in New Zealand currency) for the three MGs.

The discounted payback period represents the number of years it takes to break even from undertaking the capital investment, by discounting future cash flows, and can be mathematically expressed as (Lefley, 1996):

$$\sum_{t=0}^{DPP} I(1+i)^{-t} - \text{TNPC} = 0. \quad (43)$$

The IRR represents a discount rate that makes the net present value of all discounted cash flows equal to zero (Steffen, 2020), which can be mathematically expressed as in Eq. (44). In general, the higher the IRR, the more desirable an investment project to undertake (Gurau, 2012).

$$\sum_{t=0}^{T} \frac{CF(t)}{(1+i)^t} = 0, \quad (44)$$

where $CF(t)$ denotes the net cash inflow in the t-th year of the investment.

Table 16 presents the resulting capital budgeting metrics of the three MG investment proposals. The resulting values collectively indicate that the investment proposals represent low-risk, high-yield projects, which not only would be able to provide affordable, reliable, clean electricity to the sites of interest, but would also generate a steady revenue stream for the investors.

Table 16. Capital budgeting of the three MGs.

Sys.	PI (%)	DPP (years)	IRR (%)
MG 1	2.51	7	17.93
MG 2	2.01	12	10.55
MG 3	2.46	8	17.53

5.10. Model validation: Comparison with HOMER Pro

This section validates the effectiveness of the model in nearing the globally optimum MG sizing results by benchmarking the case of Medlands against the design of a similar system using HOMER Pro. Fig. 28 displays the layout of the system simulated in the HOMER Pro software. To match the HOMER Pro model to the proposed model, the EV-charging loads were specifically profiled in the period from 9 p.m. to 5 a.m.

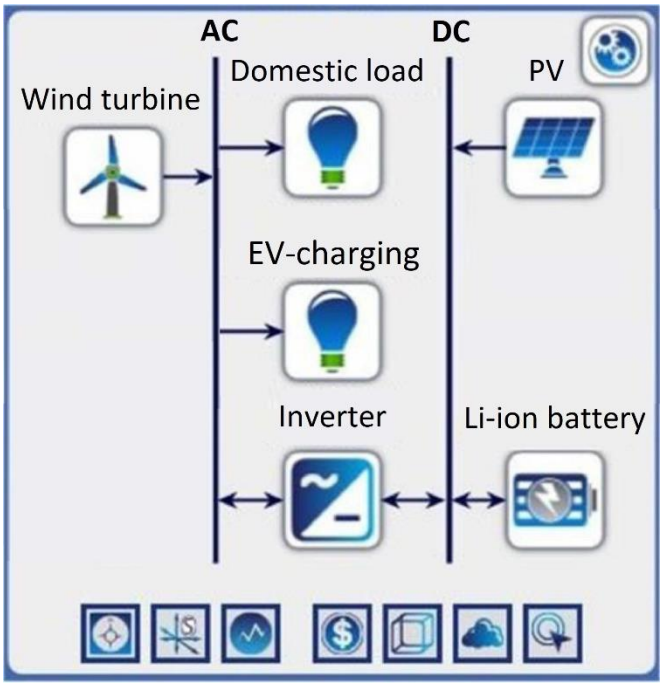

Figure 28. HOMER Pro model of the Medlands test-case system.

Table 17 presents the comparative results of the proposed model and HOMER Pro. For the proposed model, the full version with 8,760 data points was used. Also, the optimiser was selected to be the MFOA due to its verified outperformance. Furthermore, the best-case results out of the 30 trials of the MFOA were used for comparisons. It is noteworthy that given the absence of a dedicated module for EV-charging in HOMER Pro, the cost of EV chargers was added as a fixed cost to the model, similar to the proposed model where the capacity, and in turn the cost of EV-chargers is calculated exogenously to the model. Additionally, the cost of the multi-mode inverter is determined endogenously in the HOMER Pro model, whereas it is calculated outside the model based upon the peak load in the proposed model. However, given the selected reliability constraint of 100% under which the loads must always be satisfied, this does not make any difference in the optimal capacity of the inverter, as can be seen from Table 17. The table also reveals that although the percentage difference between total discounted costs in the two models is as low as 5%, with an associated lower LCOE of $0.02/kWh in the proposed model, there is a substantial difference between the resulting optimal configurations. More specifically, HOMER Pro supports a solar PV-less energy generation mix, but a larger battery storage capacity. This can be in large part attributed to the fact that the cycle-charging energy dispatch strategy in HOMER Pro is treating the residential/commercial loads and EV-charging loads in the same manner. Put differently, it allows the stationary battery storage to be discharged to the EVs, with the consequent drawing of more energy from the onsite battery bank during the light-load hours, compared to the proposed MFOA-based model, resulting in mitigated WT generation curtailment – thereby improving the economics of WT generation and undermining the economics of solar PV generation – in view of the pre-defined timing of EV charging. It should be emphasised that the total curtailed energy of the HOMER Pro model is around half

the proposed MFOA-based model with a specifically developed dispatch strategy. However, not only does the modified dispatch strategy of the proposed MG sizing model – where EV-charging loads cannot be served by releasing the energy stored in the stationary battery bank for energy efficiency reasons – result in a reduced total discounted cost solution, but it also improves the energy mix diversity necessary for energy security. On the other hand, the resilience of the system optimised by HOMER Pro against a severe outage that disrupts access to the electricity generated from the onsite renewable resources is modestly higher due to the presence of a relatively larger battery capacity – and, consequently, an improved battery bank autonomy. It should be noted that there might also be other more important factors involved in the lower cost yielded by the proposed MFOA-based model, notably using a fit-for-purpose meta-heuristic, the relative importance of which cannot be readily quantified due to the infeasibility of customising the dispatch strategy in the HOMER Pro model. Yet, collectively, the comparative results corroborate the aforementioned proposition that important dynamics are taking place around the global optima with important implications for the trade-offs between cost, energy efficiency, resilience, and security.

Table 17. Comparison of the MFOA-based model and HOMER Pro results for the Medlands case.

Output	Optimisation method	
	MFOA-based model	HOMER Pro
Total net present cost of the MG ($)	435,509	458,176
Levelised cost of energy ($/kWh)	0.09	0.11
Total curtailed energy (kWh)	41,740	22,522
PV size (no.)	102	0
WT size (no.)	3	3
Battery size (no.)	381	466
Inverter (kW)	47	47

5.11. Conclusions

This chapter has compared the efficiency of the well-established and competitively selected, state-of-the-art, herd-behaviour-oriented meta-heuristic algorithms in long-term off-grid MG planning applications. The results obtained from the application of the meta-heuristics under consideration to the MG sizing cases of interest are then comparatively evaluated. The comparative analyses of the efficiencies of the meta-heuristics have incorporated various summary statistics to systematically measure the accuracy and precision of the algorithms.

The section has then proceeded to provide comprehensive univariate sensitivity analyses that provide important insights into the robustness of the system costs and configurations to changes in load demand and power outputs of renewable energy technologies. Finally, case-specific cash flow, energy flow, and capital budgeting analyses have substantiated the technical feasibility and economic viability of the project proposals before verifying the validity of the model through a direct comparison of the results with those of the industry-leading software package for MG sizing, HOMER Pro, for the case of Medlands.

Chapter 6: Conclusions and future work

Remote, renewables-powered micro-grids (MG) have been recognised as a stepping stone towards achieving the objectives of decarbonisation and sustainable development. More specifically, localised MGs are of particular interest to areas where energy self-sufficiency and/or energy security are challenging, such as remote and island communities. The standard optimal sizing problem of stand-alone MGs seeks to determine the minimum total discounted cost associated with the variable generation, storage, and power conversion technologies that are able to reliably serve the loads subject to operational constraints. Furthermore, the wider economy-wide deep decarbonisation efforts have recently highlighted the importance of e-mobility interventions. This has given rise to the major trend of transportation and electrical energy system hybridisation to leverage the potentially significant synergies – that can provide more efficient smart, integrated energy systems – such as buffering renewable energy variability, particularly in the presence of solar photovoltaic (PV) and wind resources. However, the non-dispatchability of renewables, especially where energy storage systems are present in the candidate pool and the charging scheduling of electric vehicles (EVs) need to be coordinated, make finding the optimal strategic resource mix for MGs particularly challenging. More specifically, the nonlinearities and non-convexities involved in the relevant problem formulation make it non-amenable to exact mathematical optimisation algorithms without strong mean-field approximations, the impact of which on the optimality of the resulting solutions cannot be measured by any known means. This brings to light the importance of meta-heuristic optimisation algorithms that can be readily applied to the associated full-models of MG sizing, but at the risk of sub-optimality due to the inherently approximate dimensions involved. This is especially so in view of the so-called “no free lunch” theorem, which essentially implies that the suitable performance of no meta-heuristic can be generalised to all applications. This necessitates the comprehensive, systematic efficiency testing of state-of-the-art meta-heuristics for potential solution quality improvement when applied to NP-hard problems, including the MG capacity planning optimisation problem.

In this context, this research has sought to determine and rank a number of competitively selected, newly developed, herd-behaviour-oriented meta-heuristics in MG infrastructure planning applications. To this end, Chapter 2 has presented a comprehensive review of the literature on optimal MG sizing to determine the non-explored meta-heuristics in the field, as well as the limitations in the associated rule-based energy dispatch strategies integrated into the upper-level sizing methods, particularly in off-grid, EV-charging-load-addressable MGs. More specifically, a systematic review of the MG resource planning literature has identified the lack of attention to the following state-of-the-art meta-heuristics: the wild horse optimiser (WHO), the artificial hummingbird algorithm (AHA), the artificial gorilla troops optimiser (AGTO), the marine predator algorithm (MPA), the equilibrium optimiser (EO), and the moth-flame optimisation algorithm (MFOA). Furthermore, the review of the mainstream literature has revealed the absence of tailored EV-charging scheduling strategies in the wider MG sizing models, thereby prohibiting the associated models from producing highly efficient integrated system designs. Moreover, a number of technical, economic, social, and regulatory barriers to locally-controlled, 100%-renewable energy deployment are identified from the review. In addition, the review has identified the drivers of off-grid MG development to be addressing climate change, energy security, energy access, and socio-economic growth.

To address the identified methodological gaps in the relevant reviewed literature, Chapter 3 has presented a novel meta-heuristic-based off-grid MG sizing method, which uses net present cost valuations, the equivalent loss factor reliability index, and a specifically developed rule-based, cycle-charging dispatch strategy to determine the operational schedules of non-grid-connected MGs in the presence of EV-charging loads. Also, the chapter discusses the novel features of the formulated operational scheduling strategy, namely the minimisation of the probability of oversizing the components by discharging the battery storage to its maximum capacity during the periods where total residential/commercial loads fall short of total renewable power generation, as well as using distinct rules for serving residential/commercial and EV-charging loads. The proposed model has been parametrised for two stand-alone, battery-supported system topologies feeding residential/commercial and EV-charging loads. The first system is driven by a combination of solar PV panels and WTs, whereas the second system is driven by solar PV panels alone. A further salient feature of the proposed model is considering separate reliability indices for meeting residential/commercial and EV-charging loads, based on which distinct penalty factors have been formulated.

Chapter 4 has presented and discussed the meteorological and load demand data forecasts used to populate the notional MGs for the cases of Medlands, Tryphena, and Mulberry Grove sites on Aotea–Great Barrier Island, Aotearoa–New Zealand. The forecasted time-series data of the sites of interest – solar irradiance, wind speed, residential/commercial loads, and EV-charging loads – have also been comparatively analysed. Furthermore, the underlying differences in the devised rule-based scheduling strategy of EV-charging loads in the three cases of interest have been explained. The derived time-series data are utilised as inputs to the proposed meta-heuristic-based off-grid MG sizing model parametrised for the conceptual MGs.

The numeric simulation results obtained from the application of the proposed model to the three cases of interest are presented and discussed in Chapter 5. More specifically, using a statistics-oriented meta-heuristic performance ranking technique and based on the total net present costs obtained over 30 independent simulation runs of the three test-case problems, the following rank order has been established for the meta-heuristics under comparison: the MFOA > the AGTO > the MPA > the AHA > the PSO > the WHO > the EO. The results corroborate the previous findings on the suitability of the MFOA for MG capacity planning optimisation applications. To generate insights into the contribution of serving the EV-charging loads to the total discounted system costs, e-mobility-less simulations have also been carried out, which demonstrate that serving EV-charging loads makes up a relatively significant portion of the associated system costs. Also, for the case that integrates both solar PV and wind resources (Medlands), specific solar PV-less and WT-less simulations have shown the considerable role of the associated seasonal and day-to-day complementarities in power outputs of solar PV and WT generation systems in reducing the associated total costs. Furthermore, comprehensive univariate sensitivity analyses have explored the effects of variation in load demand, solar irradiance, and wind speed on the resulting MG cost and configuration solutions. The sensitivity analyses have also provided insights into the sensitivity of the MG sizing solutions to changes in various time-series data. Given the computational expensiveness of the problem, an effective input data reduction technique has also been developed to ensure the tractability of the sensitivity analyses. A comparison of the full (with 8,760 data points) and reduced (with 288 data points) model variants for one run of each of the three cases (using the superior MFOA algorithm) has also verified the validity of the input data reduction technique, with the percentage deviation of the total cost found to be

0.05%, 0.6%, and 2% respectively for the cases of Medlands, Tryphena, and Mulberry Grove, respectively. Moreover, comprehensive cash flow and energy flow analyses have respectively shown the financial and energy balance of the optimised MGs. In addition, specific capital budgeting analyses using the profitability index, the discounted payback period index, and the internal rate of return index have substantiated the economic sustainability of the project proposals. A comparison of the associated levelised costs of electricity with the current average retail price of domestic electricity in New Zealand have provided an additional layer of evidence on the financial viability of the projects.

6.1. Recommendations for future research

There exist several opportunities for further work to improve the practical utility of the proposed modelling framework, which can be summarised as follows:

1. Quantifying the uncertainties associated with data forecasts – notably power outputs from variable renewable energy technologies and load demand – in a probabilistic manner to tailor the MG planning decisions to the tolerable degree of risk of the communities.

2. Incorporating a hybrid opt-in/opt-out demand response programme into the proposed model to more effectively coordinate the charging of EV loads, whilst additionally considering the discharge potential of EVs for supporting highly-renewable, off-grid MGs towards reducing the capacity of capital-intensive stationary storage.

3. Characterising the interactions between the MG operator and EV owners in demand-side management programmes to compare and contrast the impact of the strategic (self-interested) and pro-social behaviours on the optimal size of the components, and in turn, the total cost of the system.

4. Comparing the efficiency of the selected meta-heuristics in other MG topologies and configurations, including grid-connected MGs and those integrating different generation and storage technologies, such as micro-hydro and hydrogen-based energy storage systems (incorporating electrolysers, hydrogen tanks, and fuel cells).

5. Considering the dynamic nature of the efficiencies of the power electronics devices and the nonlinearities in the power outputs of solar PV and wind generation plants to minimise the so-called “simulation-to-reality” gaps and better reflect reality.

Appendix A: Barriers to and drivers of MG development

This appendix summarises and sub-categorises the identified barriers to the development of highly-renewable micro-grids before outlining their drivers, identified from the review of the relevant literature. Specifically, Table A1 lists the identified technical, economic, social, and regulatory barriers, while Table A2 lists the associated drivers. The tables, additionally, provide the relevant important remarks and the corresponding notable sources.

Table A1. Summary of the barriers to the development of MGs.

Barrier	Sub-category	Remarks	Reference(s)
Technical	Non-dispatchable renewable resources	The degree of complexity of MG sizing increases as the dimension of the system components increases due to the correlations that exist between the associated uncertain factors, notably given the complementarities of different renewable energy sources.	(Kumar *et al.*, 2016)
	Energy storage complexities	There exist salient inadequacies with regard to the standards and guidelines of energy storage integration that are critical for the reliable operation of highly-renewable MGs.	(Radosavljevic *et al.*, 2016)
	Lack of operation and maintenance culture	Given that renewable energy technology is comparatively new and less optimally developed, there exists a lack of knowledge and expertise in operation and maintenance.	(Seetharaman *et al.*, 2019)
Economic	Competition with fossil fuels	Fossil fuels (mainly coal, natural gas, and oil) are still expected to supply 78% of the global energy used (aggregated over all sectors) in 2040.	(EIA, 2016)
	Subsidies of energy generation	In developing, fossil fuel-exporting countries, fossil fuel-fired power plants are still receiving significantly higher government subsidies compared to renewable energy generation schemes.	(Financial Tribute, 2021)
	Renewable energy investment with limited financing institutions	Securing financing at competitive rates with those of fossil fuel energy projects is a substantial barrier for renewable energy developers in the developing world. Accordingly, a hybrid debt-equity finance	(Krupa *et al.*, 2019)

		structure is promoted in the literature.	
	Cost of capital	Both energy-as-a-service and community-financed business models suffer from high initial capital costs – an issue that is more pronounced where more stringent lending standards are in place, making it more difficult to borrow money without having substantial credit.	(Ansari *et al.*, 2013)
Social	Symbolic aspects of facility siting	Rhetorical and communicative dimensions at the social-psychological level can positively impact the decisions of individuals and local communities involved in renewable energy siting disputes.	(Steffen *et al.*, 2018), (Devine-Wright, 2007)
	Not-in-my-backyard phenomenon	The notable reasons behind the not-in-my-backyard behaviour are found to be landscape impact, environmental degradation, noise concerns, government giveaways of public lands to private solar and wind farm developers, and lowering local property values.	(Grafström *et al.*, 2020), (Nasirov *et al.*, 2015), (Smith and Klick, 2007)
	Land use	Direct involvement of communities in renewable energy planning and land use zoning has been recognised as an effective policy to alleviate land use concerns.	(Nesamalar *et al.*, 2017), (Gross, 2020)
	Lack of skilled labour	Driving the renewable energy transformation requires additional investment and innovation in higher education, as well as long-term investments in staffing.	(Karakaya and Sriwannawit, 2015)
Regulatory	Lack of legal frameworks and standards	There is a lack of standardised legal frameworks for independent electricity generators to enter the market and invest in sustainable energy systems with energy-as-a-service business models.	(Sun and Nie, 2015), (Beck and Levine, 2004)
	Limited transmission line access	Monopoly utilities may not allow emerging renewable energy generation companies to fairly access the transmission lines.	(Zhang *et al.*, 2014), (Beck and Levine, 2004)

Liability insurance requirements	Additional liability insurance is required for the so-called "islanding" issue.	(Stokes, 2013), (Beck and Levine, 2004)
Lack of equipment standards	Effective development of the relevant standards requires extensive verification processes based on benchmarking against a set of criteria.	(Emodi *et al.*, 2014)

Table A2. Summary of the drivers of the development of MGs.

Driver	Remarks	Reference(s)
Climate change mitigation	Given the fact that energy use accounts for around two-thirds of total greenhouse gas emissions with the power generation sector recognised as a major contributor, decarbonisation of the energy sector, including the power sector, using renewables is at the forefront of climate change mitigation efforts.	(Shah Danish *et al.*, 2019)
Energy security	The use of local renewable energy systems that use well-diversified technologies has been shown in the literature to be able to increase energy security in remote, off-grid applications, whilst additionally reducing the associated energy costs.	(Verbruggen *et al.*, 2010)
Energy access	The emergence of advanced, smart MGs, accompanied by unprecedented improvements in the cost-effectiveness and efficiency of renewable and storage technologies, has provided an effective platform to accelerate the progress in electrifying remote and low-income communities.	(Shieh, Ersal and Peng, 2019)
Socio-economic growth	Off-grid, integrated, smart energy systems that produce electricity locally using renewable energy sources are found to be an effective tool for sustainable rural development with their potential to deliver multi-faceted socio-economic benefits, including net job creation and greater social inclusiveness.	(IRENA, 2017)

Appendix B

B1. Appliance classification

The classification of the considered appliances is conducted based on consumer usage patterns, power ratings, and load segments. The following three general consumption patterns were used to approximate the load duration of the appliances.

Pattern 1: Continuously running appliances, which are never switched off, such as fridges and freezers. The energy consumption of such appliances, which can be of the type single- or multi-state, depends on the season and usage per person (Larson, Davis and Uslan, 2014).

Pattern 2: Occasionally running appliances, which are often not used more than one time per day – usually in the morning and evening hours. Examples include washing machines and clothes dryers, the consumption pattern of which is, to a great extent, user-behaviour-dependent.

Pattern 3: Frequently switched on and off appliances with variable power consumption, which are run during specific periods of time; for example, lighting loads. The frequency and magnitude of the loads in this category also depend on the season and usage per person.

Table B1 indexes various household appliances and maps them to the above-mentioned three patterns.

Table B1. Indexed household appliances mapped to the defined usage patterns.

Type	Appliance	Pattern
A	Cold appliances: fridge and freezer	1
B	Audio-visual: music system, speaker, and modem	2
C	Audio-visual: television, radio, laptop, scanner, and printer	2
D	Washing: washing machine, clothes dryer, and dishwasher Others: vacuum cleaner	2
E	Cooking: microwave and coffee machine	2
G	Charging accessory: phone charger	2
H	Fan	2
F	Lighting: LED lights and tube lights	3

Furthermore, Tables B2 and B3 respectively present the detailed specifications of the residential and commercial loads considered for integration into the three MGs. The associated specifications of the appliances include the rated power (kW), the average number of devices (per household and per commercial building), the usage time (hours), and the energy consumption per day (kWh/day). The associated specifications are defined in accordance with the relevant appliance classes mentioned above.

Table B2. Detailed specifications of the residential appliances.

Appliance	Rated power (kW)	Average number of devices per household	Usage duration (h)	Total load per day (kWh/day)	Consumption type
LED lights	0.009	3	5	0.13	F
Small refrigerator	0.100	1	24	2.40	A
Phone charging unit	0.005	2	2	0.02	G
Radio	0.004	1	4	0.02	H
Computer	0.200	1	8	1.60	C
Washing machine	0.500	1	0.29	0.14	D
Dishwasher	0.500	1	1	0.5	D
Fan	0.200	1	5	1.00	H
Microwave	0.900	1	0.5	0.45	E
Internet modem	0.010	1	24	0.24	B
Scanner	0.010	1	2	0.02	C
Printer	0.005	1	0.5	0.00	C
Loudspeaker	0.050	1	0	0.00	B
Vacuum cleaner	1.000	1	0.14	0.14	D
Coffee machine	0.600	1	0	0.00	E

Table B3. Detailed specifications of the commercial appliances.

Commercial appliance	Rated power (kW)	Number of devices per commercial user	Usage duration (h)	Total load per day (kWh/day)	Consumption Type
LED lights	0.009	10	6	0.51	F
Display fridge	0.300	4	24	28.80	A
Phone charging unit	0.005	2	4	0.04	G
Radio	0.004	1	6	0.02	H
Library computers	0.200	4	4	3.20	C
Laundromat (medium and large) washer	0.500	3	12	18.00	D
Laundromat (medium and large) dryer	4.000	3	12	144.00	D
Dishwasher	0.500	1	2	1.00	D
Deep freezer	0.500	3	24	36.00	A
Fan	0.200	2	3	1.20	H
Microwave	0.900	2	4	7.20	E
Internet modem	0.010	2	6	0.12	B
Scanner	0.010	1	4	0.04	C
Printer	0.005	1	6	0.03	C
Loudspeaker	0.050	1	0	0.00	B

Vacuum cleaner	1.000	1	0.5	0.50	D
Coffee machine	0.600	1	1	0.60	E
LED tube light	18.000	1	4	72.000	F
Disco lights	0.003	1	4	0.012	F
Music system	0.025	1	4	0.100	B

B2. Energy consumption pattern

Figs. B1–B3 show the typical energy consumption profiles of the households (MGs 1–3), the commercial loads (MGs 1–3), and the pub (MG 2), respectively.

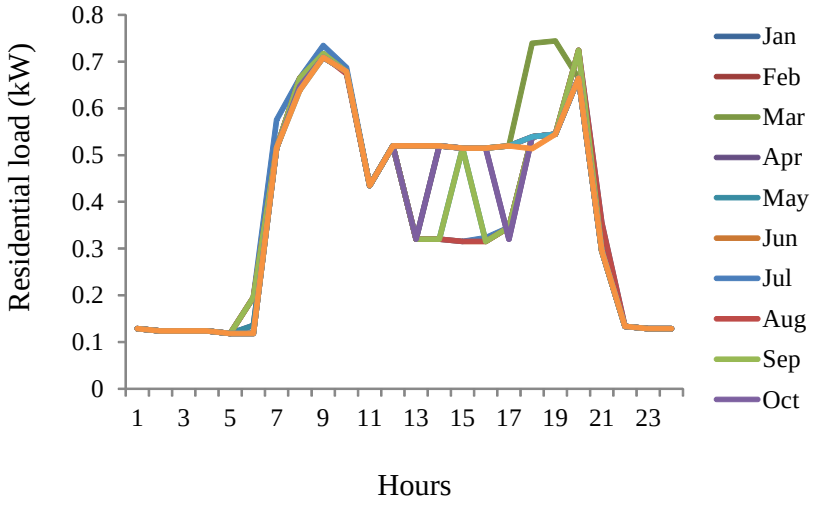

Figure B1. Monthly mean daily household energy consumption profile for the three MGs.

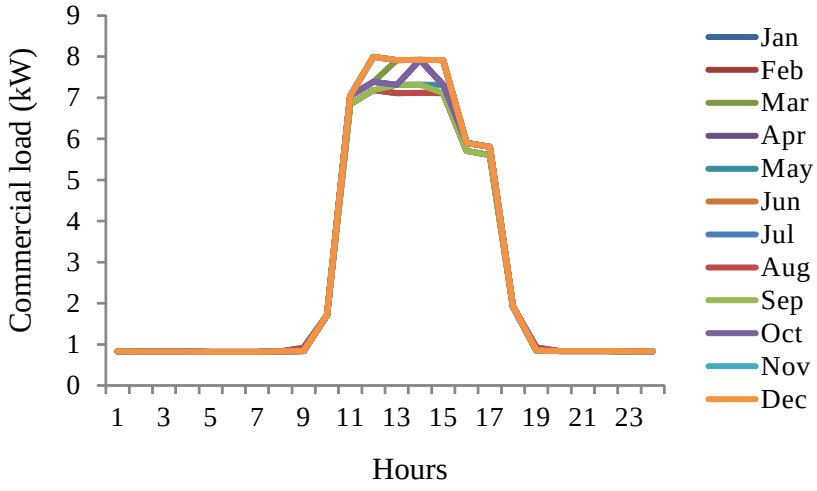

Figure B2. Monthly mean daily commercial building energy consumption profile for the three MGs.

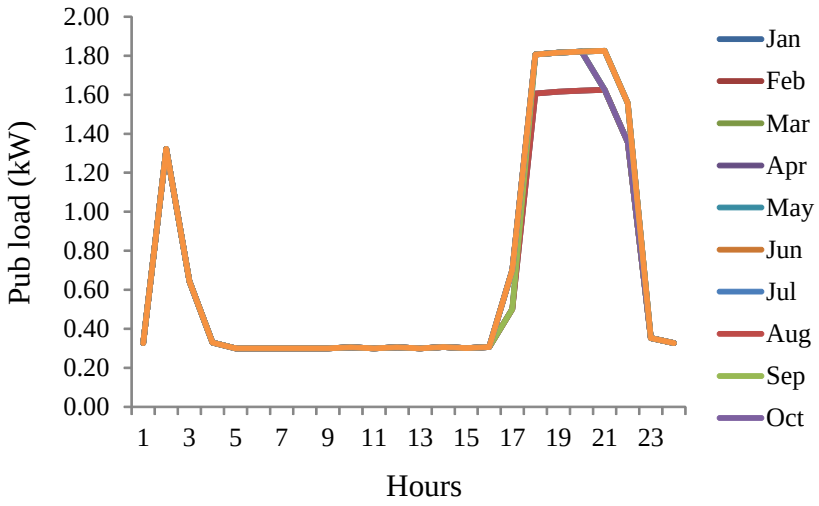

Figure B3. Monthly mean daily energy consumption profile of a pub on the Tryphena site (MG 2).

References

‘2018 Census Latest news about 2018 Census’ (2020), pp. 1–21. Available at: https://www.stats.govt.nz/2018-census/.

Abdollahzadeh, B., Soleimanian Gharehchopogh, F. and Mirjalili, S. (2021) ‘Artificial gorilla troops optimizer: A new nature-inspired metaheuristic algorithm for global optimization problems’, *International Journal of Intelligent Systems*, 36(10), pp. 5887–5958. doi: 10.1002/int.22535.

Afrooz, A. A. *et al.* (2019) ‘Retail Electricity Pricing Impacts on Demand Response and Electrical Vehicles Planning in Residential Micro-grid’, *2019 Iranian Conference on Renewable Energy and Distributed Generation, ICREDG 2019*, pp. 11–12. doi: 10.1109/ICREDG47187.2019.190267.

Agua, O. F. B. *et al.* (2020) ‘Decentralized versus clustered microgrids: An energy systems study for reliable off-grid electrification of small islands’, *Energies*, 13(17). doi: 10.3390/en13174454.

Ahmed, D. *et al.* (2021) ‘Multi-objective energy management of a micro-grid considering stochastic nature of load and renewable energy resources’, *Electronics (Switzerland)*, 10(4), pp. 1–22. doi: 10.3390/electronics10040403.

Alam, M. N., Chakrabarti, S. and Ghosh, A. (2019) ‘Networked Microgrids : State-of-the-Art and’, *IEEE Transactions on Industrial Informatics*, 15(3), pp. 1238–1250.

Alharthi, M. *et al.* (2021) ‘A Multi-Objective Marine Predator Optimizer for Optimal Techno-Economic Operation of AC/DC Grids’, *Studies in Informatics and Control*, 30(2), pp. 89–99. doi: 10.24846/v30i2y202108.

Ali, M. *et al.* (2021) ‘Design of cascaded pi-fractional order PID controller for improving the frequency response of hybrid microgrid system using gorilla troops optimizer’, *IEEE Access*, 9, pp. 150715–150732. doi: 10.1109/ACCESS.2021.3125317.

AlSkaif, T. *et al.* (2017) ‘A distributed power sharing framework among households in microgrids: a repeated game approach’, *Computing*, 99(1), pp. 23–37. doi: 10.1007/s00607-016-0504-y.

Alsmadi, Y. M. *et al.* (2019) ‘Optimal configuration and energy management scheme of an isolated micro-grid using Cuckoo search optimization algorithm’, *Journal of the Franklin Institute*, 356(8), pp. 4191–4214. doi: 10.1016/j.jfranklin.2018.12.014.

Altbawi, S. M. A., Bin Mokhtar, A. S. and Arfeen, Z. A. (2021) ‘Enhacement of microgrid technologies using various algorithms’, *Turkish Journal of Computer and Mathematics Education*, 12(7), pp. 1127–1170.

Ansari, M. F. *et al.* (2013) ‘Analysis of barriers to implement solar power installations in India using interpretive structural modeling technique’, *Renewable and Sustainable Energy Reviews*, 27, pp. 163–174. doi: 10.1016/j.rser.2013.07.002.

Augustine, N. *et al.* (2012a) ‘Economic dispatch for a microgrid considering renewable energy cost functions’, *2012 IEEE PES Innovative Smart Grid Technologies, ISGT 2012*, pp. 1–7. doi: 10.1109/ISGT.2012.6175747.

Augustine, N. *et al.* (2012b) ‘Economic dispatch for a microgrid considering renewable energy cost functions’, *2012 IEEE PES Innovative Smart Grid Technologies, ISGT 2012*, pp. 1–7. doi: 10.1109/ISGT.2012.6175747.

Badal, F. R. *et al.* (2019) 'A survey on control issues in renewable energy integration and microgrid', *Protection and Control of Modern Power Systems*, 4(1). doi: 10.1186/s41601-019-0122-8.

Baños, R. *et al.* (2011) 'Optimization methods applied to renewable and sustainable energy: A review', *Renewable and Sustainable Energy Reviews*, 15(4), pp. 1753–1766. doi: 10.1016/j.rser.2010.12.008.

Bayoumi, A. S. A., El-Sehiemy, R. A. and Abaza, A. (2021) 'Effective PV Parameter Estimation Algorithm Based on Marine Predators Optimizer Considering Normal and Low Radiation Operating Conditions', *Arabian Journal for Science and Engineering*, (0123456789). doi: 10.1007/s13369-021-06045-0.

Beck, T. and Levine, R. (2004) 'Stock markets, banks, and growth: Panel evidence', *Journal of Banking and Finance*, 28(3), pp. 423–442. doi: 10.1016/S0378-4266(02)00408-9.

Billinton, R. and Huang, D. (2008) 'Electric System Reliability Evaluation', *Power*, 23(2), pp. 418–425.

Blum, C. *et al.* (2011) 'Hybrid metaheuristics in combinatorial optimization: A survey', *Applied Soft Computing Journal*, 11(6), pp. 4135–4151. doi: 10.1016/j.asoc.2011.02.032.

Blum, C. and Roli, A. (2003) 'Metaheuristics in Combinatorial Optimization: Overview and Conceptual Comparison', *ACM Computing Surveys*, 35(3), pp. 268–308. doi: 10.1145/937503.937505.

Cagnano, A., De Tuglie, E. and Bronzini, M. (2018) 'Multiarea voltage controller for active distribution networks', *Energies*, 11(3). doi: 10.3390/en11030583.

Cetinbas, I., Tamyurek, B. and Demirtas, M. (2019) 'Energy management of a PV energy system and a plugged-in electric vehicle based micro-grid designed for residential applications', *8th International Conference on Renewable Energy Research and Applications, ICRERA 2019*, pp. 991–996. doi: 10.1109/ICRERA47325.2019.8997025.

Chaspierre, G., Panciatici, P. and Cutsem, T. Van (2017a) 'Dynamic equivalent of a distribution grid hosting dispersed photovoltaic units', *... Symposium: X Bulk Power ...*.

Chaspierre, G., Panciatici, P. and Cutsem, T. Van (2017b) 'Dynamic equivalent of a distribution grid hosting dispersed photovoltaic units', *... Symposium: X Bulk Power ...*. Available at: https://orbi.uliege.be/handle/2268/212146.

Chen, S. X., Gooi, H. B. and Wang, M. Q. (2012) 'Sizing of energy storage for microgrids', *IEEE Transactions on Smart Grid*, 3(1), pp. 142–151. doi: 10.1109/TSG.2011.2160745.

Cliflo (no date) 'CliFlo', pp. 1–2. Available at: https://niwa.co.nz/information-services/cliflo.

'Create SolarView Version: 1.1.1 ©2019 NIWA Terms and Conditions' (2019), p. 2019. Available at: https://solarview.niwa.co.nz/.

Cronin et al. (2008) 'Undertaking a literature review: a step by-step approach', *Nursing*, 17(1), p. 38. doi: 10.1097/01.NURSE.0000369871.07714.39.

Dalton, G. *et al.* (2015) 'Economic and socio-economic assessment methods for ocean renewable energy: Public and private perspectives', *Renewable and Sustainable Energy Reviews*, 45, pp. 850–878. doi: 10.1016/j.rser.2015.01.068.

Deb, K. (2001) 'Self-Adaptive Genetic Algorithms with', *Evolutionary Computation*, 9(2), pp. 197–221.

Devine-Wright, P. (2007) 'Reconsidering public attitudes and public acceptance of renewable energy technologies : a critical review', *Architecture*, Working Pa(February), pp. 1–15. Available at: http://geography.exeter.ac.uk/beyond_nimbyism/deliverables/bn_wp1_4.pdf.

Diaf, S. *et al.* (2008) 'Design and techno-economical optimization for hybrid PV/wind system under various meteorological conditions', *Applied Energy*, 85(10), pp. 968–987. doi: 10.1016/j.apenergy.2008.02.012.

Divya, K. C. and Østergaard, J. (2009) 'Battery energy storage technology for power systems-An overview', *Electric Power Systems Research*, 79(4), pp. 511–520. doi: 10.1016/j.epsr.2008.09.017.

Dragoi, E. N. and Dafinescu, V. (2021) 'Review of metaheuristics inspired from the animal kingdom', *Mathematics*, 9(18), pp. 1–52. doi: 10.3390/math9182335.

Dulal, H. B. *et al.* (2013) 'Renewable energy diffusion in Asia: Can it happen without government support?', *Energy Policy*, 59(2013), pp. 301–311. doi: 10.1016/j.enpol.2013.03.040.

Edris, A. (2012) 'Opportuunities and Challenges of Integrating Wind, Solar and other Distributed Generation & Energy Storage', *Quanta Technology*, p. 32.

EIA (2016) *International Energy Outlook 2016*. Available at: https://www.eia.gov/outlooks/ieo/pdf/0484(2016).pdf.

'Electricity cost and price monitoring' (2021) *Ministry of Business, Innovation and Employment*, pp. 23–26. Available at: http://www.mbie.govt.nz/info-services/sectors-industries/energy/energy-data-modelling/statistics/prices/electricity-prices.

Elsayed, A. T., Mohamed, A. A. and Mohammed, O. A. (2015) 'DC microgrids and distribution systems: An overview', *Electric Power Systems Research*, 119, pp. 407–417. doi: 10.1016/j.epsr.2014.10.017.

Emodi, V. N., Yusuf, S. D. and Boo, K.-J. (2014) 'The Necessity of the Development of Standards for Renewable Energy Technologies in Nigeria', *Smart Grid and Renewable Energy*, 05(11), pp. 259–274. doi: 10.4236/sgre.2014.511024.

Faramarzi, A. *et al.* (2020) 'Equilibrium optimizer: A novel optimization algorithm', *Knowledge-Based Systems*, 191. doi: 10.1016/j.knosys.2019.105190.

'Financial tribute' (2021), (December). Available at: https://www.a-tribute-to-financial-planning.com/.

Fouskakis, D. and Draper, D. (2002) 'Stochastic optimization: A review', *International Statistical Review*, 70(3), pp. 315–349. doi: 10.1111/j.1751-5823.2002.tb00174.x.

Gamarra, C. and Guerrero, J. M. (2015) 'Computational optimization techniques applied to microgrids planning: A review', *Renewable and Sustainable Energy Reviews*, 48, pp. 413–424. doi: 10.1016/j.rser.2015.04.025.

'Global Fossil Fuel consumption' (2019), pp. 1–25. Available at: https://ourworldindata.org/fossil-fuels.

Grafström, J. *et al.* (2020) 'Government support to renewable energy R&D: drivers and strategic interactions among EU Member States', *Economics of Innovation and New Technology*, 0(0), pp. 1–24. doi: 10.1080/10438599.2020.1857499.

Gross, S. (2020) 'Renewables, Land Use, and Local Opposition in the United States Executive Summary', *Foreight Policy at Brookings*, (January), pp. 1–24.

Gruber, J. K. and Prodanovic, M. (2012) 'Residential energy load profile generation using a probabilistic approach', *Proceedings - UKSim-AMSS 6th European Modelling Symposium, EMS 2012*, pp. 317–322. doi: 10.1109/EMS.2012.30.

Gurau, M. A. (2012) 'The use of Profitability Index in Economic Evaluation of Industrial Investment Projects', *Proceedings in Manufacturing Systems*, 7(1), pp. 55–58.

Haddadian, H. and Noroozian, R. (2017) 'Multi-microgrids approach for design and operation of future distribution networks based on novel technical indices', *Applied Energy*, 185, pp. 650–663. doi: 10.1016/j.apenergy.2016.10.120.

Hainz, C. and Kleimeier, S. (2012) 'Political risk, project finance, and the participation of development banks in syndicated lending', *Journal of Financial Intermediation*, 21(2), pp. 287–314. doi: 10.1016/j.jfi.2011.10.002.

Hlal, M. I. *et al.* (2019) 'NSGA-II and MOPSO based optimization for sizing of hybrid PV / wind / battery energy storage system', *International Journal of Power Electronics and Drive Systems*, 10(1), pp. 463–478. doi: 10.11591/ijpeds.v10n1.pp463-478.

Hosseinnia, H. and Tousi, B. (2019) 'Optimal operation of DG-based micro grid (MG) by considering demand response program (DRP)', *Electric Power Systems Research*, 167(October 2018), pp. 252–260. doi: 10.1016/j.epsr.2018.10.026.

Huang, Z. *et al.* (2019) 'Modeling and multi-objective optimization of a stand-alone PV-hydrogen-retired EV battery hybrid energy system', *Energy Conversion and Management*, 181(August 2018), pp. 80–92. doi: 10.1016/j.enconman.2018.11.079.

Hussain, A., Bui, V. H. and Kim, H. M. (2017) 'Optimal operation of hybrid microgrids for enhancing resiliency considering feasible islanding and survivability', *IET Renewable Power Generation*, 11(6), pp. 846–857. doi: 10.1049/iet-rpg.2016.0820.

Iqbal, M. *et al.* (2014) 'Optimization classification, algorithms and tools for renewable energy: A review', *Renewable and Sustainable Energy Reviews*, 39, pp. 640–654. doi: 10.1016/j.rser.2014.07.120.

IRENA (2013) 'International Standardisation in the Field of Renewable Energy', (March), p. 74. Available at: http://www.irena.org/DocumentDownloads/Publications/International_Standardisation_in_the_Field_of_Renewable_Energy.pdf.

IRENA (2017) 'Renewable Energy Benefits: Understanding the Socio-Economics', pp. 1–16. Available at: https://www.irena.org/-/media/Files/IRENA/Agency/Publication/2017/Nov/IRENA_Understanding_Socio_Economics_2017.pdf?la=en&hash=C430B7EF772BA0E631190A75F7243B992211F102.

Jeslin Drusila Nesamalar, J., Venkatesh, P. and Charles Raja, S. (2017) 'The drive of renewable energy in Tamilnadu: Status, barriers and future prospect', *Renewable and Sustainable Energy Reviews*, 73(January), pp. 115–124. doi: 10.1016/j.rser.2017.01.123.

Jin, S., Wang, S. and Fang, F. (2021) 'Game theoretical analysis on capacity configuration for microgrid based on multi-agent system', *International Journal of Electrical Power and Energy Systems*, 125(August 2020), p. 106485. doi: 10.1016/j.ijepes.2020.106485.

Jong, K. (1988) 'Learning with genetic algorithms: An overview', *Machine Learning*, 3(2–3), pp. 121–138. Available at: http://www.springerlink.com/index/10.1007/BF00113894.

Kaldellis, J. K. (2002) 'Parametrical investigation of the wind-hydro electricity production solution for Aegean Archipelago', *Energy Conversion and Management*, 43(16), pp. 2097–2113. doi: 10.1016/S0196-8904(01)00168-6.

Karakaya, E. and Sriwannawit, P. (2015) 'Barriers to the adoption of photovoltaic systems: The state of the art', *Renewable and Sustainable Energy Reviews*, 49, pp. 60–66. doi: 10.1016/j.rser.2015.04.058.

Karuppasamypandiyan, M. *et al.* (2019) 'An Efficient Non-dominated sorting Genetic algorithm II (NSGA II) for Optimal Operation of Micro grid', *2019 International Conference on Clean Energy and Energy Efficient Electronics Circuit for Sustainable Development, INCCES 2019*, (Nsga Ii). doi: 10.1109/INCCES47820.2019.9167747.

Karytsas, S. and Theodoropoulou, H. (2014) 'Socioeconomic and demographic factors that influence publics' awareness on the different forms of renewable energy sources', *Renewable Energy*, 71, pp. 480–485. doi: 10.1016/j.renene.2014.05.059.

Kawakami, N. *et al.* (2010) 'Development and field experiences of stabilization system using 34MW NAS batteries for a 51MW Wind farm', *IEEE International Symposium on Industrial Electronics*, pp. 2371–2376. doi: 10.1109/ISIE.2010.5637487.

Kennedy, J. and Eberhart, R. (2005) 'Particle Swarm Optimization', *Proceedings of ICNN'95-international*, 71(706), pp. 968–975. doi: 10.1299/kikaia.71.968.

Kerboua, A., Boukli-Hacene, F. and Mourad, K. A. (2020) 'Particle swarm optimization for micro-grid power management and load scheduling', *International Journal of Energy Economics and Policy*, 10(2), pp. 71–80. doi: 10.32479/ijeep.8568.

Krupa, J., Poudineh, R. and Harvey, L. D. D. (2019) 'Renewable electricity finance in the resource-rich countries of the Middle East and North Africa: A case study on the Gulf Cooperation Council', *Energy*, 166, pp. 1047–1062. doi: 10.1016/j.energy.2018.10.106.

Kumar, V., Pandey, A. S. and Sinha, S. K. (2016) 'Grid integration and power quality issues of wind and solar energy system: A review', *International Conference on Emerging Trends in Electrical, Electronics and Sustainable Energy Systems, ICETEESES 2016*, 2011, pp. 71–80. doi: 10.1109/ICETEESES.2016.7581355.

Kwon, K. H. *et al.* (2006) 'A two-dimensional modeling of a lithium-polymer battery', *Journal of Power Sources*, 163(1 SPEC. ISS.), pp. 151–157. doi: 10.1016/j.jpowsour.2006.03.012.

Larson, B., Davis, R. and Uslan, J. (2014) 'Is Your Refrigerator Running ? Energy Use and Load Shapes for Major Household Appliances', *ACEEE Summer Study on Energy Efficiency in Buildings*, pp. 235–246.

Lefley, F. (1996) 'The payback method of investment appraisal: A review and synthesis', *International Journal of Production Economics*, 44(3), pp. 207–224. doi: 10.1016/0925-5273(96)00022-9.

Lekvan, A. A. *et al.* (2021) 'Robust optimization of renewable-based multi-energy micro-grid integrated with flexible energy conversion and storage devices', *Sustainable Cities and Society*, 64(June 2020), p. 102532. doi: 10.1016/j.scs.2020.102532.

Leung, P. *et al.* (2012) 'Progress in redox flow batteries, remaining challenges and their applications in energy storage', *RSC Advances*, 2(27), pp. 10125–10156. doi: 10.1039/c2ra21342g.

Liu, X. *et al.* (2010) 'Dynamic economic dispatch for microgrids including battery energy storage', *2nd International Symposium on Power Electronics for Distributed Generation Systems, PEDG 2010*, (2), pp. 914–917. doi: 10.1109/PEDG.2010.5545768.

Liu, Z. *et al.* (2020) 'Optimal planning and operation of dispatchable active power resources for islanded multi-microgrids under decentralised collaborative dispatch framework', *IET Generation, Transmission and Distribution*, 14(3), pp. 408–422. doi: 10.1049/iet-gtd.2019.0796.

Lu, T. *et al.* (2017) 'Interactive Model for Energy Management of Clustered Microgrids', *IEEE Transactions on Industry Applications*, 53(3), pp. 1739–1750. doi: 10.1109/TIA.2017.2657628.

Mahmoud, M. S., Azher Hussain, S. and Abido, M. A. (2014) 'Modeling and control of microgrid: An overview', *Journal of the Franklin Institute*, 351(5), pp. 2822–2859. doi: 10.1016/j.jfranklin.2014.01.016.

Manfren, M., Caputo, P. and Costa, G. (2011) 'Paradigm shift in urban energy systems through distributed generation: Methods and models', *Applied Energy*, 88(4), pp. 1032–1048. doi: 10.1016/j.apenergy.2010.10.018.

Mavrotas, G. (2009) 'Effective implementation of the ε-constraint method in Multi-Objective Mathematical Programming problems', *Applied Mathematics and Computation*, 213(2), pp. 455–465. doi: 10.1016/j.amc.2009.03.037.

MBIE (2020a) 'Energy in New Zealand', *Energy & Buildings Trends*, p. 71.

MBIE (2020b) 'Wind Generation Stack Update: Version 2.0: Final', (June).

Mendes, G., Ioakimidis, C. and Ferrão, P. (2011) 'On the planning and analysis of Integrated Community Energy Systems: A review and survey of available tools', *Renewable and Sustainable Energy Reviews*, 15(9), pp. 4836–4854. doi: 10.1016/j.rser.2011.07.067.

Mirjalili, S. (2015) 'Moth-flame optimization algorithm: A novel nature-inspired heuristic paradigm', *Knowledge-Based Systems*, 89(July), pp. 228–249. doi: 10.1016/j.knosys.2015.07.006.

Mohseni, S. *et al.* (2019) 'Stochastic Optimal Sizing of Micro-Grids Using the Moth-Flame Optimization Algorithm', *IEEE Power and Energy Society General Meeting*, 2019-Augus, pp. 0–4. doi: 10.1109/PESGM40551.2019.8973570.

Mohseni, S., Brent, A. C., Burmester, D., *et al.* (2021) 'Lévy-flight moth-flame optimisation algorithm-based micro-grid equipment sizing: An integrated investment and operational planning approach', *Energy and AI*, 3, p. 100047. doi: 10.1016/j.egyai.2021.100047.

Mohseni, S., Brent, A. C., Kelly, S., *et al.* (2021) 'Strategic design optimisation of multi-energy-storage-technology micro-grids considering a two-stage game-theoretic market for demand response aggregation', *Applied Energy*, 287(January), p. 116563. doi: 10.1016/j.apenergy.2021.116563.

Mohseni, S. and Brent, A. C. (2020) 'Economic viability assessment of sustainable hydrogen

production, storage, and utilisation technologies integrated into on- and off-grid micro-grids: A performance comparison of different meta-heuristics', *International Journal of Hydrogen Energy*, 45(59), pp. 34412–34436. doi: 10.1016/j.ijhydene.2019.11.079.

Mohseni, S., Brent, A. C. and Burmester, D. (2019) 'A demand response-centred approach to the long-term equipment capacity planning of grid-independent micro-grids optimized by the moth-flame optimization algorithm', *Energy Conversion and Management*, 200(October), p. 112105. doi: 10.1016/j.enconman.2019.112105.

Monfared, H. J. *et al.* (2019) 'A hybrid price-based demand response program for the residential micro-grid', *Energy*, 185, pp. 274–285. doi: 10.1016/j.energy.2019.07.045.

Mosbah, M., Arif, S. and Mohammedi, R. D. (2017) 'Multi-objective optimization for optimal multi DG placement and sizes in distribution network based on NSGA-II and fuzzy logic combination', *2017 5th International Conference on Electrical Engineering - Boumerdes, ICEE-B 2017*, 2017-Janua, pp. 1–6. doi: 10.1109/ICEE-B.2017.8192171.

Mumtaz, F. and Bayram, I. S. (2017) 'Planning, Operation, and Protection of Microgrids: An Overview', *Energy Procedia*, 107(September 2016), pp. 94–100. doi: 10.1016/j.egypro.2016.12.137.

Nasirov, S., Silva, C. and Agostini, C. A. (2015) 'Investors' perspectives on barriers to the deployment of renewable energy sources in Chile', *Energies*, 8(5), pp. 3794–3814. doi: 10.3390/en8053794.

Nikmehr, N. and Najafi Ravadanegh, S. (2015) 'Optimal Power Dispatch of Multi-Microgrids at Future Smart Distribution Grids', *IEEE Transactions on Smart Grid*, 6(4), pp. 1648–1657. doi: 10.1109/TSG.2015.2396992.

'NIWA CliFlo National Climate Centre' (2020). Available at: https://cliflo.niwa.co.nz/.

O. Bilal, B. *et al.* (2013) 'Study of the influence of load profile variation on the optimal sizing of a standalone hybrid PV/Wind/Battery/Diesel system', *Energy Procedia*, 36, pp. 1265–1275. doi: 10.1016/j.egypro.2013.07.143.

Okedu, K. E., Salmani, A. L. and Waleed, Z. (2019) 'Smart Grid Technologies in Gulf Cooperation Council Countries: Challenges and Opportunities', *International Journal of Smart Grid*, 3(2), pp. 92–102. Available at: https://www.researchgate.net/profile/Kenneth-Okedu-2/publication/334029620_Smart_Grid_Technologies_in_Gulf_Cooperation_Council_Countries_Challenges_and_Opportunities/links/5d13068092851cf4404c3dff/Smart-Grid-Technologies-in-Gulf-Cooperation-Council-Countr.

Pahle, M., Pachauri, S. and Steinbacher, K. (2016) 'Can the Green Economy deliver it all? Experiences of renewable energy policies with socio-economic objectives', *Applied Energy*, 179, pp. 1331–1341. doi: 10.1016/j.apenergy.2016.06.073.

Papageorgiou, A. *et al.* (2020) 'Climate change impact of integrating a solar microgrid system into the Swedish electricity grid', *Applied Energy*, 268(April), p. 114981. doi: 10.1016/j.apenergy.2020.114981.

Park, N. M. (2021) 'Aotea , Great Barrier Island ~ A World of its Own', pp. 1–10. Available at: https://www.greatbarrierislandtourism.co.nz/.

Puchinger, J. and Raidl, G. R. (2006) 'Combining Metaheuristics and Exact Algorithms', pp. 1–12. Available at:

http://link.springer.com/10.1007/11499305_5%0Ahttp://link.springer.com/10.1007/11890584_1.

Radosavljević, J., Jevtić, M. and Klimenta, D. (2016) 'Energy and operation management of a microgrid using particle swarm optimization', *Engineering Optimization*, 48(5), pp. 811–830. doi: 10.1080/0305215X.2015.1057135.

Rajesh, P., Shajin, F. H. and Umasankar, L. (2021) 'A Novel Control Scheme for PV/WT/FC/Battery to Power Quality Enhancement in Micro Grid System: A Hybrid Technique', *Energy Sources, Part A: Recovery, Utilization and Environmental Effects*, 00(00), pp. 1–17. doi: 10.1080/15567036.2021.1943068.

Ramadan, A. *et al.* (2021) 'Parameter estimation of modified double-diode and triple-diode photovoltaic models based on wild horse optimizer', *Electronics (Switzerland)*, 10(18). doi: 10.3390/electronics10182308.

Ramli, M. A. M., Bouchekara, H. R. E. H. and Alghamdi, A. S. (2018) 'Optimal sizing of PV/wind/diesel hybrid microgrid system using multi-objective self-adaptive differential evolution algorithm', *Renewable Energy*, 121, pp. 400–411. doi: 10.1016/j.renene.2018.01.058.

Rasouli, B. *et al.* (2019) 'Optimal day-ahead scheduling of a smart micro-grid via a probabilistic model for considering the uncertainty of electric vehicles' load', *Applied Sciences (Switzerland)*, 9(22). doi: 10.3390/app9224872.

Razmi, H. and Doagou-Mojarrad, H. (2019) 'Comparative assessment of two different modes multi-objective optimal power management of micro-grid: Grid-connected and stand-alone', *IET Renewable Power Generation*, 13(6), pp. 802–815. doi: 10.1049/iet-rpg.2018.5407.

Sahu, P. C., Prusty, R. C. and Panda, S. (2020) 'Frequency regulation of an electric vehicle-operated micro-grid under WOA-tuned fuzzy cascade controller', *International Journal of Ambient Energy*, 0(0), pp. 1–18. doi: 10.1080/01430750.2020.1783358.

Samy, M. M. and Barakat, S. (2019) 'Hybrid Invasive Weed optimization-Particle Swarm optimization Algorithm for Biomass/PV Micro-grid Power System', *2019 21st International Middle East Power Systems Conference, MEPCON 2019 - Proceedings*, pp. 377–382. doi: 10.1109/MEPCON47431.2019.9008156.

Sarkar, J. and Bhattacharyya, S. (2012) 'Application of graphene and graphene-based materials in clean energy-related devices Minghui', *Archives of Thermodynamics*, 33(4), pp. 23–40. doi: 10.1002/er.

Seetharaman *et al.* (2019) 'Breaking barriers in deployment of renewable energy', *Heliyon*, 5(1), p. e01166. doi: 10.1016/j.heliyon.2019.e01166.

'Senwei - Model SWT-50kw - Variable Pitch Wind Turbine' (2021), pp. 1–5. Available at: https://www.energy-xprt.com/products/senwei-model-swt-50kw-variable-pitch-wind-turbine-675204.

Shah Danish, M. S. *et al.* (2019) 'A sustainable microgrid: A sustainability and management-oriented approach', *Energy Procedia*, 159, pp. 160–167. doi: 10.1016/j.egypro.2018.12.045.

Shieh, S. Y., Ersal, T. and Peng, H. (2019) 'Power Loss Minimization in Islanded Microgrids: A Communication-Free Decentralized Power Control Approach Using Extremum Seeking', *IEEE Access*, 7, pp. 20879–20893. doi: 10.1109/ACCESS.2018.2889840.

Sims, R. E. H., Rogner, H. H. and Gregory, K. (2003) 'Carbon emission and mitigation cost

comparisons between fossil fuel, nuclear and renewable energy resources for electricity generation', *Energy Policy*, 31(13), pp. 1315–1326. doi: 10.1016/S0301-4215(02)00192-1.

Smith, E. R. A. N. and Klick, H. (2007) 'Explaining NIMBY Opposition to Wind Power', 1(9), pp. 1689–1699.

SolarView (2019) 'Create SolarView Version: 1.1.1', p. 2019. Available at: https://solarview.niwa.co.nz/.

Steffen, B. *et al.* (2018) 'Opening new markets for clean energy: The role of project developers in the global diffusion of renewable energy technologies', *Business and Politics*, 20(4), pp. 553–587. doi: 10.1017/bap.2018.17.

Steffen, B. (2020) 'Estimating the cost of capital for renewable energy projects', *Energy Economics*, 88, p. 104783. doi: 10.1016/j.eneco.2020.104783.

Stewart and Essenwanger (1978) '1520-0450%281978%29017_1633%3Afdowsn_2.0.co%3B2.pdf'.

Stokes, L. C. (2013) 'The politics of renewable energy policies: The case of feed-in tariffs in Ontario, Canada', *Energy Policy*, 56, pp. 490–500. doi: 10.1016/j.enpol.2013.01.009.

Su, J., Lie, T. T. and Zamora, R. (2019) 'Modelling of large-scale electric vehicles charging demand: A New Zealand case study', *Electric Power Systems Research*, 167(November 2018), pp. 171–182. doi: 10.1016/j.epsr.2018.10.030.

Sun, P. and Nie, P. yan (2015) 'A comparative study of feed-in tariff and renewable portfolio standard policy in renewable energy industry', *Renewable Energy*, 74, pp. 255–262. doi: 10.1016/j.renene.2014.08.027.

Suresh, J. and Ganesh, V. (2019) 'An IBSMF Optimization Technique used Distribution system with Renewable Energy Sources', *IOP Conference Series: Materials Science and Engineering*, 623(1). doi: 10.1088/1757-899X/623/1/012013.

Ton, D. T. and Smith, M. A. (2012) 'The U.S. Department of Energy's Microgrid Initiative', *Electricity Journal*, 25(8), pp. 84–94. doi: 10.1016/j.tej.2012.09.013.

Verbruggen, A. *et al.* (2010) 'Renewable energy costs, potentials, barriers: Conceptual issues', *Energy Policy*, 38(2), pp. 850–861. doi: 10.1016/j.enpol.2009.10.036.

Vergara, P. P., Torquato, R. and Da Silva, L. C. P. (2015) 'Towards a real-time Energy Management System for a Microgrid using a multi-objective genetic algorithm', *IEEE Power and Energy Society General Meeting*, 2015-Septe, pp. 9–13. doi: 10.1109/PESGM.2015.7285956.

Wadood, A. *et al.* (2021) 'Application of Marine Predator Algorithm in Solving the Problem of Directional Overcurrent Relay in Electrical', pp. 1–5.

Van Wyk, M. and Taole, M. (2015) 'Planning , Designing and Conducting Educational Research Chapter 10', *Educational research*, pp. 164–185.

Xu, F. *et al.* (2018) 'A multi-objective optimization model of hybrid energy storage system for non-grid-connected wind power: A case study in China', *Energy*, 163, pp. 585–603. doi: 10.1016/j.energy.2018.08.152.

Yakout, A. H. *et al.* (2021) 'Optimal Fuzzy PIDF Load Frequency Controller for Hybrid Microgrid

System Using Marine Predator Algorithm', *IEEE Access*, 9, pp. 54220–54232. doi: 10.1109/ACCESS.2021.3070076.

Yang, H., Lu, L. and Zhou, W. (2007) 'A novel optimization sizing model for hybrid solar-wind power generation system', *Solar Energy*, 81(1), pp. 76–84. doi: 10.1016/j.solener.2006.06.010.

Yi, T. *et al.* (2020) 'Joint optimization of charging station and energy storage economic capacity based on the effect of alternative energy storage of electric vehicle', *Energy*, 208, p. 118357. doi: 10.1016/j.energy.2020.118357.

Yin, T., Zhang, Z. and Jiang, J. (2021) 'A Pareto-discrete hummingbird algorithm for partial sequence-dependent disassembly line balancing problem considering tool requirements', *Journal of Manufacturing Systems*, 60(August 2020), pp. 406–428. doi: 10.1016/j.jmsy.2021.07.005.

Zaki Diab, A. A. *et al.* (2019) 'Application of different optimization algorithms for optimal sizing of pv/wind/diesel/battery storage stand-alone hybrid microgrid', *IEEE Access*, 7, pp. 119223–119245. doi: 10.1109/ACCESS.2019.2936656.

Zaki Diab, A. A. *et al.* (2020) 'Fuel cell parameters estimation via marine predators and political optimizers', *IEEE Access*, 8, pp. 166998–167018. doi: 10.1109/ACCESS.2020.3021754.

Zhang, C. *et al.* (2018) 'Energy storage system: Current studies on batteries and power condition system', *Renewable and Sustainable Energy Reviews*, 82(December 2016), pp. 3091–3106. doi: 10.1016/j.rser.2017.10.030.

Zhang, H. *et al.* (2014) 'Political connections, government subsidies and firm financial performance: Evidence from renewable energy manufacturing in China', *Renewable Energy*, 63, pp. 330–336. doi: 10.1016/j.renene.2013.09.029.

Zhao, Haoran, Guo, S. and Zhao, Huiru (2018) 'Comprehensive performance assessment on various battery energy storage systems', *Energies*, 11(10). doi: 10.3390/en11102841.

Zhu, W. H. *et al.* (2013) 'Energy efficiency and capacity retention of Ni-MH batteries for storage applications', *Applied Energy*, 106, pp. 307–313. doi: 10.1016/j.apenergy.2012.12.025.